Novel Quadruple-mode, Dual-mode and Dual-band Dielectric Resonator Filters and Multiplexers

by

Mohammad Memarian

A thesis
presented to the University of Waterloo
in fulfillment of the
thesis requirement for the degree of
Master of Applied Science
in
Electrical and Computer Engineering

Waterloo, Ontario, Canada, 2009

AUTHOR'S DECLARATION

I hereby declare that I am the sole author of this thesis. This is a true copy of the thesis, including any required final revisions, as accepted by my examiners.

I understand that my thesis may be made electronically available to the public.

Mohammad Memarian

Abstract

Dielectric resonators offer high-Q (low loss) characteristics which make them ideal for filters with narrow bandwidth and low insertion loss specifications. They are mainly used in satellite and wireless system applications. Such applications desire the highest performance filters with the lowest amount of size and mass, which has been the main motivation for size reduction techniques invented over the past three decades for these filters. In addition with the emergence of different communication system technologies, several bands are now required to be supported by a single front-end, calling for emergence and development of dual-band and multi-band filters. To date few work has been done in the area of dual-band dielectric resonator filters. Dielectric resonators filters are important components in many communication systems, when a group of such filters are brought together to perform multiplexing of RF channels. These multiplexer systems tend to be fairly complex and bulky in design, and there is strong desire to reduce their size and mass to the maximum extent possible.

Novel quadruple-mode, dual-mode, and dual-band filters as well multiplexers are presented in this thesis. The first ever quadruple-mode dielectric resonator filter using the simple cylinder structure is reported in this work. A cylindrical dielectric resonator sized appropriately in terms of its diameter and height is shown to operate as a quadruple-mode resonator, which is achieved by having two mode pairs of the structure resonate at the same frequency. Single-cavity, quad-mode filters and higher order 4n-pole filters are realizable using this quad-mode cylindrical resonator, offering significant size reduction for dielectric resonator filter applications. The structure of the quad-mode cylinder is then simplified by cutting lengthwise along the central axis of the cylinder, to produce a half-cut cylinder suitable for operation in a dual-mode regime. Novel dual-mode, 2n-pole filters are realizable using this half-cut cylinder, by making the two resonances equal in frequency. The dual-mode half-cut filter is shown to be a strong contender for replacing existing dual-mode filters used in satellite and wireless applications, as it offers superior size and mass characteristics.

By making the resonances unequal in frequency, novel dual-band filters and multiplexers are further realizable, by carrying separate frequency bands on different resonant modes of the structure. The first true orthogonal mode dual-band dielectric resonator is presented in this work, using the half-cut structure. Multiplexers are also derived from these dual-band resonators, which greatly reduce size and mass of many-channel multiplexers at the system level, as each two channels are overloaded in one physical branch.

Full control of center frequencies of resonances, input and inter-resonator couplings are achievable, allowing realization of microwave filters with different bandwidth, frequency, and return loss specifications, as well as advanced filtering functions with prescribed transmission zeros. Spurious performance of the half-cut cylinder can also be improved by cutting one or more through-way slots between opposite surfaces of the resonator. Size and mass reduction achieved by using the full and half-cut resonators described in this thesis, provide various levels of size reduction in microwave systems, both device and system level.

Acknowledgements

There are many whom I thankful to, but I am most grateful to the god almighty, for giving me the blessing of life, and all the blessings that come in life.

I would like to sincerely thank my supervisor and mentor, professor R. R. Mansour. His supervision, ideas, encouragement, and guidance made my research possible and fruitful, and his great personality made this a pleasant and wonderful journey. I will be forever grateful to him for introducing me to the world of RF/Microwave engineering, and for allowing and encouraging me to progress in it. I would not have been able to achieve all this during the past two years without his supervision.

I would like to thank Dr. M. Yu for his constructive comments throughout my research, and COMDEV Ltd. for their support. In addition, I would like to thank the Natural Sciences and Engineering Research Council of Canada (NSERC) and Ontario Graduate Scholarship (OGS) for their support of my research. I would like to also thank the reviewing readers of this thesis.

My warm wishes and thanks to my friends and colleagues in the CIRFE group, and CIRFE lab manager B. Jolley, and to all my friends over the past years.

And most importantly my deepest appreciation goes to my family, whom I love and cherish dearly. Your great care, love, wisdom, and fountain of emotions have helped to progress in different chapters of my life thus far.

To my parents

Table of Contents

List of Figures

List of Tables

Chapter 1
Introduction

1.1 Motivation

Dielectric resonator filters have tremendous applications in satellite and wireless communication systems. Their low loss capabilities is the main driving force for using this technology for filters and multiplexers in microwave systems. After their early analysis by Cohn [9] in the 1960s, dielectric resonators were not significantly utilized in commercial applications until the 1970s and 1980s, when more advanced ceramic materials were devised which had good dielectric attributes, low-loss performance and other important characteristics. Since then, various materials, shapes, forms, and modes of operation have been reported in the literature and used commercially for dielectric resonator filters. Most of these efforts are to somehow improve one or more characteristics of the dielectric resonator filter, be it having less size and mass, better filtering performance, etc.. One of the most important of all these characteristics is size and mass. Many attempts such as the dual-mode operation [23], became legendary work in this area as they offered an alternative smaller device, with comparable performance to their predecessor. Such devices are more attractive for applications that dielectric resonator filters are mainly intended for. For example a satellite orbiting the earth, would require as small as possible size and as light as possible devices to be launched with it.

In addition, many wireless systems have emerged over the years that have opened the door for invention of dual-band and multiband filters. Such filters would need to handle different frequency passbands with different characteristics (e.g. bandwidth), simultaneously. So far limited work has been done that show dual-band filters with low loss capabilities, as these devices have so far been mainly realized with planar structures which are quite limited in Q.

Multiplexing systems, which are essentially a collection of channel filters, are widely used in microwave systems. They have different applications, such as an IMUX or an OMUX, and are realized with various techniques. Nevertheless, these crucial system components tend to be bulky, heavy, and can become fairly complex in design.

The motivation behind this thesis is to find solutions to better achieve size and mass characteristics, with comparable performance to existing alternatives for microwave systems. This thesis aims to address size issues in different levels of microwave systems, be it at the filter device level, or at the system level.

1.2 Objectives

The objective of this thesis is three fold:

1) Propose solutions for dielectric resonator filters that reduce size and mass compared to existing solutions.
2) Propose solutions for dual-band dielectric resonator filters, harnessing their high-Q and maintaining compact size.
3) Propose possible solutions that could be used at a system level for multiplexing devices in microwave systems, to achieve size and complexity reduction.

1.3 Scope

This thesis mainly aims to introduce new structures and schemes for size reduction in areas of microwave systems that utilize dielectric resonator filters and multiplexers. One example of such application is the satellite payload. It should be noted that some of the ideas and structures mentioned in this thesis, especially those in later chapters, maybe applicable to other technologies and or shapes, and therefore this work presents some of the possibilities, and in no way aims to define the limits of the proposed concepts.

1.4 Thesis Organization

The organization of this thesis is as follows. Following the introduction, a literature review of work done so far in the area of dielectric resonator filters is presented, as well as dual-band filters and multiplexers.

Chapter 3 introduces the first ever quadruple-mode dielectric resonator filter using a simple cylinder structure. Designs and measurement results are presented. Also a novel dual-mode half-cut dielectric resonator filter is introduced in this chapter which is derived from the quadruple mode filter. Various aspects of the design are discussed, as well as spurious improvement techniques and comparison with existing technology, and measurement results are presented.

Chapter 4 is dedicated to a novel dual-band dielectric resonator filters, using the half-cut or full cylinder structure. Again various design details are discussed. Several designs are presented as well as measurement results showing the validity of the proposed concepts.

Chapter 5 introduces a novel two-channel dielectric resonator based multiplexer device. Several designs are presented showing the validity of the proposed concept. The performance of the device is investigated and various techniques are presented to reach a good compromise. Various applications of

the proposed design and its impact on the system level, including many channel multiplexing systems are presented.

In final chapter the major conclusions and contributions from this work are briefly summarized followed by suggestions for possible future work.

Chapter 2
Background

2.1 Introduction

In this chapter we cover some of the major work that has been done to-date mainly in the area of microwave bandpass dielectric resonator filters. Dual-band filters, and multiplexer/diplexer systems are also briefly discussed, with more focus on dielectric resonator based devices.

2.2 Microwave Bandpass Filters

Microwave bandpass filters exist in all satellite, radar, and wireless communication systems, and are used to separate certain frequencies from a spectrum of frequencies. They are commonly realized using one or more resonators, coupled to each other. Broadly speaking, a resonator is any physical element that stores both magnetic and electric energy in a frequency-dependent way. At the resonance frequency, the stored electric and magnetic energies in the resonator are equal. The simple model for an ideal resonator is a capacitor/inductor system, where at resonance the magnetic and electric energy is exchanged between inductor and capacitor respectively, having a resonance frequency $f = 1/2\pi\sqrt{LC}$.

DR filters are realized with various technologies. At microwave frequencies, potentially any three-dimensional structure can be used to realize a resonator in which internal electric and magnetic field distributions are determined by the shape and size of the overall structure, and its boundary conditions. The resonance is sustained in the structure indefinitely, if no losses were to be present. In reality all structures exhibit some loss and therefore the resonance would be decaying unless more energy is supplied. Q or quality factor, measures the structure`s loss capability to sustain the resonance, and is defined as Q = ω.(energy stored / average power loss) = 2π(energy stored / energy dissipated per cycle) [1]. High-Q filters are much required in applications where only low insertion loss (IL) can be tolerated. Achieving low IL is challenging in filters with narrow bandwidth, e.g. satellite applications, and normally requires Q of up to 10,000-20,000.

A full cycle of filter design first starts with the filter specifications. The specification such as the filter type (e.g. Chebyshev, elliptic, …), return loss, number of poles, and location of transmission zeros are used to determine the ideal characteristic polynomials of the filter. Higher order filters typically provide higher out of band rejection, and transmission zeros are placed in the ideal response to further

improve the rejection of response and create sharp roll-offs to the sides of the passband. The recursive technique introduced by Cameron, in [1] and [2] is one method to arrive at these polynomials, which can be used generally for both symmetric and asymmetric response filters. The next step is to translate these polynomials into a prototype electrical circuit from which a real microwave filter can be designed. There are two methods, namely the classical circuit synthesis [3], and the direct coupling matrix approach [4]-[6]. Design of microwave filters using the coupling matrix approach was first introduced by Atia and Williams in 1970s [4] and has been widely used since.

Once the desired coupling matrix is achieved, the filter can be implemented with different physical realizations, e.g. microstrip, or waveguide, or DR filters. The design of the physical filter from here after involves modeling, approximations, EM simulations and partial and global optimizations in order to arrive at physical dimensions of the entire filter. There are various methods and models depending on the technology used to design the filters based on its subcomponents, e.g. resonators and coupling values. A comprehensive description of these methods are available in literature e.g. [1]. Once the design dimensions are found, the filter is fabricated. Normally a tuning stage is also required after the filter is fabricated with the design dimensions, to compensate for differences between simulated design and the actual fabricated filter.

Of course not every coupling matrix arrangement maybe realized with every filter technology and type. For example, some cross couplings maybe easier to realize in a dual-mode filter, or more than one source to load coupling may not even be realizable with waveguide technology. Therefore a coupling matrix maybe required to be converted to other arrangements via a series of similarity transformations [7] and [8], to suite the type of filter and its technology. For detailed description of N and N+2 coupling matrix representation of microwave filters and the relations governing their theory the reader is referred to literature such as [1].

Some classes of microwave resonators and filters include lumped element, planar (microstrip, CPW), coaxial, waveguide, dielectric, and superconductor type. Each class has application specific advantages and disadvantages. Two key features of any filter are its size and loss capabilities or Q. Figure 2-1 shows a comparison between the Q performance and size of some of the major microwave filter technologies. It can be seen that there always exists a trade-off between size and energy loss. In general, higher Q means bulkier technology.

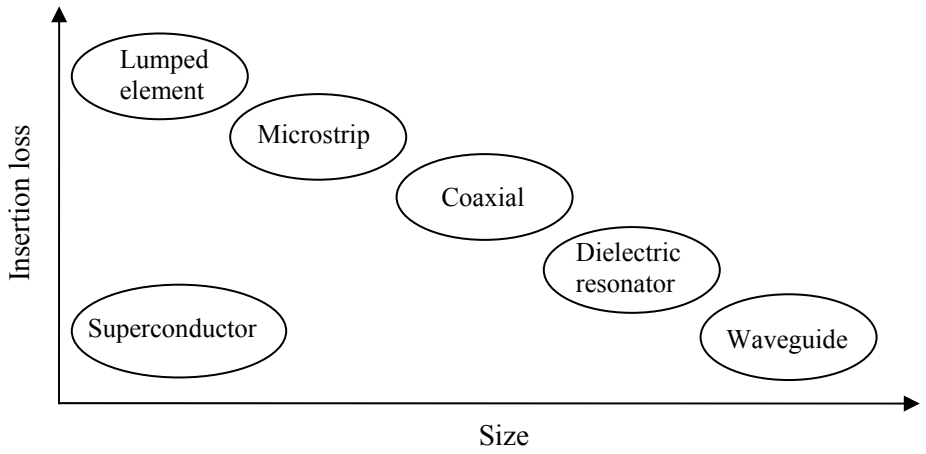

Figure 2-1: Comparison of microwave filter technologies in terms of size and insertion loss [1].

2.3 Dielectric Resonators and Dielectric Resonator Filters

Dielectric resonators have found significant applications in the area of low loss (high Q) microwave filters. DR filters are mainly utilized in satellite and base station technologies, where low insertion loss is required with narrow bandwidth filter specifications, e.g. 1% fractional bandwidth [1]. In general DR filters miniaturize waveguide filters by loading the cavity with some form of dielectric, decreasing the wavelength of resonance, and hence achieving same resonance frequency with smaller size. As depicted in Figure 2-1, compared to lumped element and microstrip resonators, dielectric resonators (as well as coaxial and waveguide resonators) tend to be bulkier in size and more complex in design, but offer superior Q values. In present microwave technologies, dielectric resonators offer Q values in the range of 3,000 to 30,000 at 1 GHz [1]. This is orders of magnitude higher than planar technologies. For this reason, dielectric resonator filters are often favored for use in satellite/space communication and wireless base station applications, where low loss and high power can be overriding design considerations.

Any formation of a dielectric material can potentially be used as a dielectric resonator. However certain shapes have found to be more practical, due to theory of operation as well as fabrication considerations. The most popular shape of dielectric resonators is the cylindrical shape analyzed in the classic work of Cohn [9]. The other shape is the rectangular box shape also reported in [9], though it has not found equal application as the cylindrical. Other shapes of DRs and modifications to the cylindrical and rectangular shapes have also been reported in the literature, all having certain advantages and applications. A dielectric resonator cavity normally comprises of a dielectric resonator made from a high-

permittivity material ($10 < \varepsilon_r < 100$) mounted inside a metallic housing, using a support with a low-permittivity material ($\varepsilon_r' < 10$). Though most of the field is concentrated inside the dielectric, it is still placed inside a cavity to prevent radiation losses of the remaining fields, and to better guide the waves. The dielectric resonator resonates at a frequency lower than the metal cavity's fundamental mode of propagation, to avoid resonance of waveguide modes. Figure 2-2 shows a common dielectric resonator loaded cavity.

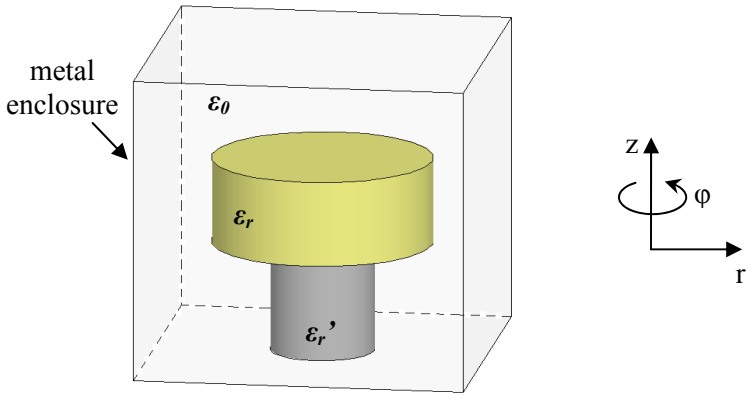

Figure 2-2: Cylindrical DR placed in a metal cavity.

Loss in dielectric resonator filters mainly come from the losses in the dielectric resonator itself, as well as losses at the metal cavity walls the dielectric is placed in. Several other losses exist, including losses in the support, losses due to adhesive between dielectric and support, losses due to any coupling or tuning mechanism, e.g. tuning screw, and even fabrication issues such as oil from fingers when handling the DR [1]. The loss due to the dielectric itself is the dominating form of loss at resonance frequency, as most of the field is trapped inside the dielectric.

Over the years and with advances in material engineering, dielectric materials have been introduced that provide high permittivity, as well as low dielectric losses at microwave resonance frequencies. They are commercially available in various forms and sizes, e.g. [10]. The general dispersion rule of the resonator dictates that for a specific DR material operating in a certain mode and with constant permittivity within a frequency range, the higher the operating frequency, the higher the losses in the dielectric material. Therefore a more comprehensive metric for the loss capabilities of a dielectric is *Q.f,* which is typically a constant over a wide frequency range. Typical low-loss commercial dielectrics are now available with *Q.f* of 40,000 for relative permittivity of above 30-40 [10]. These material not only offer superior low-loss capabilities, but are also considerably temperature stable, which is another characteristic that is highly desired for certain applications where the filter is operating in harsh and

varying environmental conditions.

2.4 Modes in a Dielectric Resonator

A dielectric resonator, similar to other 3D structures, has many modes of resonance. There are in fact infinite number of modes, that can resonate inside the dielectric and satisfy all boundary conditions. These modes can be decomposed to TE, TM and Hybrid TE/TM to the main axis of the cylinder. There have been different naming conventions for the modes inside a DR, e.g. [11], or [12]. One mode designation that simplifies the naming of the modes in DR is that proposed by Zaki et al., in [13], which will be used throughout this thesis exclusively. The modes are designated as TEH_{0m}, TME_{0m}, TMH_{0m}, TME_{0m}, HEH_{nm}, HEE_{nm}. The first two letters indicate whether the modes are Hybrid (HE), Transverse Electric (TE) or Transverse Magnetic (TM). The third letter (E or H) indicates whether the symmetry plane half way between the two caps of the DR, indicated as z = 0 in the side view shown in Figure 2-3, is an electric wall or magnetic wall, respectively. That is whether the E-field of the mode is tangential to the plane (magnetic wall) or perpendicular (electric wall). The order of the angular or φ variation of the field (*cos(nφ)* or *sin(nφ)*) is denoted by the first subscript "n". The second subscript "m" is the order of the resonant frequency, m = 1 being the lowest resonant of the particular mode with angular variation *cos(nφ)* or *sin(nφ)*. It can be seen that with this mode designation, for all the TE and TM modes, n=0. Note that this convention does not indicate the radial (r) nor the axial (z) field variations. It orders the modes according to their resonance frequency [13].

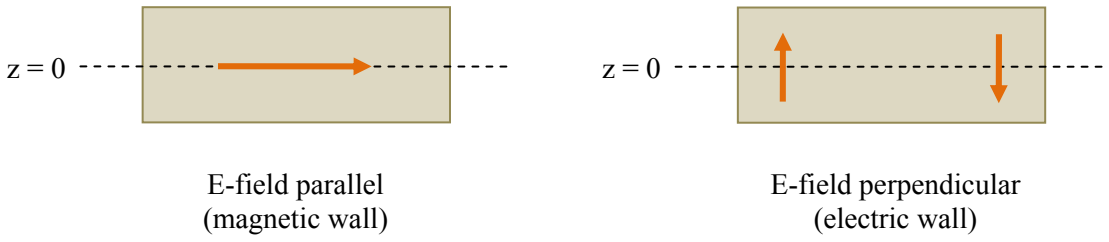

Figure 2-3: Mode designation based on the nature of the symmetry plane placed half-way between the two caps of the dielectric resonator.

The existence of different modes at certain resonance frequencies depends on the geometry and size of the resonator. For a cylindrical DR, the diameter to height ratio dictates the order of modes in

frequency. A mode chart of a DR is shown in Figure 2-4. This chart shows how for a specific dielectric material, the resonance frequency of different modes vary if the diameter to height ratio (D/L) is varied. Mode charts are a useful tool for initial design of DR cavities and to better understand the behavior of modes. Some available mode charts published to date are those of Rebsch [14], Courtney [15], Kobayashi [16]and [17], Zaki et al. [13] and [18].

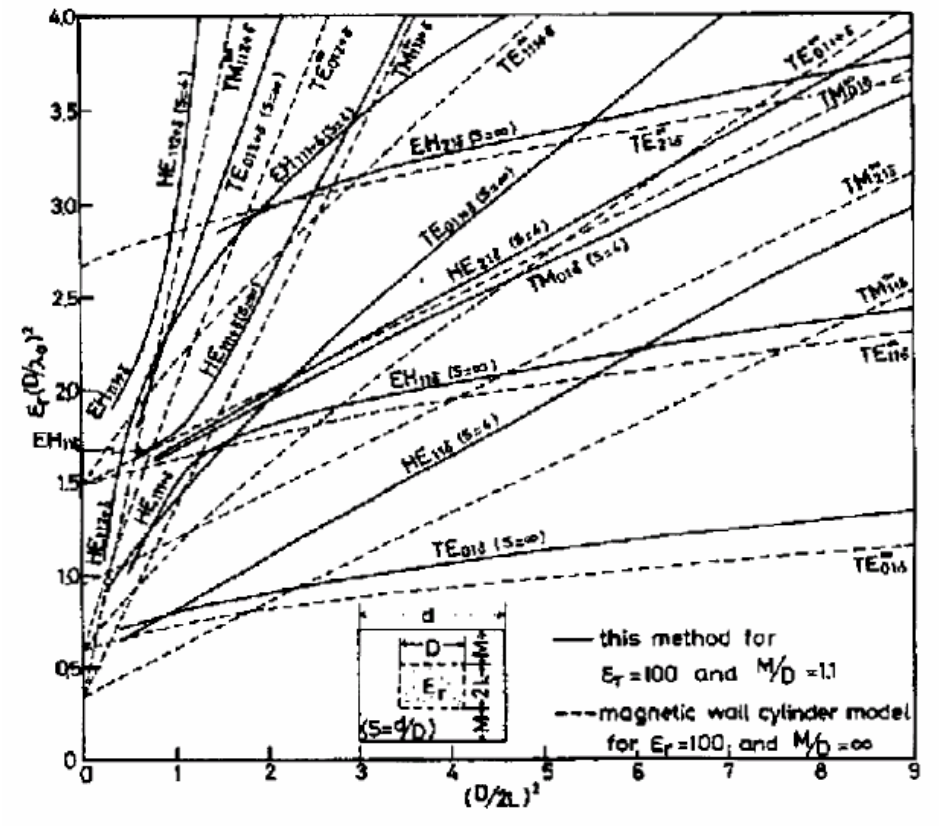

Figure 2-4: Mode chart of a cylindrical DR placed in a metal cavity [17].

2.5 Multi-mode Dielectric Resonator Filters

Microwave resonators can be single or multi-mode resonators. A single-mode resonator supports only a single field distribution at the resonator's desired resonance frequency. Correspondingly, a dual-mode resonator supports two field distributions and a triple-mode resonator supports three different field distributions at the operating frequency. The intention for using a higher number of modes is mainly size reduction, as one physical resonator is overloaded with more than one electrical resonator, and each electrical resonator is supported by a mode distribution. Multi-resonant modes, such as dual and triple-

modes supporting a plurality of field distributions at the same frequency, normally arise from the degeneracy of the modes. Usually, the different field distributions in a degenerate mode are orthogonal modes of a similar field distribution, and are created due to symmetries in the resonator. Thus, dual modes have been mainly realized with resonators having 90-degree radial symmetry (e.g. cylindrical and rectangular waveguide cavities and resonators [5]), while triple modes are supported for example in cubic waveguide cavities or circular cavities with certain modes, [19], [20], and [21]. Figure 2-5 shows an example of a dual-mode, triple-mode and quadruple-mode filters in different technologies.

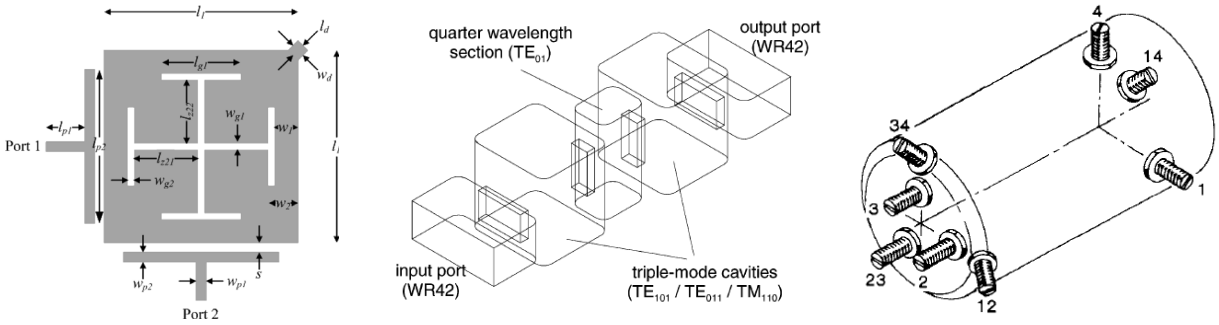

Figure 2-5: (left) dual-mode filter in microstrip [22], (middle) triple-mode filter in waveguide [19], and (right) quadruple-mode cavity in circular waveguide [20] technologies .

Dielectric resonator filters are commonly operated as single-mode resonators [9], dual-mode resonators [23], and less commonly as triple-mode [24] and [25], and quadruple-mode resonators [26]. For cylindrical dielectric resonator discussed so far, with a typical mode chart of Figure 2-4, the first few modes, namely the TEH, TME, HEE_{11}, HEH_{11}, have been popular choices for filter design. The TEH mode is the most popular and common operating mode, which is also known as the $TE_{01\delta}$ mode. This mode is a single mode and has an azimuthal electric field distribution shown in Figure 2-6 (left). This mode of operation has been extensively used both in academic literature and commercially for satellite and wireless applications. The TME is also a single mode resonance and can potentially be used for single mode DR filters, though due to size, the TEH mode is the more favorable solution. A TEH mode filter using modified cylindrical resonator is shown in Figure 2-6 (middle and right).

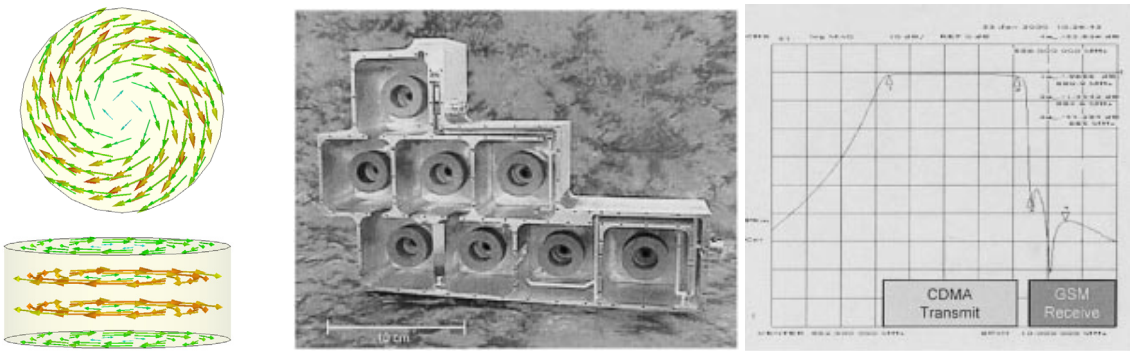

Figure 2-6: (left) E-field of the TEH mode in cylinder DR, (middle) multi-pole $TE_{01\delta}$ (TEH) single mode DR filter (middle) structure and (right) response for cellular base-station application [27].

The first significant contribution to reduction of size in DR filters was introduced by Fiedziuszko [23], showing that is it is possible to realize dual-mode DR filters. Dual-mode operation is preferred in satellite applications for size and mass savings reasons. An example of such filter is shown in Figure 2-7. Here the degeneracy of the HEH_{11} or the HEE_{11} is utilized to realize compact DR filters, with less overall size and mass than the single mode TEH type filters. Cruciform irises were used for inter-cavity couplings. In dielectric resonators, generally the electric energy is mainly concentrated inside the DR, while the magnetic energy is more available outside the resonator. Therefore for coupling between resonators, typically magnetic coupling, such as irises shown in Figure 2-7 are used. This dual-mode resonator, since its introduction, has received extensive attention in the literature and also been used in commercial applications. The original work of [23] was later further analyzed and extended by Zaki et al. [28], Kobayashi et al. [29], and Guillion et al. [30]. The filters initially introduced in [23] were axially mounted, as shown in Figure 2-7, which are less mechanically stable, but this work was later extended to planar mounted DRs in [31].

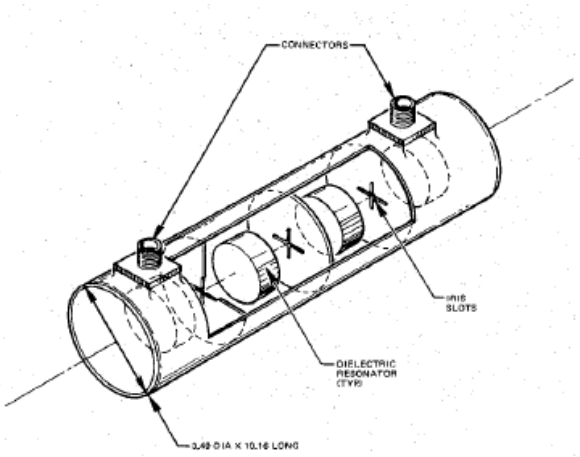

Figure 2-7: Axially mounted dual-mode DR filter configuration of [23].

Figure 2-8 shows a triple-mode DR cavity introduced by Hunter et al. in [24] and [25]. Here, the DR is chosen such that three degenerate mode distributions co-exists at the same frequency, hence the cubic shape. Some coupling and tuning mechanisms are also shown in the figure.

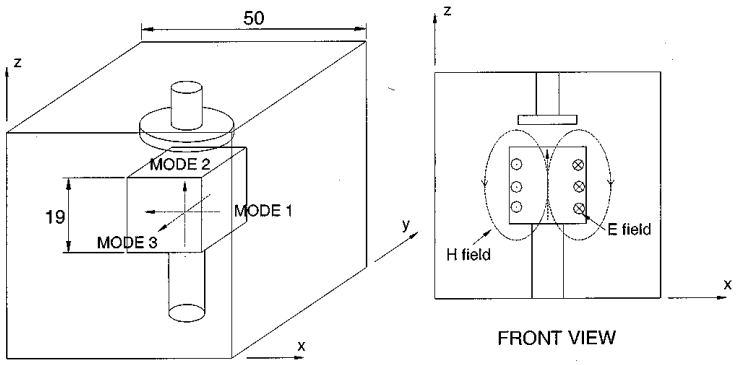

Figure 2-8: Triple-mode $TE_{01\delta}$ resonator from [25].

A quadruple-mode dielectric resonator filter has also been realized, introduced by Hattori et al. in [26]. This resonator is shown in Figure 2-9. Here the shape is modified to achieve four resonances in the same cavity. The concept was used in [26] to realize a 2 GHz band quadruple mode dielectric resonator filter for cellular base station, having a compact size for WCDMA applications.

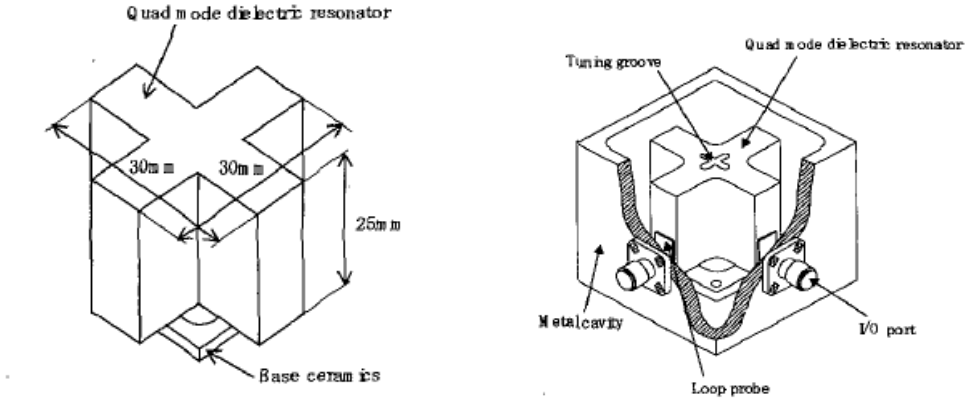

Figure 2-9: Quadruple-mode dielectric resonator (left) and (right) filter from [26].

The incentive for using dual-mode or higher order modes of operation is principally for size reduction benefits, which is an important factor for applications such as satellite systems, but this is achieved at a price. Although dielectric resonators can come in various forms and shapes, not all forms are easy to fabricate. This is mainly due to the high temperature and pressure required when firing the ceramic. Triple mode and quadruple mode DR filters known to date are very few, and mainly due to complications in fabrication and tuning, comparatively less interest has been generated in their utilization. In order to realize a quadruple-mode dielectric resonator, aside from fabrication complexities of the resonator shapes, independent or near independent control over the coupling and tuning of each of four modes is required, which generally results in a complex overall coupling scheme involving a large number of tuning and/or coupling screws. Although tuning and coupling schemes are also necessary for single-mode and dual-mode and add some design complexity to these filters, the added design complexities are more noticeable in triple-mode dielectric resonators, and are even more pronounced in presently known realizations of quadruple-mode dielectric resonators. Simple multi-mode resonators are attractive alternatives to single-mode dielectric resonators, especially considering that dielectric resonators already tend to be bulky, and any size reduction is highly desirable for their intended application.

2.6 Other DR filters

Aside from the DR filters discussed, other forms of DRs with modified shapes have been used independently or alongside other resonators. In [32] a dual-mode filter with conductor loaded dielectric resonators has been shown to yield size reduction compared to coaxial filters for the 900 MHz frequency applications. An alternative structure uses grounded dielectric rods operating in the single mode [33]. This provides less volume reduction, but with a simpler physical structure. A compact filter with good spurious

response was demonstrated in [34] by placing high-Q TM dielectric rod resonators coaxially in a TM_{01} cut-off circular waveguide. This single mode resonator is bigger than the TEH mode resonator, but has higher Q and better spurious performance. There are also reports of TEM-mode resonators with Q_u of less than 1000, for very compact configurations [35] and [36]. More recently Zhang et al. [37] introduced a dielectric resonator filter configuration implemented as a single piece of a high-K ceramic substrate. It uses the TEH_{01} fundamental mode, and reduces the cost of assembly and integration.

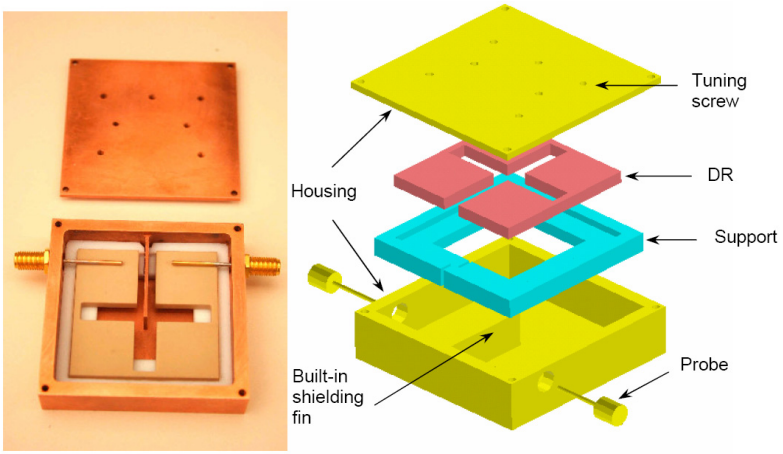

Figure 2-10: 4-pole filter made with high-K dielectric substrate [37].

Several size reduction techniques other than multi-mode filters have also been introduced in the years. The most famous of these is the quarter-cut image type resonator introduced in [38]. Here the typical TEH mode is used, but only a quarter of the resonator is utilized, along with metallization at the two ends of the cut surface. The placement of the metal walls allow for existence of the same TEH mode distribution in the remaining quarter-cut, as the field at the metal walls need to completely orthogonal, which is the same behavior as the field in the original resonator. The resonator has a high unloaded Q over 7000 and its construction provides a sufficient thermal diffusion path to the metal housing.

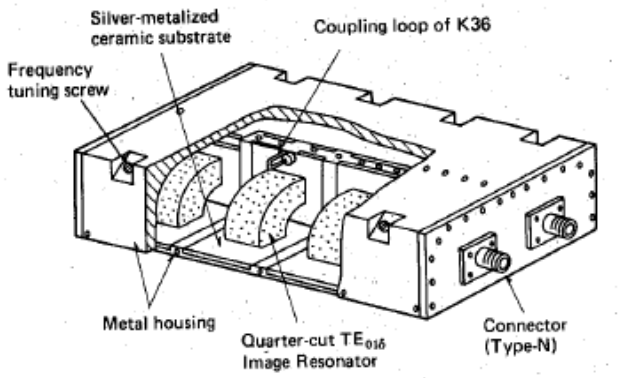

Figure 2-11: Basic construction of quarter-cut $TE_{01\delta}$ image resonator filter [38].

Another size reduction technique is using the imperfect magnetic wall technique as done by Mansour et al. in [39] to realize single mode half-cut dielectric resonator and quasi dual-mode half-cut dielectric resonator filters. The full cylinder is cut in half along its axis, which resonates with half of a single component of the HEH_{11} mode. The half HEH_{11} mode can be sustained in the remaining half-cut resonator due to the magnetic boundary condition formed at the cut location. Figure 2-12 shows a comparative picture between the conventional TEH DR filter and the half-cut DR filter.

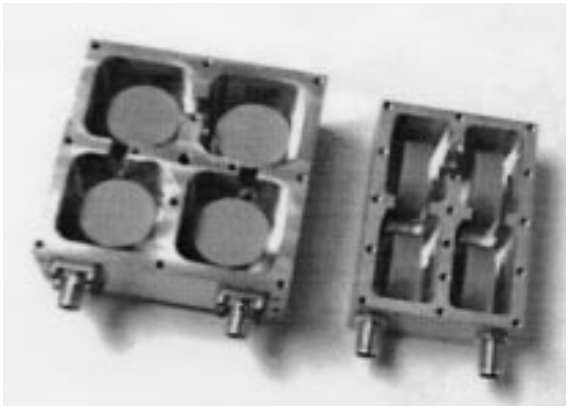

Figure 2-12: Comparison between single-mode full, and single-mode half-cut resonator filters [38].

2.7 Spurious Considerations

In addition to Q and resonator size, spurious performance is an important design consideration. The spurious free window of a filter is the frequency separation between the operating frequency (also known as center frequency) of the filter, and the frequency of the closest undesired transmission.

Normally the non-operating spurious modes that are not at the operating frequency create spurious transmissions from the input to output of the filter, and thereby limiting the filtering capabilities. The closer the spurious modes of a filter to the operating range, the poorer the response is. Different techniques have been used in the past to improve the spurious free window of a filter. One method is to add a helper low-pass filter after the main filter, which rejects the out of band frequencies due to spurious modes, and only transmits the operating band [1]. The addition of the helper filter does not render the main filter useless, as the main filter is still required to attain an accurate response with narrow bandwidth. However size increase, added design complexity, and insertion loss degradation are some major consequences of this method.

Another method for spurious enhancement is using dissimilar resonators, or mixed modes in filters. For dielectric resonators, this idea was utilized in [40]. Various resonators operating in different modes, each having different spurious free windows are coupled together to realize a filter. The overall filter would however not have overlapping spurious modes, and its spurious free window should theoretically be as good as the first common spurious mode.

The other method which is probably the most popular approach, is reshaping the resonator [41], [42], [43] and [44]. The idea is to analyze the field distribution of the operating and spurious modes, and alter the shape of the resonator such that the operating modes are unaffected, but the spurious modes are terminated or pushed much higher in frequency. The most popular of such alterations ever presented is introduction of a hole inside a cylindrical DR as analyzed in [44], also shown in Figure 2-6 (middle). Here the operating mode is still the TEH mode, which has an azimuthal circulation around the hole. The introduction of the hole in the middle of the resonator along its axis hardly affects this operating mode. However higher order modes such as the HEH, HEE and especially TME, all are significantly affected and are pushed much higher in frequency. According to [27], the spurious free window is improved from 30% of center frequency to 50% of center frequency. Of course altering the shape of the resonator does come at a price. Although the operating mode is not affected significantly, it is normally increased in frequency by some noticeable amount. This means that in order to achieve the same frequency, the resonator needs to be made larger, to compensate for the frequency shift. [44] discusses finding the optimum size and mode separation.

2.8 DR Calculation Techniques

Accurate calculation of resonant frequency, Q-factor, coupling coefficients and field distribution for DRs mounted in cavities or in free space is fairly complicated. To date, much work has been done to

come up with models and techniques for accurate calculations for DRs. These attempts can be divided into simple models and rigorous analysis techniques.

The first order model, the second order Cohn model [9] and Itoh-Rudokas model [45] are examples of simple models. The least accurate model is the first order model. It assumes perfect magnetic wall (a.k.a. perfect magnetic conductor or PMC) boundary conditions on all surfaces of the DR, solving the field inside of this PMC wall cylindrical cavity. The main reason for the large inaccuracy is that this model assumes all field is concentrated inside the DR, and assumes zero field outside. In reality none of the DR walls are PMC, but rather imperfect magnetic wall, owing to the finite relative permittivity of the dielectric to the outside material. The second order Cohn model [9] allows for some accuracy by removing the PMC condition on the two end caps of the DR, and assumes two waveguides attached to the two ends of the DR. The two waveguides have PMC on their sidewalls, and are under cutoff, allowing for modeling of leakage of evanescent field, outside of the two end caps. These fields would be exponentially decaying in the direction of the axis of the cylinder. The two waveguides can be terminated at some distance from the DR with an electric wall (PEC) boundary condition, allowing the modeling of walls of the cavity that the DR is normally placed in. This model is limited as it still assumes zero field anywhere radialy outward of the DR's sidewalls. This is however corrected in the pertubational correction to the Cohn model [12]. Here, the same field is assumed for the sidewalls of the DR as the PMC BC in the second order Cohn model, but it equates this field with the field on the other side of the DR. This model then uses perturbation in volume of resonator. The Itoh-Rudokas model [45] offers further improvement, as it does not assume PMC B.C. on any walls, rather it starts the model using a dielectric waveguide rod, ensuring the continuity of both electric and magnetic field on the two sides of the sidewalls of the DR. There is also a variational method correction to the Itoh-Rudokas model [12], utilizing reaction formulas to arrive at more accurate frequency calculation results that are less prone to errors due to inaccuracies in the field modeling.

The simple models all lack accuracy to a great degree for modern filter design, and therefore over the years, rigorous analysis techniques have been introduced, or borrowed for solution to DR problems. All these methods start from the Maxwell's equations for the entire problem space and aim to solve the field, which is the main reason for their accuracy over the simplified field assumed in the simple models. They work based on repeated approximation attempts towards the exact solution and therefore can be theoretically repeated to yield sufficient accuracy. Some of the rigorous methods include the general FEM (Finite Element Method) and Finite Difference Time Domain (FDTD) methods available in

full wave solver software such as [46] and [47] respectively. The axial mode matching technique [11], radial mode matching technique [13] and [18], the Galerkin-Rayleigh-Ritz method [12], the differential mode-matching [48], and the Green's function/integral equation method [49] and [50], all customized for the DR inside cavity or in free space, are other examples of rigorous analysis techniques. They all have their own merits and disadvantages depending on the exact configuration of the problem, calculation complexity, modes analyzed and other factors.

It should be noted that for the purposes of this work, using a full wave solver is inevitable and deemed to be the most practical and efficient method. Therefore Ansoft HFSS was used exclusively in calculations and simulations of this thesis, which is a FEM based full wave solver.

2.9 Dual-Band Filters

In the past decade there has been a significant growth in emergence of different wireless communication systems. Such market and the scarce available frequency spectrum demand systems and devices that can handle these different technologies simultaneously and efficiently. As microwave filters are important components in any wireless communication system, to date various dual-band and multi-band filters have been introduced [51]-[59], to allow filtering of various bands within a single device. In the filter synthesis stage, analytical methods [51], or optimization techniques [52] have been presented to reach the desired coupling matrix. Some of the typical technologies that have so far been used to realize dual-band filters have been planar microstrip [52], multiple-coupled coaxial [53], and Waveguide structures [52] and [54], all having application specific advantages and disadvantages. It is fair to say most of the contributions in the area of dual-band filters have been mostly implemented with planar filters. However a drawback that any filter in such technologies exhibit is its relatively higher Insertion Loss (IL) compared to waveguide and dielectric resonator filters, especially for narrow band applications due to the limited Q. Only recently work such as [54] have investigated possible dual-band features of waveguide technologies. On the other hand waveguide filters tend to be quite bulky, and as discussed earlier, DR filters have shown to offer significant high Q values with smaller size than waveguide filters. Therefore it is imperative that the DR technology be somehow used in the area of dual-band and multi-band filters to harness their high-Q feature.

To date very few work has been presented that realize dual-band filters in DR technology. Chen et al. proposed a tunable dielectric-resonator filter that happened to present a dual-passband behavior [58]. However, the observed dual-band characteristic of that dielectric-resonator filter was not explained and

investigated. Very recently, Zhang et al. [59] have shown a realization of a dual-band DR filter. The resonators were fabricated from high-K ceramic substrates. This was achieved by placing two physical dielectric resonators of different frequencies in a metal cavity. There are however some limitations in this design as we shall see more in chapter 4.

Several techniques have been used thus far to realize dual-band filters. Recent designs of these types of filters involve cross-coupled resonators, as in the single-band case. Coupling schemes, which generate transmission zeros between the bands, as well as in the upperband lower stopbands, have been presented. More compact realizations in dual-mode cavities were introduced in [56] and [57]. The design is based on a network of cross-coupled resonators in order to generate the required number of transmission zeros. The method has its own limitations mainly due to the sensitivity of the cross coupled topology. Recently [54] proposed the approach of using orthogonal modes of a rectangular (non-square) waveguide to realize the two bands of the dual-band filter.

2.10 Multiplexer Systems

Multiplexers are used in communication systems, and their primary goal is to either split a wideband frequency spectrum into a number of narrowband signals (RF channels), or to combine a number of RF channels into a single composite wideband signal. Depending on this splitting or combining feature, they are referred to as RF channelizers or RF combiners respectively. In addition, a two channel multiplexer can be used as a diplexer or duplexer, configured to separate the transmit and receive frequency bands in a common device. Multiplexers have many applications in satellite payloads, wireless systems, and electronic warfare (EW) systems. In all cases, multiplexers are realized with two or a collection of microwave filters, and possibly some additional components. Microwave filters are the main building block of any multiplexing system [1].

Figure 2-13 (left) shows a simplified block diagram of a typical satellite payload. The satellite payload in orbit acts as a repeater. It receives the uplink signal coming from earth, amplifies it using the HPA, and transmits it back to earth. Some practical constraints of the HPA require that the wideband signal received from the antenna be channelized, which is achieved using the IMUX or the input multiplexer. The amplified narrowband signals coming out of the HPA are then combined back using the Output MUX (OMUX), and transmitted back to earth via the common antenna. In satellite payloads IMUX and OMUX determine the characteristics of the RF channels and have significant impact on the performance of the payload. Typically a number required for the IMUX and OMUX network ranges from 48 to well over 100 [1].

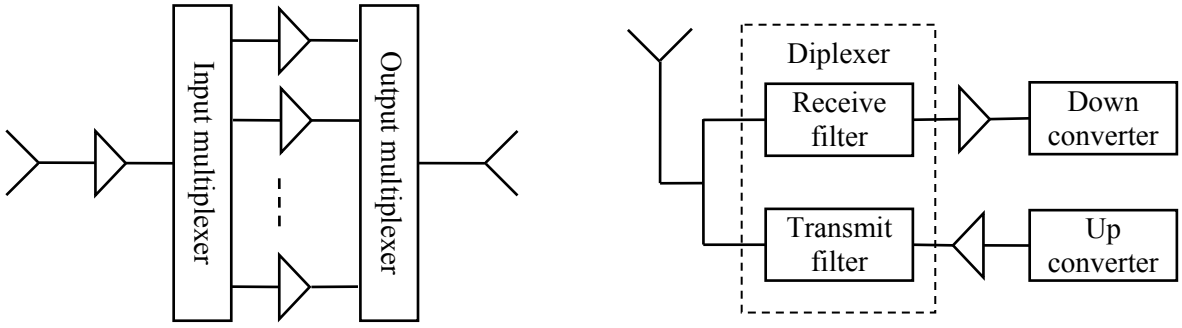

Figure 2-13: Simplified block diagram of (left) satellite payload and (right) base station front end [1].

Diplexers are used in wireless telephony base stations, operating in the worst climatic environments. A block diagram of a typical front end of a base station is shown in Figure 2-13 (right). The purpose of the receive filter is to reject the out of band interference prior to LNA and down conversion, and the transmit filter is placed after the HPA and used to the limit the out of band signals generated by the transmit chain.

Another application of multiplexers for wireless systems is when a wireless base station needs to transmit various frequency channels in different directions by using directive antennas. In such a case a multiplexer is needed to separate the overall band into separate channels. Another application is in cases where the base station needs to provide services to a number of independent operators that are licensed to operate only in specific channels within the frequency band covered by the base station. In EW systems, multiplexers are used in switched filter banks for wideband receivers [1].

There have been various advances since the 1970s in the area of multiplexers. Some of these works are [60]-[65]. Different techniques and schemes have been proposed over the years for multiplexing. The most commonly used multiplexing techniques are hybrid-coupled, circulator-coupled, directional filter, and manifold-coupled multiplexers. Table 2-1 from [64] provides a summary of comparison between the merits and disadvantages of these well known methods.

Table 2-1: Comparison among various multiplexer configurations [64]

	Hybrid Coupled MUX	Circulator Coupled MUX	Directional Filter MUX	Manifold coupled MUX
Advantage	+ Amenable to modular concept + Simple to tune, no interaction between channel filters + Total power in transmission modes as well as reflection mode is divided only 50% of the power is incident on each filter; power handling is this increased and susceptibility to voltage breakdown is reduced.	+ Requires one filter per channel + Employs standard design of filters + Simple to tune; no interaction between channel filters + Amenable to modular concept	+ Requires one filter per channel + Simple to tune, no interaction between channel filters + Amenable to modular concept	+ Requires one filter per channel + Most compact design + Capable of realizing optimum performance for absolute insertion loss, amplitude and group delay response
Disadvantage	- Two identical filters and two hybrids are required for each channel. - Line lengths between hybrids and filters require precise balancing to preserve circuit directivity. - Physical size and weight of multiplexer is greater than in other approaches	- Signals must pass in succession through circulators, incurring extra loss per trip - Low-loss, high power ferrite circulators are expensive - High level of Passive Inter-Modulation (PIM) products that in other configurations	- Restricted to realize all-pole functions such as Butterworth and Chebyshev - Difficult to realize bandwidths greater than 1%	- Complex design - Tuning of multiplexer can be time-consuming and expensive - Not amenable to a flexible frequency plan; i.e. change of a channel frequency would require a new multiplexer design.

DR filters, owing to their low-loss and comparatively less size, have tremendous applications for multiplexing systems, especially satellite applications. [23] originally proposed dual-mode DR filters employed for input multiplexers of satellite payloads. [65] implements a 3-channel multiplexer using a ridge waveguide manifold, and utilization of dual-mode and triple-mode DR filters. The design has size reduction, power handling, and good electrical performance for C-band output multiplexing applications. [63] also shows application of DR filters for multiplexers.

Chapter 3

Quadruple-Mode and Dual-Mode Dielectric Resonator Filters

3.1 Introduction

In this chapter two novel, compact, yet simple dielectric resonator filter types are presented. First a new quadruple mode dielectric resonator filter is presented, using a simple cylindrical structure. Secondly, a dual-mode half-cut dielectric resonator filter is presented and analyzed.

3.2 Quadruple-Mode Dielectric Resonator

A cylindrical dielectric resonator resonates with different mode distributions at different frequencies. Some of the lower order modes of a dielectric resonator are the TEH_{01} (TEH hereafter), HEH_{11}, HEE_{11} and TME_{01} modes. An example mode chart of a dielectric resonator was presented in previous chapter. Consider Figure 3-1 showing a portion of a typical DR mode chart. The chart shows change in resonance frequencies of the modes for different ratios of the Diameter (D) over height (L) of the structure. The results obtained are for a dielectric resonator placed in a cubic cavity of dimensions 1in x 1in x 1in. D is kept constant while L is varied.

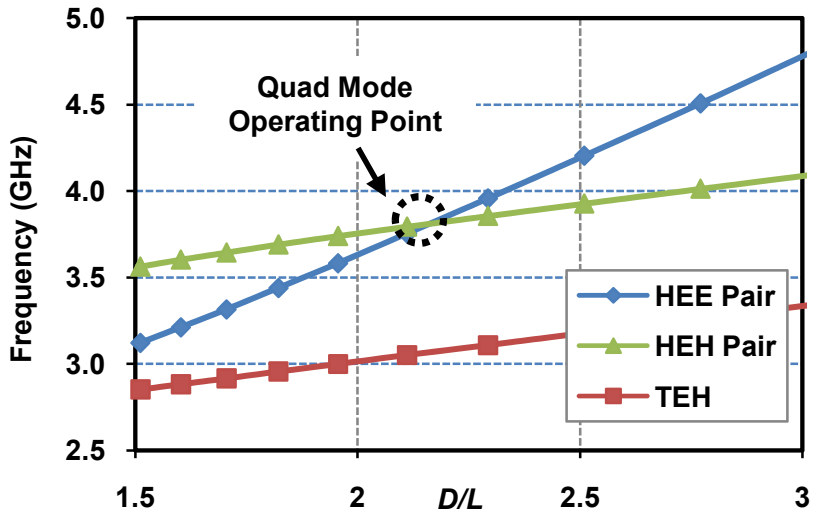

Figure 3-1: Mode chart of a cylindrical dielectric resonator. D = 17.78 mm, $\varepsilon_r = 38$, 25.4 mm x 25.4 mm x 25.4 mm cavity, L varying.

From the mode chart, we observe a very unique phenomenon for *D/L* ratios slightly higher than 2, designated in figure. At this ratio, the mode pairs of HEH_{11} and HEE_{11} coincide in resonant frequency. The idea of the quadruple-mode resonator is to size the cylinder at this ratio, such that four resonant modes (two pairs) are achieved all at the same frequency. Such cylindrical DR would then resonate in a quadruple-mode fashion. The top views of these four modes of interest are shown in Figure 3-2. Each mode pair has two orthogonal components rotated by 90 degrees.

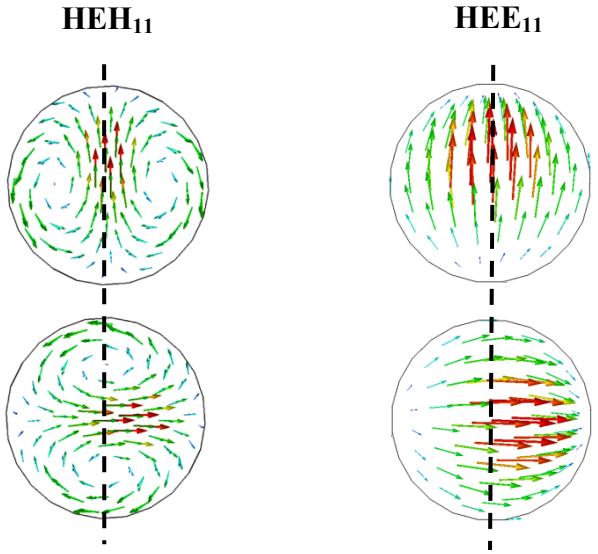

Figure 3-2: Top view of E field distribution of orthogonal mode pairs, (left column) HEH_{11} at the middle of the resonator and (right column) HEE_{11} modes. Each mode has two orthogonal components which are 90 degrees rotated. The components in top row have field lines parallel to the surface going into page designated by dashed line, while the bottom row components are perpendicular to the surface.

In view of the field distribution of the two modes, the E-fields of the four modes are concentrated such that they do not coincide with each other. This is theoretically supported as these modes are eigenmodes of the structure. The side view of Figure 3-3 helps better clarify this fact. The E field of HEH_{11} mode is mainly concentrated in the middle of the resonator, while that of the HEE_{11} mode is mainly concentrated at the top and bottom of the resonator. Thus, the four modes can coexist at the same frequency and be theoretically controlled independently. The resonator can be used as a building block for a "quad-mode" dielectric resonator filter, which yields a considerable size reduction.

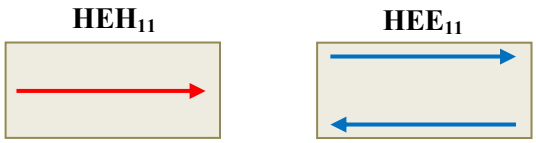

Figure 3-3: Side view of E-field of (left) HEH_{11} mode which is concentrated mainly near the middle and (right) HEE_{11} mode which is concentrated mainly at the top and bottom of the resonator.

To date cylindrical DRs have only been used as single mode and dual-mode resonators in filters. Here we are demonstrating that it is indeed possible to operate the same simple structure in a quadruple-mode fashion, by proper choice of the resonator dimensions. Generally a good starting point for finding the dimensions of the quad-mode resonator is $D/L\sim2$, with D found from models e.g. [12] or [13] , based on the desired center frequency and dielectric material. The dimensions are then refined and optimized using a full wave solver to yield the exact quad mode operating point.

3.3 Quad-Mode Dielectric Resonator Filter

In this work we demonstrate the first ever quadruple-mode dielectric resonator filters using the cylindrical resonator. The filters presented here are single cavity filters having four electrical resonators, yielding a 4-pole filter. In fact higher order filters, such as 8 or 4n pole filters (n integer) can be constructed using this building block. It should be noted that these resonators may also be combined with other types of resonators, in mixed mode filters.

A possible configuration for a four pole filter using the quad-mode resonator is shown in Figure 3-4. A cylindrical resonator of diameter D and height L is placed inside a cylindrical cavity of diameter D_c and height L_c. Probes are placed at X_p away from the center of the cavity and at 90 degrees from each other, extending from the top or bottom walls of the cavity. The 90 degrees separation is essential to excite the orthogonal modes. The length of the probes (H_p), as well as X_p, determines the amount of input/output coupling. Several tuning and coupling screws are placed as shown in the diagram, and their locations are justified as follows. The screws opposite each probe are for a combination of tuning and coupling of the two components of HEH_{11} and HEE_{11} that align with the probes. The screws positioned at 45 degrees are for coupling between the two orthogonal components of the mode pair. The vertical screws are located X_s away from the center of the cavity, penetrating into the cavity from the top or bottom walls. The horizontal screws extend from the side of the cylinder and are exactly equidistant from the top and bottom walls.

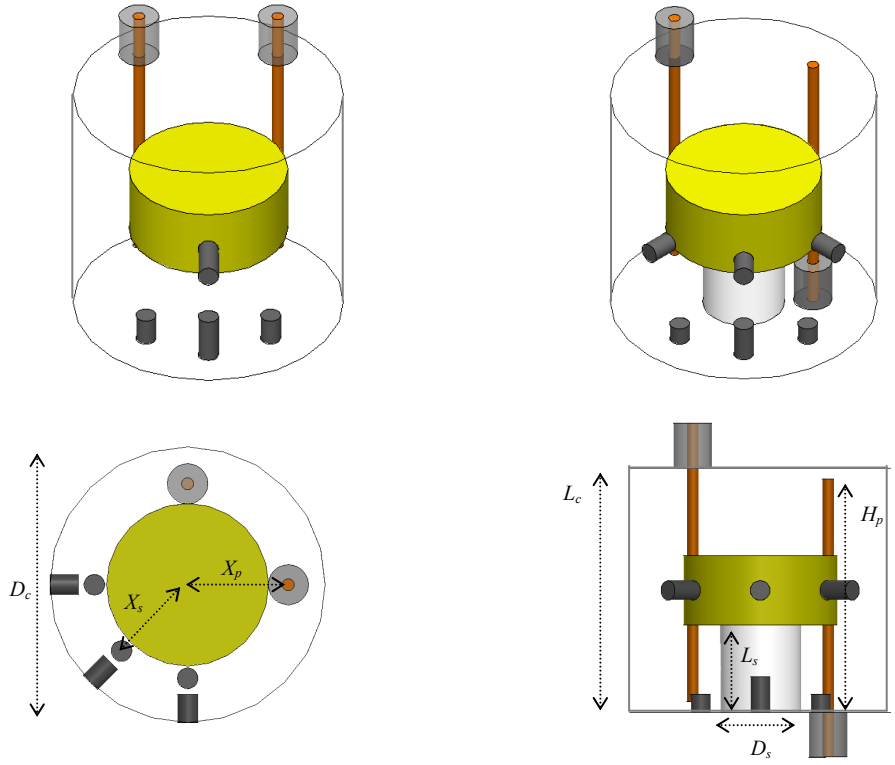

Figure 3-4: Structure of the quad-mode 4 pole filter with (top left) transmission zero on sub-passband frequency, D=17.145 mm, L=7.747 mm, D_c=29.15 mm, L_c=27.2 mm, X_p=10.57 mm, H_p=25 mm, and (top right) transmission zeros on both sides of passband, D=17.145 mm, L=7.747 mm, D_c=29.15 mm, L_c=27.2 mm, X_p=10.67 mm, H_p=26 mm, D_s=9 mm, L_s=9.73 mm. The dielectric resonator is centered in cavity for each case.

The first filter has the structure of Figure 3-4 (top left) and has a return loss = 10 dB, and fractional bandwidth of 1.35% with a centre frequency of 3.683 GHz. The response of the filter is shown in Figure 3-5. The whole structure was designed and simulated using Ansoft HFSS [46]. We can see a steep out of band rejection on one side of the passband, due to the existence of transmission zero.

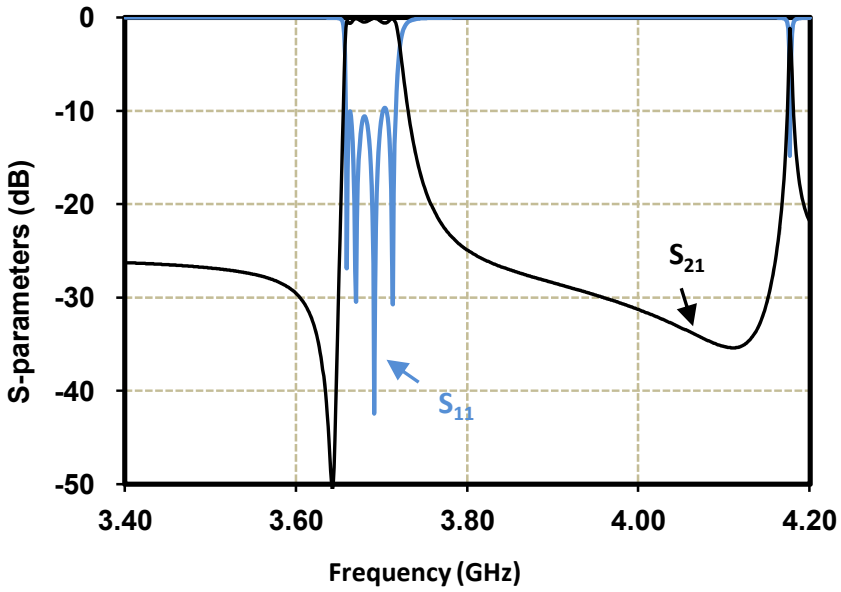

Figure 3-5: Simulated S-parameter response of 4-pole filter in Figure 3-4.

Due to the compactness of the filter and existence of cross couplings, we can realize different transmission zeros in this structure. In fact, if the same filter structure is used with the output probe now reversed in polarity as shown in Figure 3-4 (top right), we can achieve transmission zeros on both sides of the passband.

3.4 Quad-Mode Dielectric Resonator Filter Measurement Results

The structure in Figure 3-4 (top right) is used to design, simulate and fabricate the second four pole filter with return loss = 15 dB, center frequency of 3.666 GHz, and percentage bandwidth of 1%. The structure is similar to the previous example, with an addition of a low permittivity support of radius D_s and a height of L_s now holding the resonator centered in the cavity, and the polarity of the output probe reversed. The response of the filter is shown in Figure 3-6. It can be seen that there are transmission zeros on both sides of the passband in this case. A measured spurious free window of 480 MHz and an insertion loss varying between 0.4 dB to 0.6 dB over the passband is observed.

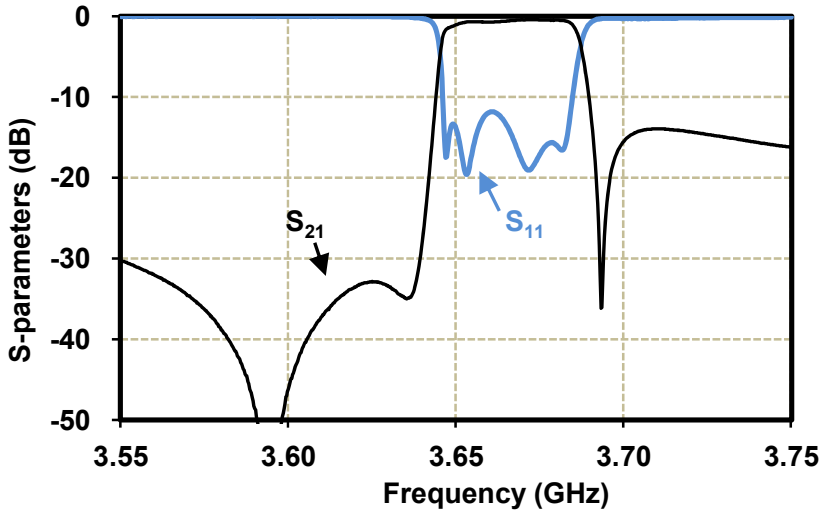

Figure 3-6: Measured S-parameter response of 4-pole filter of Figure 3-4 (top right).

The single cavity 4-pole filter configurations of Figure 3-4 both have direct coupling between the source and load, as the I/O probes are placed in the same cavity. This causes the out of bound rejection of the filter to deteriorate. This problem is actually alleviated in higher order filters. For example a two cavity 8-pole filter would have isolation between the two probes, as the input and output are placed in separate quad mode cavities. Another method is to design a six pole filter with one single cavity quad-mode resonator, and two single-mode cavities for I/O coupling.

The fabricated filter is shown in Figure 3-7. The dielectric is a Trans-tech Inc. cylindrical dielectric resonator, with supplier provided permittivity of $\varepsilon_r \approx 45.6$, and a loss tangent of 7.77×10^{-5} at 4 GHz. As shown in Figure 3-4 (top right), the dielectric resonator is mounted on a Teflon support with $\varepsilon_r \approx 2.1$. The cavity is made of Aluminum and ANSI 2-56 type screws were used for coupling and tuning. There are several sources of loss in this prototype that can be improved to yield the full potentials of the resonator to achieve higher Q. The losses in Aluminum walls, losses in Teflon support, losses in adhesive between resonator and support, and type of screws can be improved.

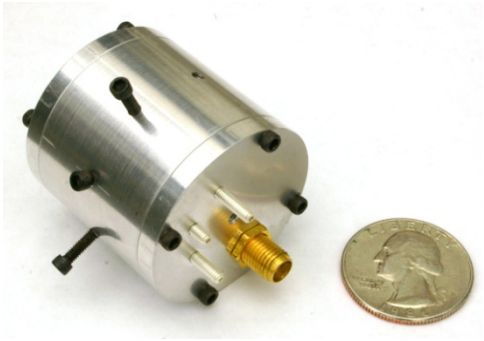

Figure 3-7: Fabricated quadruple mode filter.

3.5 Half-Cut Dielectric Resonator

The four-resonator full cylinder structure can be simplified to design a new class of dual-mode dielectric resonator filters. Consider a single component from the HEH_{11} and HEE_{11} modes that are aligned with each other, i.e. the two components in the top row of Figure 3-2. These modes have their E fields tangential (or H fields normal) to the plane going into the page, designated by the dashed line. The complete tangential E field suggests that a magnetic wall boundary condition placed over the surface of the plane, would not disturb these two mode components.

Therefore we can cut the cylinder in half, and still yield the same field distribution in the remaining half. This is because that by cutting the cylinder in half, a magnetic wall is effectively formed at the surface of the cut as shown in Figure 3-8. The magnetic wall formed by the cutting however is an imperfect magnetic wall. The "imperfect" wall means that the waves will have some leakage at the interface, which is due to the finite relative permittivity of the dielectric to air. This means that the half cut structure will resonate at a slightly higher frequency than before.

Figure 3-8: Formation of the half-cut dual-mode resonator from a quad-mode resonator. The sidewall is now an imperfect magnetic wall.

The additional orthogonal components of the degenerate HEE_{11} and HEH_{11} modes are shown in Figure 3-2 (bottom row). The cut will however remove these second components, since there would be no dielectric material to complete their path. In fact, these two components will be deformed to meet the new boundary condition at the magnetic wall. They become confined to a much smaller path, and are pushed much higher in frequency. The half-cut resonator will now have only two resonances close to the previous resonance frequencies.

The idea of the half-cut dual-mode resonator is to utilize these two new half modes resonating at the same frequency. The two half modes now require less size than their full cylinder counterparts; which is slightly more than half the size they originally occupied in the quad-mode resonator. We refer to these two operating modes of interest as $½HEH_{11}$ and $½HEE_{11}$. This is somewhat a simplification to the quad-mode resonator concept discussed earlier, but utilizes similar operation principal. The modes are shown in Figure 3-9.

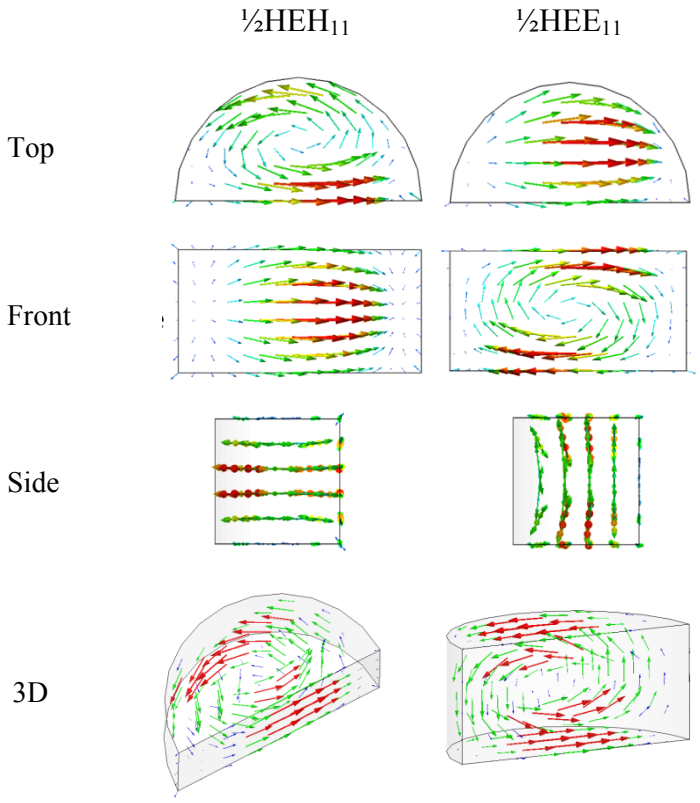

Figure 3-9: Views of the E field distribution of (left column) $½HEH_{11}$ and (right column) $½HEE_{11}$ modes of the half cylinder dielectric resonator. The modes are orthogonal.

In [39] a single-mode resonator was reported using a half-cut structure which allowed some size reduction. This work demonstrates that by properly sizing the half-cut resonator, a dual-mode resonator can exist in the half-cut structure, therefore allowing further size reduction.

3.6 Dual-Mode Half-Cut Dielectric Resonator Filter

In order to realize any filter function with specific bandwidth and return loss, one would need to have full control over the resonance frequency, the amount of inter-resonator couplings, and the amount of input output/couplings. The following discusses how full control of these parameters is achieved using the half-cut resonator as a building block.

3.6.1 Center Frequency Control

Given a half cylinder with dielectric material with dielectric constant ε_r in free space, there exists one unique value for *D* and *L* that results in the desired (½HEH$_{11}$, ½HEE$_{11}$) dual-mode resonance. Since the two modes are eigenmodes of the structure, they are orthogonal, and can coexist at the same frequency without coupling.

To design a dual-mode cavity the operating modes must resonate at the same frequency equal to the centre frequency of the filter. Qualitatively, the frequency of the ½HEH$_{11}$ is mainly dependent on the circulating electrical path of the E field in the half circle cross section seen in top view of the left column of Figure 3-9. The ½HEE$_{11}$ mode however is mainly circulating in an orthogonal fashion to the ½HEH$_{11}$, and its resonance frequency is mainly dependent on the size of the rectangular shape of the cut seen in front view of right column in Figure 3-9. Therefore the sizing of the diameter strongly affects the frequency of ½HEH$_{11}$ and the height strongly affects the frequency of ½HEE$_{11}$. Other views clarify the orthogonality of the modes. Figure 3-10 shows a new mode chart for the half-cut resonator. Here the diameter of the half cylinder is kept constant, and the height (*L*) is varying. It can be seen that a change in *L* has a more significant impact on the resonant frequency of the ½HEE$_{11}$ mode.

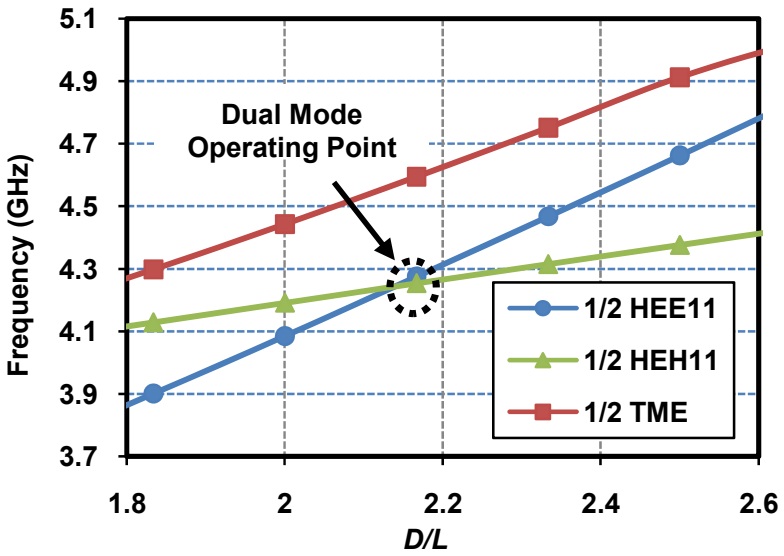

Figure 3-10: Mode chart of a half-cut cylindrical dielectric resonator, D = 17.78 mm, $\varepsilon_r = 38$, 25.4 mm x 25.4 mm x 25.4 mm cavity, L varying.

Analytic models and mode charts, refined with full wave solvers may be used to arrive at the exact dimensions for the dual mode resonator. In general a good starting point is $L \approx D/2$, and D determined from the models, e.g. [12], for the frequency of operation. Qualitative justification of this relation is seen in views of Figure 3-9. The two orthogonal modes would almost have the same circulating electrical path if the height and radius of the resonator are equal.

3.6.2 Intra-Cavity Coupling

As each cavity contains two resonators, a controllable intra-cavity coupling scheme is required. An effective coupling mechanism supporting various coupling amounts between the two orthogonal modes is a metal screw or rod placed as shown in Figure 3-11, designated by Screw 1. The screw attracts fields of one mode and causes it to leak to the other mode.

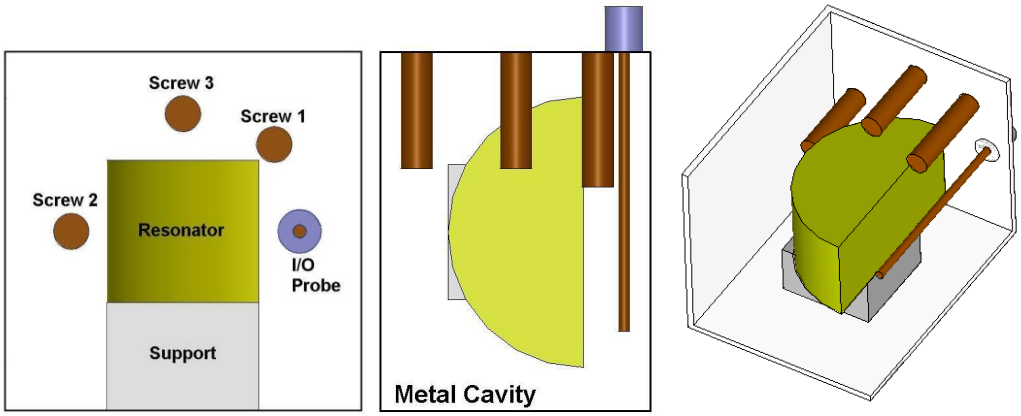

Figure 3-11: (left) front view and (right) top view and (right) 3D view of the dual mode cavity with coupling and tuning mechanisms. Screw 1 for intra-cavity coupling, Screw 2 for tuning of ½HEH$_{11}$, and Screw 3 for tuning of ½HEE$_{11}$. The I/O probe placement as shown only couples energy to ½HEH$_{11}$.

Various parameters such as distance of the screw from the edge of the resonator, length and diameter of screw have effect on the coupling amount. Using an eigenmode solver, the cavity, dielectric resonator and coupling screw are simulated together, and the first two resonant frequencies are found. The coupling coefficient, *k*, is given in [1] by:

$$k \approx \frac{f_2 - f_1}{f_2}. \qquad (1)$$

By sweeping the design variable (e.g. screws size), the desired coupling is interpolated. For cases where strong coupling values are required, it is usual for the screw length to become considerably long, especially considering that the fields of the modes are strongest near the middle of the resonator. If the coupling screw is extended from the sidewall as shown in Figure 3-11, it could give rise to unwanted propagation and resonance of coaxial mode in the cavity close to the filter centre frequency. This unwanted resonant frequency is dependent on the length of the screw being approximately equal to quarter of wavelength. To overcome this issue, a dielectric-metal screw can be used instead, avoiding contact of the metal screw to the cavity walls.

3.6.3 Inter-Cavity Coupling

An effective method for inter-cavity coupling is to use polarization discriminant irises in the cavity walls. For coupling of the ½HEH$_{11}$ mode, a vertical iris is required, as shown in Figure 3-15. A

horizontal iris however couples the ½HEE$_{11}$ mode. This is somewhat intuitive when considering the iris as a waveguide under cutoff, passing mainly one polarization of field. In either case, parameters such as width, thickness and length of iris determine amount of coupling.

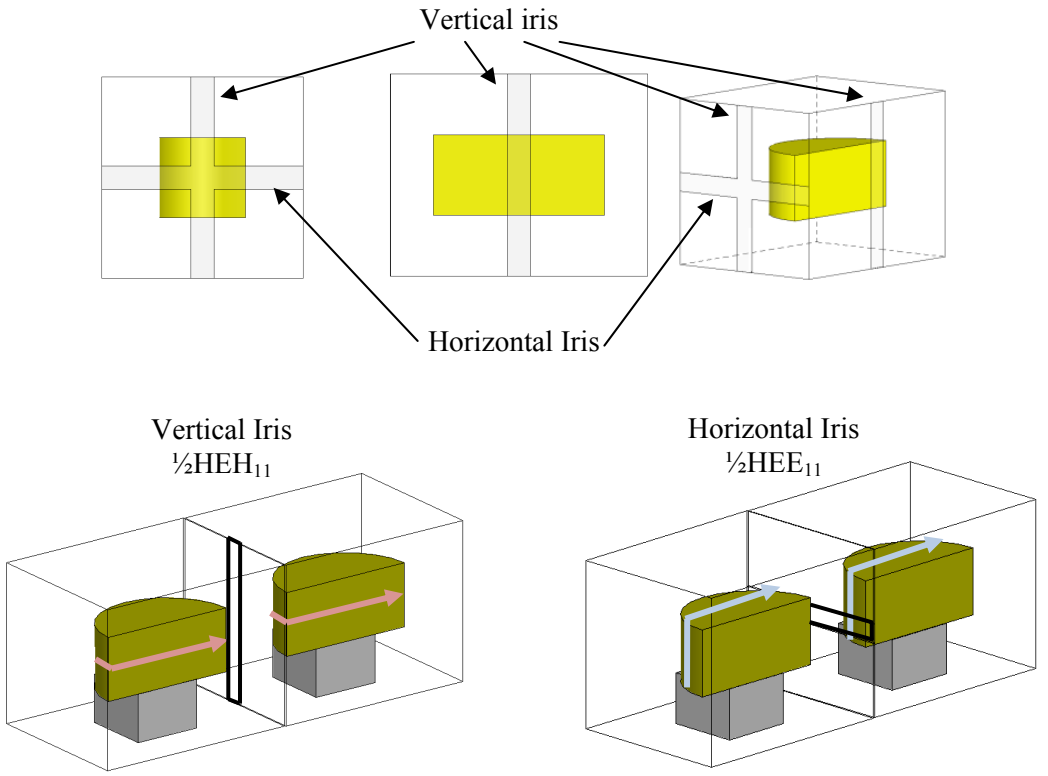

Figure 3-12: (top row) Orthogonal coupling irises (bottom row) coupling of modes through their corresponding iris.

The coupling coefficient can be computed using either the S-parameter method [1], or by finding eigenmodes and using (1), or alternatively using a symmetry plane placed in the middle of the iris, finding the even and odd (f_e, f_m) resonances of the mode coupled, and from [1] using the formula

$$k = \frac{f_e^{\,2} - f_m^{\,2}}{f_e^{\,2} + f_m^{\,2}} . \qquad (2)$$

Figure 3-13 shows the variation of the coupling amounts for different iris widths of a vertical iris. It can be seen that the vertical iris significantly controls the amount of coupling of the ½HEH$_{11}$ mode, while keeping the coupling of the ½HEE$_{11}$ almost constant over the range. A similar graph can be plotted for the horizontal iris showing almost independent coupling of the ½HEE$_{11}$.

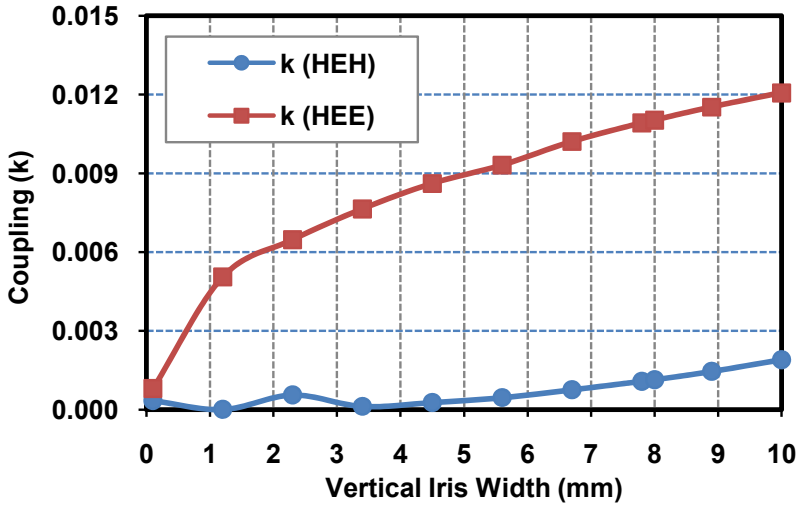

Figure 3-13: Variation of the HEH and HEE coupling amounts as a function of vertical iris width (HEH coupling iris). Vertical iris allows HEH coupling while minimizing HEE coupling.

Figure 3-14 shows realizable filter topology configurations with the two cavities (4 resonators) and I/O. We can realize cross-couplings between non-adjacent resonators, e.g. between 1 and 4 in Figure 3-14 (left). These cross-couplings are shown with dashed lines. These couplings are useful in realizing advanced filtering functions, with controlled prescribed transmission zeros.

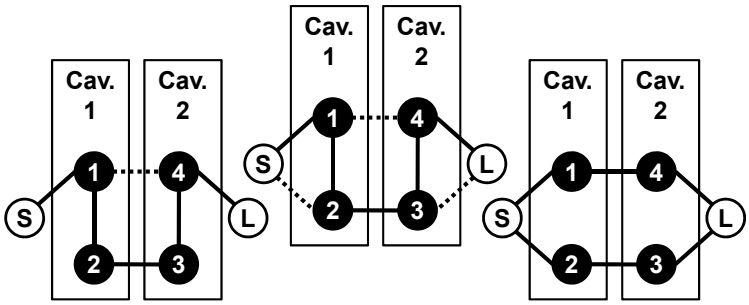

Figure 3-14: Advanced coupling methods between two cavities and Source/Load. (left) the folded formation containing a Cascade Quadruplet (middle) folded with multiple input/output (right) parallel connected two branch lines.

In Figure 3-14 (left), the familiar folded filter is realized. In fact, the four resonators and their couplings, is in essence a Cascade Quadruplet (CQ) formation similar to [8]. This formation of couplings of four resonators can be used to construct asymmetric dual-mode filters similar to those realized in [8],

with the aid of cross polarized irises.

To construct 2n pole filters (n integer), either configuration of Figure 3-15 (top row) or (bottom row) can be used. For example in the top row of Figure 3-15, we see that the four cavities are arranged in a straight configuration. Note that two CQs, i.e. (1,2,3,4) and (5,6,7,8), can be realized if desired. Moreover, the filter arrangement can also be turned as shown in the bottom row of Figure 3-15. Here resonators 4 and 5 would need to be of the ½HEH$_{11}$ type, to allow for the coupling through the side wall via a vertical iris. Resonators 3 and 6 would then have almost zero coupling. In the turned configuration, aside from the CQs formed between (1,2,3,4), and (5,6,7,8), more cross couplings can be realized by introducing another vertical iris between the cavities that contains resonators 1 and 8 (both ½ HEH$_{11}$), again through a vertical iris.

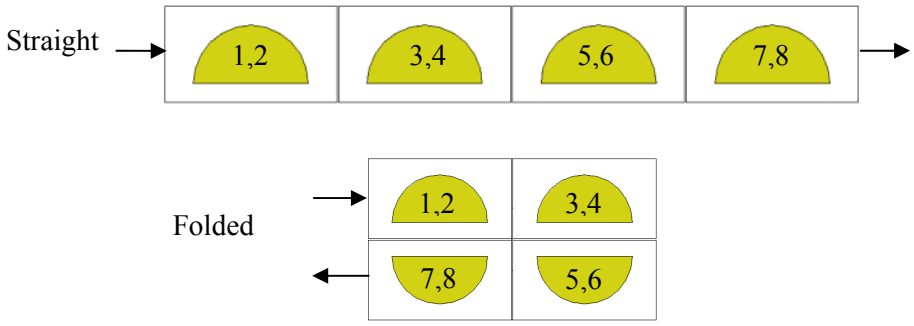

Figure 3-15: 8-th order filter with (top row) straight arrangement of resonators and (bottom row) folded arrangement of same resonators.

Negative coupling values in the coupling matrix can be realized by proper selection of the relative location of coupling screws and irises. For example, consider the inter-cavity coupling from ½HEE$_{11}$ mode (blue/dark) to ½HEH$_{11}$ mode (white), shown in Figure 3-16 (left), and assume that the designated orientation of circulation occurs for these two modes as a consequence of the coupling. Now if Screw 1 in the figure is moved to the other edge of the resonator, as in Figure 3-16 (right), the leakage of the mode from ½HEE$_{11}$ to ½HEH$_{11}$ will be to the opposite side, and causes a reverse circulation of the ½HEH$_{11}$ compared to the previous case. This means, that if a second cavity is now placed in conjunction with this cavity, the coupling between the two ½HEH$_{11}$ modes (through vertical iris) can be chosen as positive or negative, depending on the screw locations chosen in each cavity.

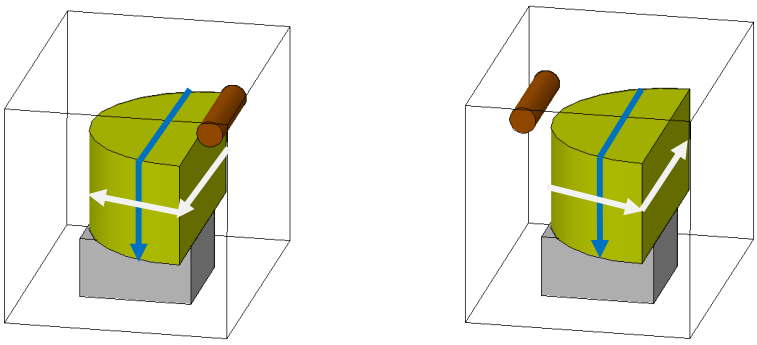

Figure 3-16: Reversing the circulation of the coupled mode by changing coupling screw location. The coupling is from ½HEE$_{11}$ (solid blue) to ½HEH$_{11}$ (white).

3.6.4 Input coupling

Input coupling to the filter is realized using either coaxial probes or waveguides. Length of probe and its distance from the resonator, allow for realization of various input coupling values. A probe placed as in Figure 3-11 would only couple energy to the ½HEH$_{11}$ mode, as the other mode is orthogonal. In fact the probe can be placed such that the energy is coupled to both modes simultaneously, realizing the input coupling scheme shown in Figure 3-14 (center and right). For waveguide coupling, either a horizontal or vertical iris is used to couple to the desired mode, with the appropriate iris size, as shown in Figure 3-17. A slanted iris or using both irises together allows for a concurrent coupling of energy to the first two resonators.

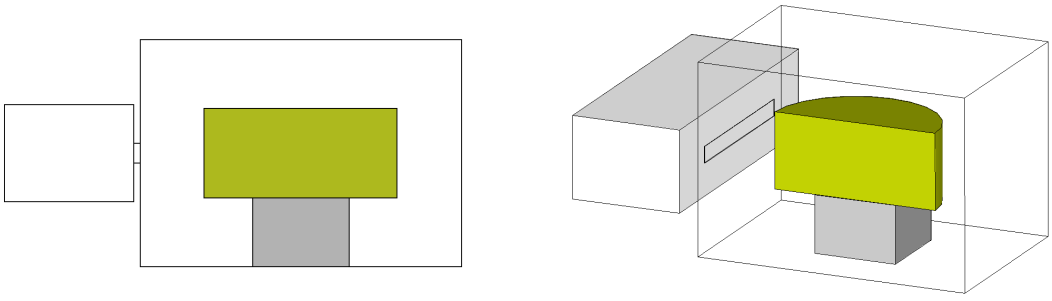

Figure 3-17: Waveguide input coupling using iris. Horizontal iris couples energy to ½HEE$_{11}$ mode.

The input coupling can be calculated by simulating the coupling structure and finding the maximum of the group delay, τ_{max}, which occurs at the center frequency. This techniques is described in [1]. τ_{max} is related to the angular frequency $\omega_0 (=2\pi f_0)$, and Q_e according to

$$\tau_{\max} = \frac{4Q_e}{\omega_0} \quad (3),$$

and Q_e is in turn related to the input coupling resistance R_1, center frequency f_0, and bandwidth BW, according to

$$Q_e = \frac{f_0}{BW \times R_1} \quad (4).$$

3.6.5 Tuning

Since exact sizes with ceramic resonators are normally hard to achieve, along with deviations in supplier's dielectric constant, and other fabrication tolerances tuning of center frequencies of resonators is essential [1]. Metal screws parallel to the main sides of the resonator provide considerable tuning range. In the configuration shown in Figure 3-11, Screw 2 tunes ½HEH_{11} and Screw 3 tunes ½HEE_{11}. They tune the modes almost independently, due to orthogonality of modes.

3.7 Half-Cut Dielectric Resonator Filter Measurement Results

The practicality of the previous discussions is demonstrated by two filter examples. Each filter has a 25 dB return loss, 4-pole (two cavities), and 1% bandwidth filter. The discussed methods were used in the design along with Ansoft HFSS. The chosen centre frequency was based on available material in our lab, and design at other microwave frequencies is equally possible.

3.7.1 Basic Half Cut

The first filter was designed using the basic half-cut cylinder resonator for the center frequency of 2.513 GHz, and two transmission zeros at 2.359 GHz and 2.597 GHz. The N+2 coupling matrix of the filter is

$$M = \begin{pmatrix} 0 & 1.141 & 0.051 & 0 & 0.003 & -0.001 \\ 1.141 & -0.060 & 1.056 & 0 & 0.054 & 0.003 \\ 0.051 & 1.056 & 0.074 & 0.783 & 0 & 0 \\ 0 & 0 & 0.783 & 0.074 & 1.056 & 0.051 \\ 0.003 & 0.054 & 0 & 1.056 & -0.060 & 1.141 \\ -0.001 & 0.003 & 0 & 0.051 & 1.141 & 0 \end{pmatrix} \quad (3).$$

The simulated structure is shown in Figure 3-18. The resonators were cut from ceramic disks with $\varepsilon_r \approx 38$ and supplier provided approximate loss tangent of $5\text{x}10^{-5}$ at 2.5 GHz, mounted on a Teflon based support with $\varepsilon_r \approx 2.1$, and Aluminum metal enclosures and iris. The ceramic resonators were cut using waterjet cutting, a low cost, simple, and accurate method. The advantage of using waterjet cutting is that chipping of the ceramic hardly occurs, making it a very favorable solution for shaping dielectric ceramics. Breaking or chipping of the ceramic, especially at the edges, is a common problem when using other machining techniques.

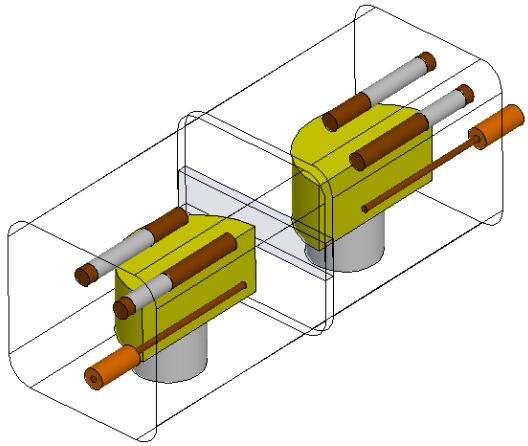

Figure 3-18: Simulated structure of the dual-mode half-cut four-pole filter.

S-parameter measurement results for the first filter using the basic half cut resonator are shown in Figure 3-19, and the group delay over the passband is shown in Figure 3-20. An insertion loss of less than 0.26 dB was measured in passband.

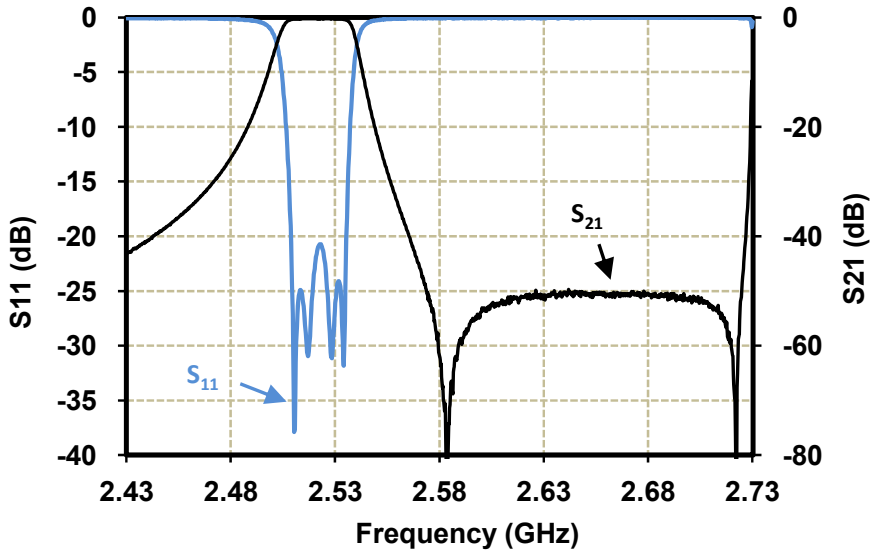

Figure 3-19: Measured S-parameter of four pole filter with half cut resonator. Resonator has dimensions *D*=30 mm, *L*=13.9 mm, and is centered in a 35 mm x 35 mm x 45 mm cavity.

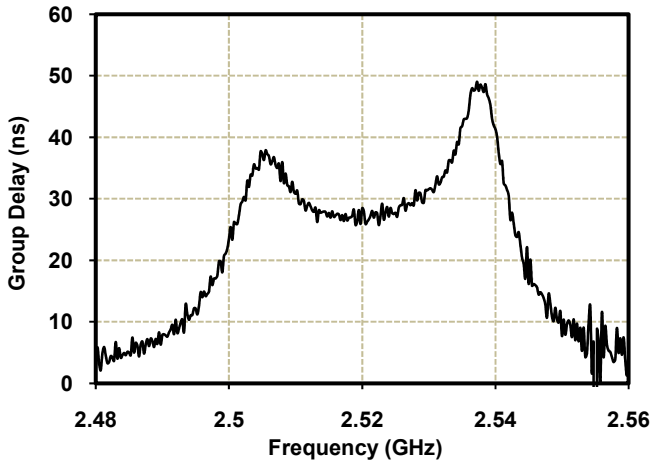

Figure 3-20: Group delay of filter with half-cut resonator derived from S-parameters measurements.

The fabricated filter is shown in Figure 3-21. Several sources of loss exist including loss in the Teflon support, Aluminum walls, lossy adhesive between resonator and support, etc., which can be improved to reach the full potential of the resonator.

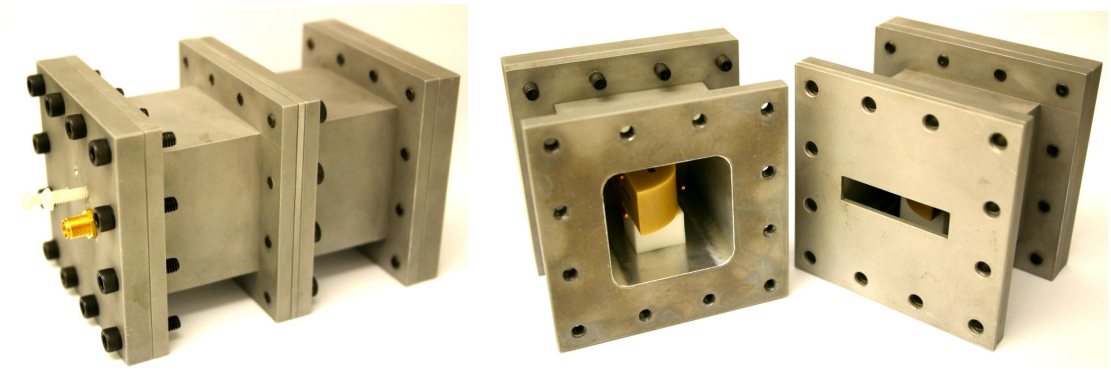

Figure 3-21: Fabricated four pole filter with basic half-cut resonators.

3.7.2 Spurious Improvement

An advantage of the proposed dual-mode half-cut structure over traditional HEH_{11} dual mode filters [23] is that there is no lower resonance (i.e. TEH) than the operating modes. The higher resonant modes are the spurious. Since we are using a $D/L \approx 2$, the spurious seen in Figure 3-19 is closer than a traditional HEH_{11} filter of [23]. We can remove this spurious by placing through way slots to terminate the path of E field for the higher resonances. Using these slots, the frequency of the ½HEH_{11} and ½HEE_{11} is not affected significantly, as their E field is tangential to the slots. The two spurious modes that are removed are shown in Figure 3-22. Depending on the amount of spurious free windows that are acceptable, one or two slots may be used.

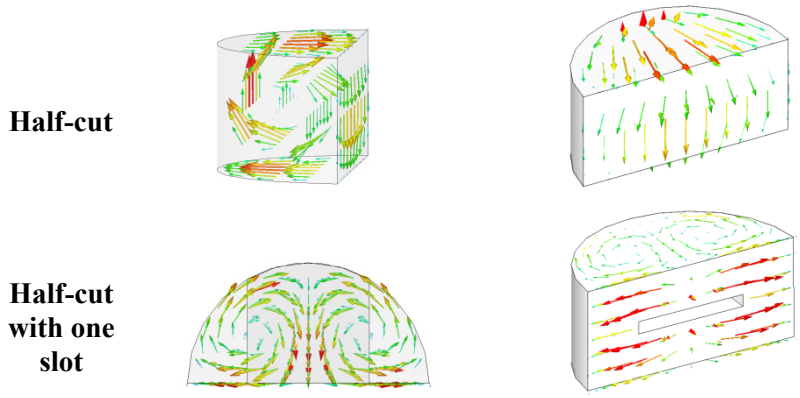

Figure 3-22: Views of the next highest resonant mode (spurious resonance) for, (top row) the basic half cut and (bottom row) half-cut with one horizontal slot.

The second filter fabricated uses a resonator shown in the inset of Figure 3-23. Response in Figure 3-23 shows how the spurious free window is improved to about 600 MHz for center frequency of

2.7 GHz. The fabricated filter is shown in Figure 3-24.

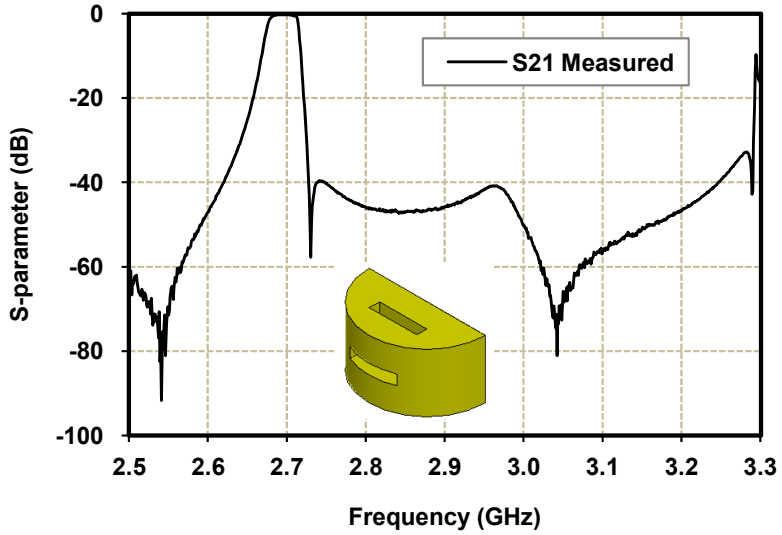

Figure 3-23: Measured S-parameter of four pole filter with improved spurious. Spurious free window is increased to 600 MHz for center frequency of 2.7 GHz. The filter uses resonators with two through way slots as shown in inset. *D*=30 mm, *L*=13.9 mm, Cavity 35 mm x 35 mm x 45 mm, slot width 2 mm, slot length 11 mm.

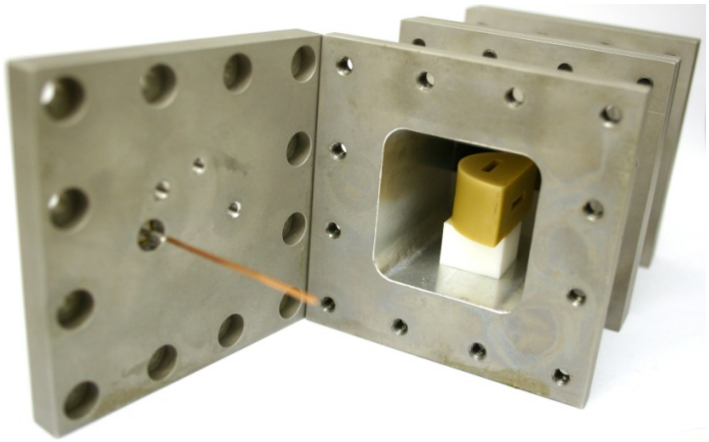

Figure 3-24: Fabricated 4 pole (two cavity) filter.

3.8 Comparison

This section discusses the size reduction and tradeoffs achieved by using the two filter types presented in this chapter. The benchmark for comparison of the dual-mode half-cut resonator is the traditional HEH_{11} dual-mode filter of [23], as it is the best solution known to date for dual-mode operation of DR filters.

3.8.1 Quad-Mode Filter

The size reduction achieved with the proposed quad-mode filter is significant. Compared to a single mode TEH, ¼ of the cavities are required, and compared with traditional HEH dual-mode filters, ½ as many cavities are required.

The modes used, are the HEH_{11} and HEE_{11} mode pairs. For example, we consider a quad-mode resonator at 3.751 GHz, with loss tangent of 7.77×10^{-5}, and $\varepsilon_r = 38$, inside a Copper cylindrical cavity. A D = 17.145 mm, L = 7.468 mm, D_c = 29.15 mm, and L_c = 25.4 mm, yields the four resonant modes close to 3.751 GHz. The Q of each mode as calculated from the eigenmode solver of Ansoft HFSS is shown in Table 3-1. It can be seen that the two HEH_{11} mode components have a higher Q than the HEE_{11} mode pair, which is due to the nature of the modes. This means that the total dielectric losses of one quad-mode resonator, is slightly higher than the total losses of two cylinders working in the traditional HEH_{11}. The latter would only use modes 3 and 4 of the table. Note the first mode of the resonator is actually the TEH mode which is not shown in the table.

Table 3-1: f_0=3.751 GHz, $\varepsilon_r = 38$, Loss Tangent = 7.77×10^{-5}, Copper Cavity

	Resonance Frequency (GHz)	Q (eigenmode solver)
Mode 1	3.7505	11918
Mode 2	3.7505	11918
Mode 3	3.7517	13519
Mode 4	3.7517	13519

3.8.2 Half-Cut vs. Traditional HEH Dual-Mode Filters

The proposed dual-mode half-cut dielectric resonator filter allows easy planar mounting, and uses less lateral space than planar mounted HEH_{11} filters [18], making it both a stable and compact

solution. Table 3-2, shows a comparison between the proposed cavity and a planar mounted HEH_{11} cavity [23], designed for the same spurious performance. It is seen that close to 50% size reduction is achieved by the proposed design, at the expense of some reduction in Q. When comparing the resonators, there are three factors that need to be considered, the volume of the cavity, the Q of the resonators, and the spurious free window. Therefore in order to make a fair comparison, one parameter (spurious) is kept equal, while the other two are analyzed. The benchmark is designed based on optimum parameters reported by Zaki et al. in [28]. We see that size reduction is achieved at the expense of some Q. but the question arises, is the size reduction achieved worth the trade-off of Q. This question is best answered by looking at the fourth row of Table 3-2, showing the Q/Volume metric of the two resonators. It is clearly seen that a much better trade-off is achieved between Q and volume using the half-cut structure, compared to the traditional full cylinder dual-modes.

In another comparison, if cavities were to have equal Q by reducing size of the traditional HEH_{11} cavity, not only is the spurious of the HEH_{11} cavity is too close making it unusable, the HEH_{11} cavity will still be 20% larger.

Table 3-2: Comparison at 4GHz, $\varepsilon_r = 38$, Q_u=12250, Copper Cavity.

	Traditional HEH_{11} dual-mode resonator	Proposed half- cut dual-mode resonator
Cavity volume	14.3 cm^3	6.86 cm^3
Spurious free window	750 MHz	790 MHz
Q (eigenmode)	11450	8200
Q/Volume	801 cm^{-3}	1196 cm^{-3}

3.9 Conclusions

We have demonstrated the first ever quadruple mode dielectric resonator using a cylindrical structure. We also presented the half-cut dual-mode dielectric resonator filter derived from the quad-mode resonator. These structures are shown to achieve significant size and mass reduction, compared to existing dielectric resonator filter technologies. They are shown to be versatile and are strong contenders for high Q filter applications.

Chapter 4
Dual Band Dielectric Resonator Filters

4.1 Introduction

In this chapter we introduce a new type of dual-band filter, which is realized using dielectric resonators. The structure used is the half-cut DR. The structure is shown to be versatile in terms of supporting two separate bands with full control over the fractional bandwidths and center frequencies of the two bands. Frequency control, inter-resonator and input coupling schemes of each band are discussed. Moreover, it is demonstrated that owing to the unique formation of modes in the structure, a simple separate filter design for each band can be carried out. Different order filters are designed and measurement results are presented, validating the practicality of the proposed structures.

4.2 Half-Cut Resonator and Cavity

The half-cut DR structure was introduced in Chapter 3 as the building block of a new class of dual-mode DR Filters. The half-cut structure is made from cutting a cylindrical DR of high ε_r (~ 30-50, typically ceramic) into half along its axis, as shown in Figure 4-1 The DR is planar mounted on a support of low ε_r inside a metal enclosure, either in an upright, or a mushroom type configuration.

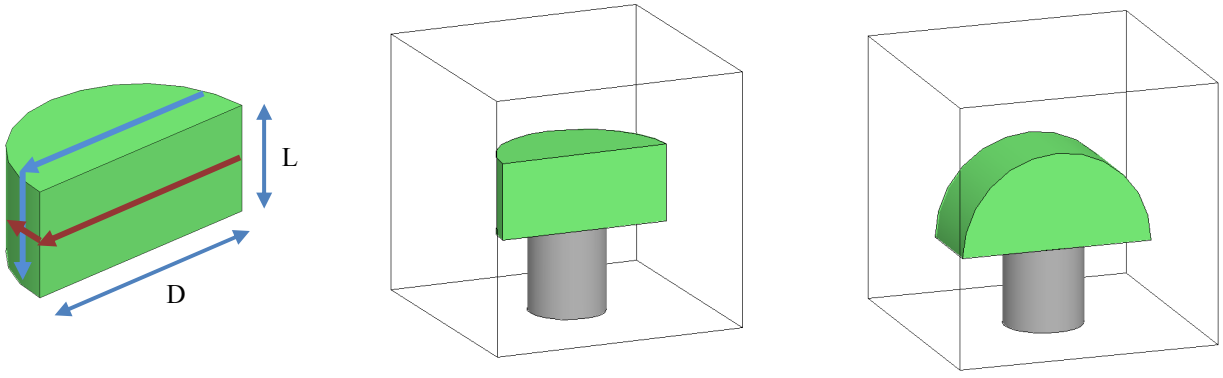

Figure 4-1: half-cut DR (left) placed inside a metal cavity (middle) upright and (right) mushroom type configuration.

The dual-mode cavity in Chapter 3 uses the two orthogonal modes ½HEE$_{11}$ and ½HEH$_{11}$. These

modes are one half of a single component of modes from their full cylinder counterparts. In Chapter 3 the two modes were made to resonate at equal frequency, by proper sizing of the resonator's diameter (D) and height (L). A ratio of *D/L~2* roughly yields equal frequency resonances.

4.3 Dual-Band Dielectric Resonator

The two ½HEE$_{11}$ and ½HEH$_{11}$ modes of interest can be made to resonate at different frequencies. This is the basis of the dual-band filter presented in this chapter. The idea is to implement each band of the dual-band filter, on one of these two operating modes. An analogous concept in [54] is utilized for realizing dual-band waveguide filters.

We saw that by using different D/L ratios, f_H the resonant frequency of the ½HEH$_{11}$, can become less than or greater than f_E, the frequency of ½HEE$_{11}$ mode. Qualitatively, starting from f_H=f_E (i.e. *D/L~2*), if L is reduced, f_H remains almost unchanged, while f_E is increased. On the other hand, decreasing D pushes f_H higher in frequency, while having less effect on f_E. This behaviour was visually justified by inspecting the path of the E field of modes shown in Figure 3-9. Hence it is possible to achieve a single cavity loaded with a single half-cut resonator that has two different frequency orthogonal resonances.

In dual-band filters, it is required to have the capability of separate and different bandwidths at different center frequencies. Based on filter theory, this means it is required to have separate control over 1) the amounts of input/output coupling to each band, 2) inter-resonator couplings of each band, and 3) center frequencies of resonators in each band. This section discusses how these requirements are met.

4.3.1 Center Frequency Control

The center frequency of the two bands is dictated by the resonant frequency of the two modes. In the mode chart of the half-cut DR shown in Figure 4-2, the amount of frequency separation of the two modes for different *D/L* ratios is presented. It can be seen that various frequency separation between the two bands can be supported with the structure. The two modes can be equal frequency, or be at different frequencies, by increase or decrease of *D/L*. Here we see two regions of dual-band operation. Choosing which size ratio mainly depends on availability and ease in fabrication of cylinders with certain aspect ratios over other ratios. In this work we normally choose *D/L* > dual-mode point. That is the region to the right of the dual-mode operating point in the mode chart of Figure 4-2. In this configuration the ½HEH$_{11}$ mode is resonating at a higher frequency than the ½HEE$_{11}$ mode. Hence the lower band of the filters presented here are realized with the ½HEE$_{11}$ mode, and the higher band with ½HEE$_{11}$.

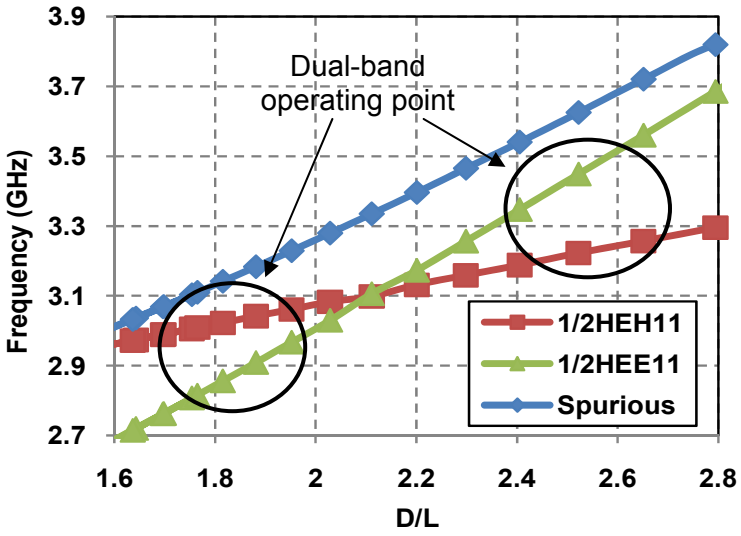

Figure 4-2: Mode chart of a half-cut DR, ε_r=45, D=0.9in, L_d varying.

In order to arrive at the desired frequencies for the two bands, mode charts and approximate models similar to [12] can be used to find a starting point for dimensions of the structure, and then simulated and corrected with full-wave solvers.

4.3.2 Inter-resonator Coupling

Similar to the dual-mode half-cut filter, utilizing polarisation discriminant irises as shown in Figure 4-3 allows for independent control of inter-resonator coupling in each band. Here we have the simultaneous presence of the horizontal and vertical iris, enabling almost independent coupling of the ½HEE$_{11}$ and ½HEH$_{11}$ modes respectively. Aside from using two orthogonal irises, one slanted iris may also be used to couple the both modes simultaneously.

The coupling amount can be calculated by simulating the two resonators and coupling irises together. By finding the frequency of the first four eigenmodes of the full coupling structure, the coupling amounts of the first and second band, k and k', is

$$k \approx \frac{f_2 - f_1}{f_2},$$

$$k' \approx \frac{f_4 - f_3}{f_4} \qquad (1).$$

Alternatively, to reduce computation, a symmetry plane can be placed half way between the two cavities and in the middle of the irises, to calculate the odd and even mode resonances [1]. The coupling amounts in this case would be

$$k = \frac{f_e^{\,2} - f_m^{\,2}}{f_e^{\,2} + f_m^{\,2}},$$

$$k' = \frac{f_e'^{2} - f_m'^{2}}{f_e'^{2} + f_m'^{2}} \qquad (2).$$

In either case the physical dimensions of the two irises; width, height and thickness, are determining factors on amount of coupling.

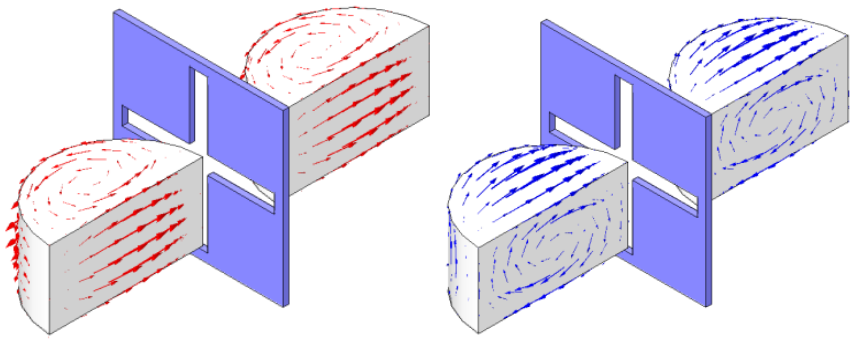

Figure 4-3: Polarization discriminant irises for coupling of the orthogonal modes between cavities. (Left) coupling of ½HEH$_{11}$ through vertical iris, and (right) coupling of ½HEE$_{11}$ through horizontal iris.

4.3.3 Input/Output Coupling

On contrary to the dual-mode filter of Chapter 3, in the dual-band filter, we need simultaneous input coupling to the two resonances of the half-cut resonator. The input and output coupling of the filter can still be easily realized using one probe. The location of the probe as well as its length determines the amount of coupling to the first and last resonator of each band. As shown in Figure 4-4, a probe placed parallel to one of the edges of the DR allows for simultaneous coupling to both the ½HEE$_{11}$ (dashed blue) and ½HEH$_{11}$ (solid red) modes. Moving the probe closer to one mode and farther from other increases one

coupling and decreases the other, while moving the probe diagonally away from both modes decreases the coupling simultaneously.

Similarly to the dual-mode resonator, we can use the maximum of group delay method to determine and quantify the amount of input coupling to the two bands simultaneously.

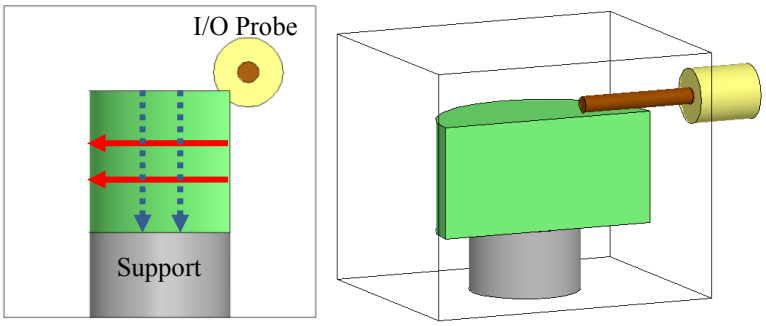

Figure 4-4: Input/Output coupling probe with simultaneous coupling to both ½HEH$_{11}$ (solid red) and ½HEE$_{11}$ (dashed blue) modes.

If the desired method of input connection to the filter is waveguide coupling rather than using probes, similar polarisation discriminant irises discussed previously can be used to couple energy to the first/last cavity, simultaneously to the two modes. Again, the physical dimensions of the iris determine the amount of coupling to each mode.

4.3.4 Spurious Enhancement

The spurious performance of the filter is also of importance. In the half-cut structure discussed so far, the operating modes are the first and second eigenmodes of the structure. Therefore there are no spurious resonances below the operating bands. The third eigenmode is the first spurious, which for D/L ratios of interest, has an E field distribution shown in Figure 4-5.

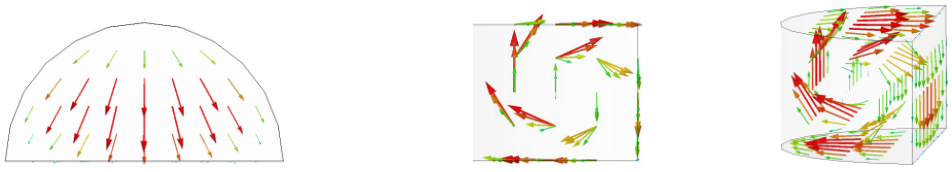

Figure 4-5: E field distribution of the spurious (third eigenmode) of half-cut DR.

As it can be seen in the figure, the path of the E field for the spurious is orthogonal to the path of the E field of the two operating modes. In Chapter 3 it was shown that placing through way slots in the resonator, terminates the path of E field for the spurious mode, while leaving the operating modes unaffected. Figure 4-6 shows the possible alterations that can be made to the basic half cut resonator.

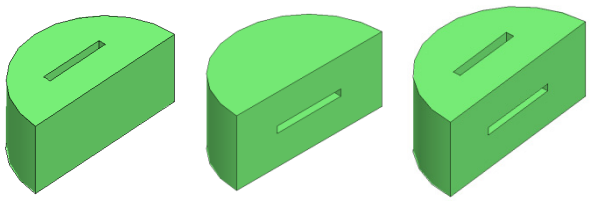

Figure 4-6: Alterations to the half-cut structure for spurious enhancement.

Table 4-1 shows a comparison of the spurious performance of the three different shapes. f and f' are the frequencies of the lower and upper bands. The resonators are adjusted in each case to have resonances close to 4 and 4.4 GHz, to compare their spurious, which is designated in the last column. It can be seen that a spurious free window of 1.3 GHz for the lower band and 900 MHz for the upper band is achieved with the two slot structure.

Two slots remove an additional spurious mode, higher than the one shown in Figure 4-5, and provide a higher spurious free window. Each shape may be used depending on the amount of spurious acceptable for the application, and level of complexity for fabrication.

Table 4-1: Spurious Improvement Comparison, ε_r=45

Type	f (GHz)	f' (GHz)	$f_{spurious}$ (GHz)
Original Half-Cut	3.96	4.38	4.56
Vertical Slot	3.96	4.38	4.77
Horizontal Slot	4.02	4.39	5.20
Two Slots	3.98	4.39	5.33

4.4 Filter Design Example

The filter topology of N-cavity dual-band filters are that of Figure 4-7, where each band is

realized with an inline filter, riding on one of the modes. The resonators of the lower frequency band are 1 to N, and of the higher frequency band are 1' to N'.

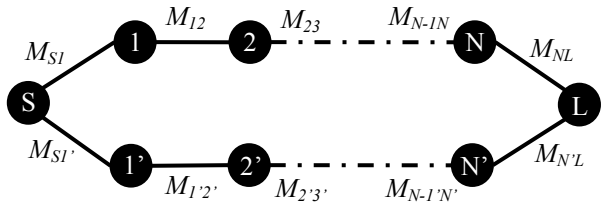

Figure 4-7: Filter topology of the dual-band 2xN-poles filter.

4.4.1 Four-cavity Dual-Band filter

Figure 4-8 shows the structure of a 4 cavity, 2x4-poles dual-band filter. Previous discussions were used in the design stage, and the full structure was simulated in Ansoft HFSS. The filter is probe fed at two ends (electric coupling), and uses cross irises (magnetic coupling) to realize inter-resonator couplings for each band. The resonator used is the modified half-cut with one slot.

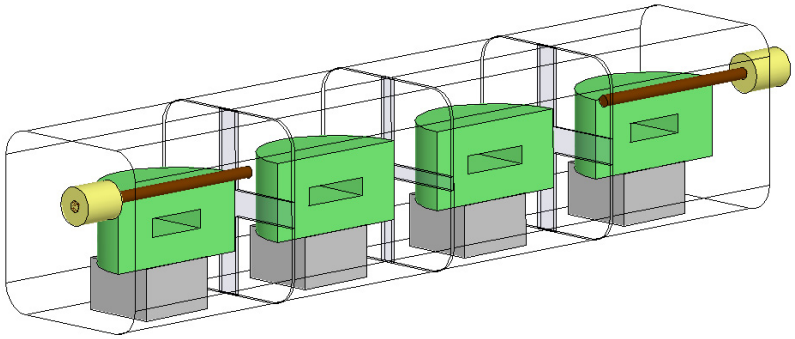

Figure 4-8: Structure of the dual-band 4-cavity (2x4-poles) filter.

The filter has f = 4.05 GHz and f' = 4.45 GHz, with 25 dB return loss and 1% bandwidth in each band. The simulation response of the designed dual-band filter is provided in Figure 4-9. A simulated spurious free window of 600 MHz starting from the higher band was achieved.

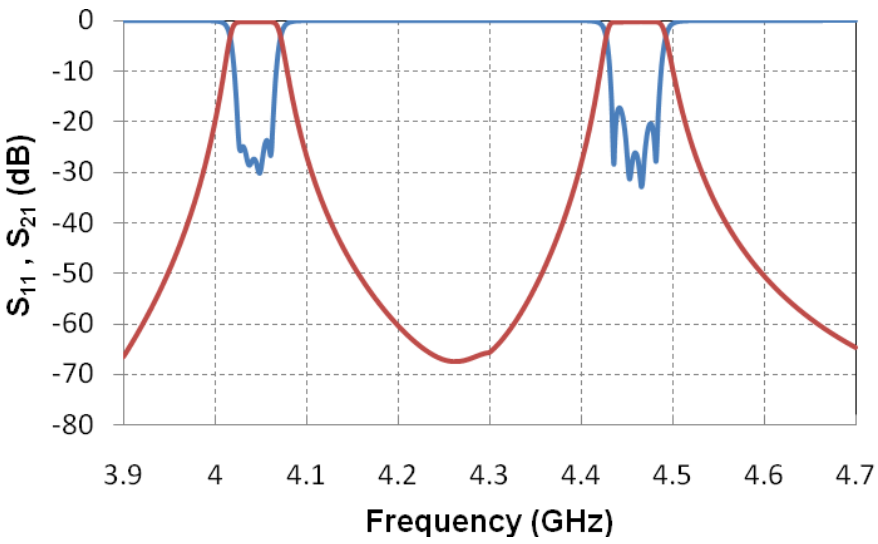

Figure 4-9: Simulated response of the dual-band 4-cavity filter

4.4.2 Three-cavity Dual-Band filter

Figure 4-10 shows the structure and arrangement of the cavities of the next design, for a 3-cavity dual-band filter.

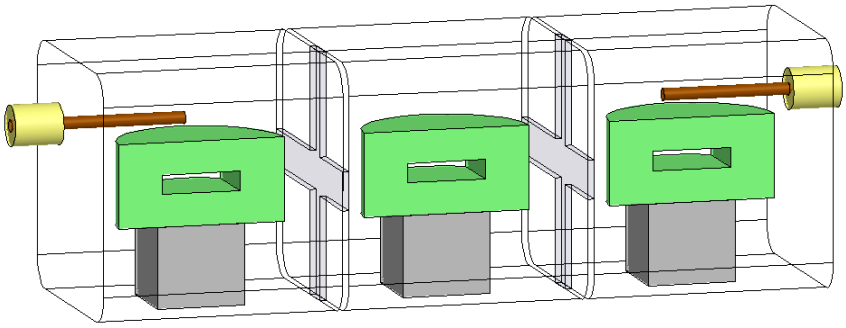

Figure 4-10: Structure of Dual-Band 3-cavity filter with probe input.

Figure 4-11, shows the simulation response of the designed dual-band 3-cavity filter, with bands at 4 and 4.42 GHz, return loss = 25 dB, and fractional bandwidth of 1% on each band.

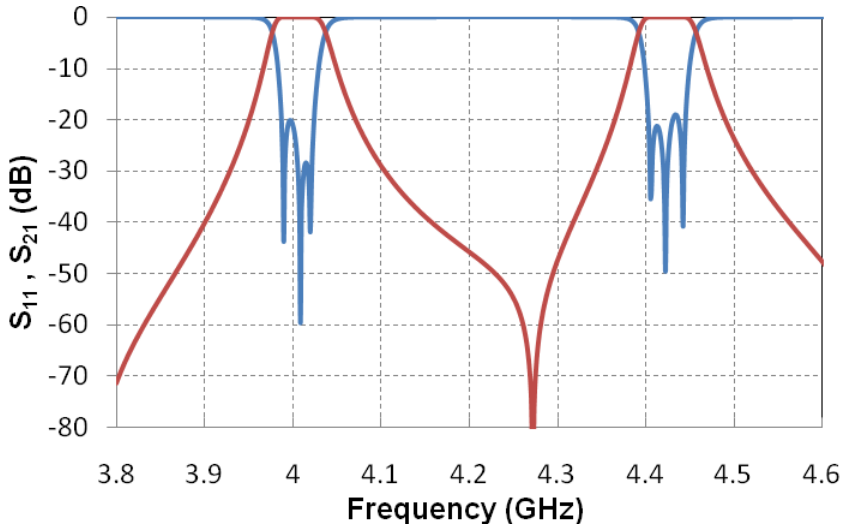

Figure 4-11: Simulated response of dual-band 3-pole filter with inter-band TZ.

The two bands are designed separately by each orthogonal mode. As it can be seen, there exists an inter-band Transmission Zero (TZ) at 4.27GHz. The explanation for this TZ is due to the order of the two filters. In each cavity, the two modes are 180˚ out of phase for frequencies between the two bands. Therefore, for odd order filters, the number of total phase reversals in each cavity is an odd multiple of 180˚, and hence the two signal paths can subtract at the output and create a TZ. For waveguide cavity filters, this concept is also presented in [54] for an odd order dual-band filter using two polarisations of the waveguide.

4.4.3 Inter-band Transmission Zero for even order filters

For even order filters however, the same separate inline design doesn't introduce an inter-band TZ, as we saw with the 2x4 pole design. This is because the two inter-band signals coming from the two paths go through even number of 180˚ phase reversals, and always add up constructively. In order to introduce a TZ, one of the coupling values in the two bands must have a different sign. For example, in the dual-band N+2 coupling matrix of a 4 cavity filter we have

$$M = \begin{pmatrix} 0 & 1.152 & 0 & 0 & 0 & 1.152 & 0 & 0 & 0 & 0 \\ 1.152 & -10.15 & 1.041 & 0 & 0 & 0 & 0 & 0 & 0 & 0 \\ 0 & 1.041 & -10 & 0.772 & 0 & 0 & 0 & 0 & 0 & 0 \\ 0 & 0 & 0.772 & -10 & 1.041 & 0 & 0 & 0 & 0 & 0 \\ 0 & 0 & 0 & 1.041 & -10 & 0 & 0 & 0 & 0 & \mathbf{\pm 1.152} \\ 1.152 & 0 & 0 & 0 & 0 & 10 & 1.041 & 0 & 0 & 0 \\ 0 & 0 & 0 & 0 & 0 & 1.041 & 10 & 0.772 & 0 & 0 \\ 0 & 0 & 0 & 0 & 0 & 0 & 0.772 & 10 & 1.041 & 0 \\ 0 & 0 & 0 & 0 & 0 & 0 & 0 & 1.041 & 10.15 & 1.152 \\ 0 & 0 & 0 & 0 & \mathbf{\pm 1.152} & 0 & 0 & 0 & 1.152 & 0 \end{pmatrix} \quad (1).$$

When the dual-band filter is designed and the sign of M_{4L} and $M_{4'L}$ are both positive, no TZ exists. However, choosing the negative sign for M_{4L} while keeping $M_{4'L}$ unchanged results in an inter-band TZ. This sign reversal means having negative output coupling to the last resonator for only one band. Physically, this can be realized in the dual-band structure by placing the probe according to the arrangement shown in Figure 4-12. Here the output probe is moved down close to an adjacent edge of the resonator, causing output coupling for $\frac{1}{2}HEE_{11}$ mode to reverse in polarity, but keeping the same polarity for the $\frac{1}{2}HEH_{11}$ mode. It should be noted, that if the probe would be placed along the edge diagonally across the original location, both modes would reverse in polarity and the inter-band TZ would again disappear, as the total number of phase reversals of the two bands would not add up destructively at the output to create a TZ.

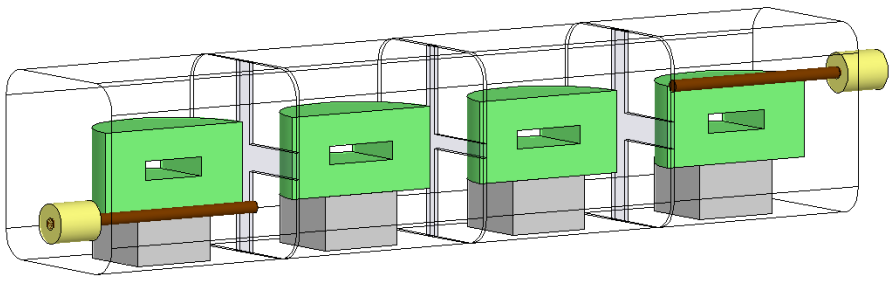

Figure 4-12: Structure of 4-cavity (even order) filter with inter-band TZ.

In such placement, all the couplings remain with the same sign for one band, while for the other

band, the last resonator's circulation of the mode is in opposite direction with the probe, causing a negative coupling. Figure 4-13 shows how the change of the probe location creates an inter-band TZ in the simulation response of the 2x4-pole dual-band DR filter. The two responses are overlaid and are otherwise identical

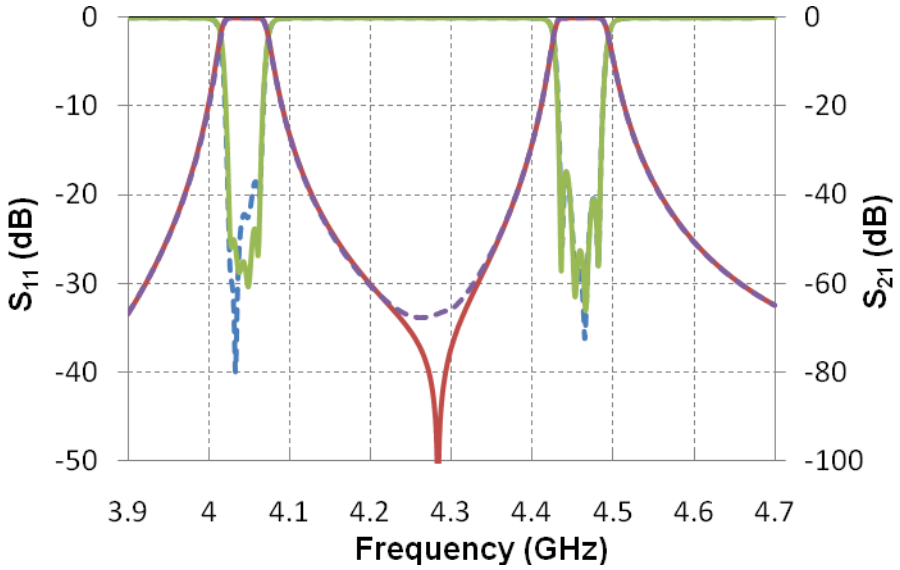

Figure 4-13: Simulated response of the Dual-Band 4-pole filter, (dashed) without inter-band TZ, and (solid) with inter-band TZ.

4.5 Measurement Result

A dual-band 2-cavity filter (2x2-poles), with RL = 15 dB and percentage Bandwidth of 1% on two bands, at center frequencies of 3.98 and 4.42 GHz was designed, built and tested. The filter structure is shown in Figure 4-14.

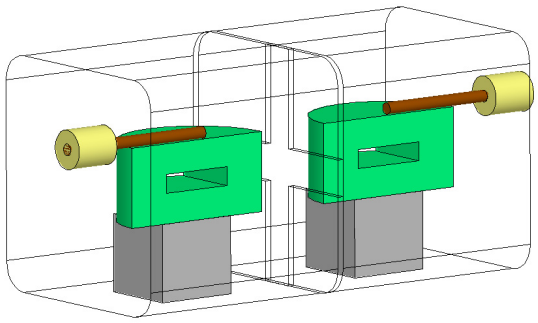

Figure 4-14: Structure of the dual-band 2-cavity (2x2-poles) filter.

The response of the measured results is shown in Figure 4-15. The resonator structure used is the half-cut with one horizontal slot, shown in Figure 4-6 (middle). A measured insertion loss of 0.5 dB and 0.6 dB are attained on the lower and upper bands respectively, and a spurious free window of 600 MHz starting from the higher band was measured.

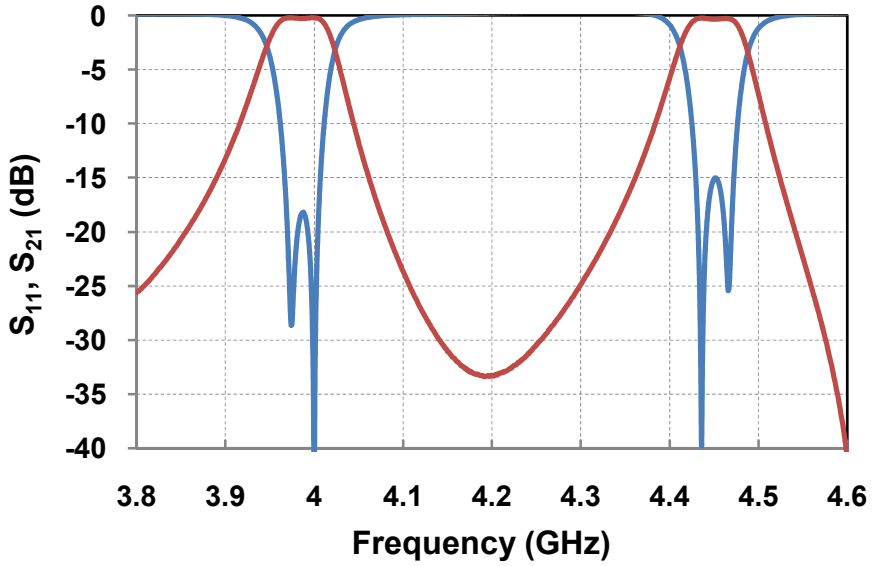

Figure 4-15: Measured response of dual-band 2-cavity filter.

The fabricated filter is shown in Figure 4-16. The ceramics used had *εr~45.6*, a supplier provided Q_u=12250 at 4 GHz, and were mounted on Teflon supports of *εr~2.1*, inside aluminum enclosures with silver coating.

The ceramics were once again shaped using waterjet cutting. The method provides ease of shaping the resonator from the widely available cylindrical form, as it is a well established structure, making water-jet cutting highly beneficial from a practical perspective. This way the costly production procedures with high pressure and temperature is avoided. Nevertheless these structures can be molded from scratch without cutting.

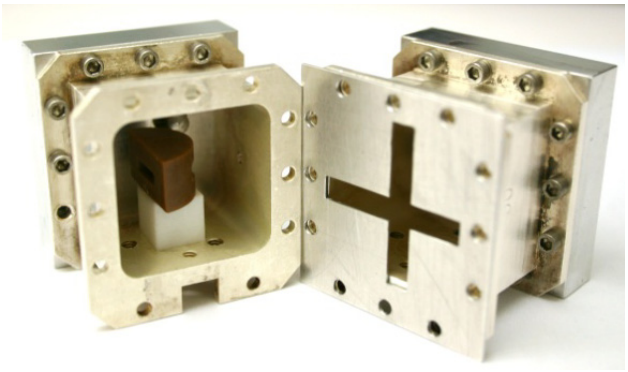

Figure 4-16: Fabricated dual-band 2-cavity (2 x 2 poles) filter.

4.6 Comparison with Existing Solutions

As mentioned in Chapter 2, there exists very few works to date that realize dual-band filters in dielectric resonator technology. Here we briefly mention some of the major benefits of dual-band dielectric resonator filter presented in our work.

An important note should be made about the dual-band filter in this chapter. To our knowledge, this is the first true dual-band dielectric resonator which is realized using two orthogonal modes of a structure. A similar concept in a different technology would be the work done by Amari et al. [54] using waveguides. Very recently, R. Zhang et al. [59], introduced a dual-band filter realized in dielectric resonator technology. However the filters in [59] do not use a single physical dual-band resonator. Rather, two resonators of different frequencies are placed in the same cavity. Therefore although the cavity is dual-band, two single band resonators are joined together. Our work however is the first in its kind to introduce a true dual-band dielectric resonator, and consequently dual-band cavity. The resonator of our work is quite compact, as the two bands are circulating in the same physical resonator in an orthogonal fashion.

There are also limitations in the couplings of the work in [59], as the inter-cavity couplings are realized with windows close to each resonator. However the orthogonal mode coupling presented here provides an ease in controllable design of the couplings for each band. There also exists the potential for unwanted and stray inter-band couplings in [59], due to the parallel placement of the two different frequency resonances in the cavity. Again, the orthogonality of the modes in our structure helps in completely isolating the two bands.

The spurious mode of the dual-band resonator of [59] was reported to be at best pushed up to

700 MHz away from the upper band at 5.6 GHz. From Table 4-1, the spurious mode of the half-cut resonator with two slots can be pushed up to 900 MHz away from the upper band at 4.4 GHz. This translates to a 1.145 GHz spurious free window if the upper band were to be at 5.6 GHz, which is 400 MHz (60%) more than the resonator in [59]. Another issue with [59] is the loss capabilities of the resonator, only capable of achieving certain Q levels, due to the shape and usage of a dielectric substrate. The dual-band resonator in this chapter are formed from the traditional cylinder, using the high-Q HEH and HEE modes.

4.7 Conclusions

This chapter has demonstrated the feasibility of realizing dual-band dielectric resonator filters. The novel half-cut dual-band dielectric resonator configuration having two orthogonal modes has been proposed for this purpose. The proposed filter structure makes it possible to independently control both the bandwidths and center frequencies of the two bands. Practicality of the designs is demonstrated via measurement. This filter is the first ever true orthogonal-mode dual-band dielectric resonator.

Chapter 5
Dielectric Resonator Multiplexers

5.1 Introduction

In this chapter we introduce novel multiplexer devices that are more compact than existing solutions used in satellite and wireless systems. The structures are then investigated for their potential applications in different areas of RF systems.

5.2 Combined Multiplexer

The dual-band filters presented in Chapter 4 receive a spectrum of frequencies at one input and transmit two passbands at the designed frequencies to a single output port. Such device however has the potential to be modified to realize a very compact two channel multiplexer. If the two passbands are not transmitted to a common output port, but rather each band is transmitted to a different output port, we can realize a two channel multiplexer. This routing of bands can be done in the last stage of the dual-band filter, realizing the two channel multiplexer. The benefit of this design is considerable size and mass reduction as we shall further see. Simply put, a typical two channel multiplexer which requires two separate physical filters, now only requires one physical branch of filter.

Consider the last cavity of the dual-band half-cut filter introduced in the previous chapter, and its common output port which are shown in Figure 5-1 (left). In Chapter 4, this common output probe is identical to the common input probe and simultaneously couples into both the ½HEH_{11} and the ½HEE_{11} modes. This last cavity can be modified according to the Figure 5-1 (right), by using two orthogonal probes, so that each probe exclusively couples only to one mode. Since each band is realized with one mode, each port would then theoretically only collect energy from one band only.

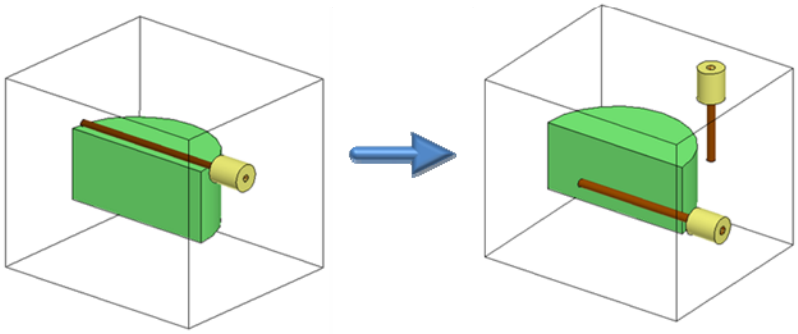

Figure 5-1: Modifying the output resonator of the dual-band half-cut filter to realize a multiplexer.

5.3 Basic 2x2-pole MUX

A simple 2x2-pole dual-band half-cut filter can be modified accordingly to create a two channel 2-pole diplexer. The structure is shown in Figure 5-2. Port 1 is the common port which couples frequencies of the first and second channel simultaneously to the first resonator of each band as shown. Port 2 couples to mode ½HEE$_{11}$. This mode is used to carry the filter with the lower frequency band. Port 3 couples waves to the ½HEH$_{11}$ mode. This mode is used to carry the filter with higher frequency band. It can be seen that the two-filter system is otherwise similar to the dual-band filter that was discussed previously. For example, the same coupling irises discussed previously are used to realize inter-resonator coupling for each filter. Here again the vertical iris couples ½HEH$_{11}$ and horizontal iris couples ½HEE$_{11}$.

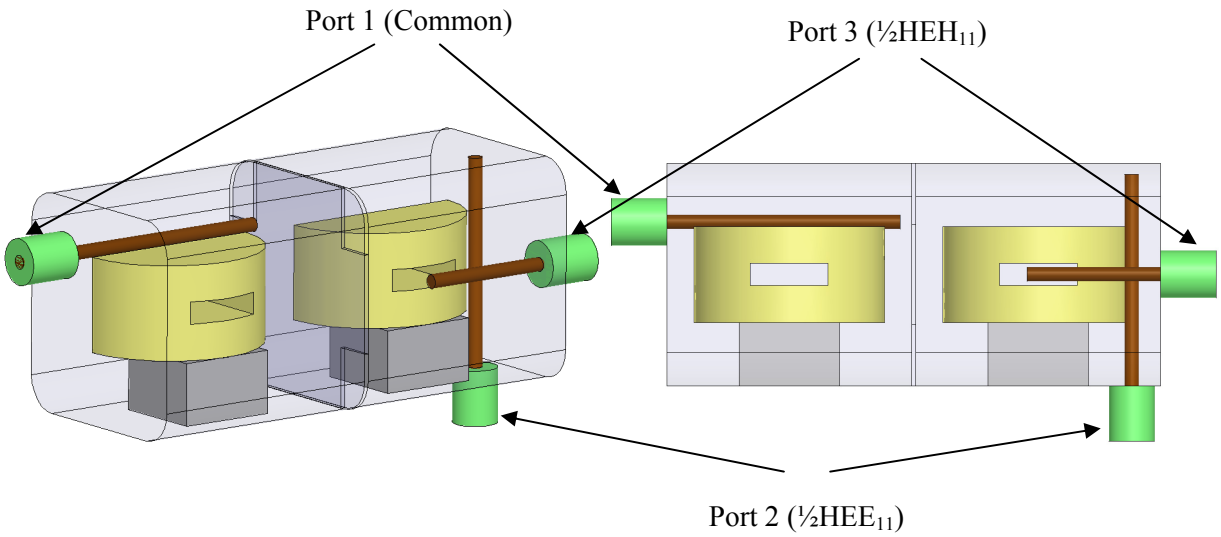

Figure 5-2: Two channel multiplexer with 2-pole channels (2x2-poles) realized with half-cut resonators.

The two cavity device now has two separate filters, each 2-pole. The design center frequencies are 4.03 GHz and 4.425GHz, with bandwidths of 1% each. The filters have return loss of 14 dB and 13 dB respectively. The response of the multiplexer system is shown in Figure 5-3. The spurious performance of the filter is 1.15 GHz for the lower frequency filter and 615 MHz for the higher frequency filter. The resonators of designs presented in this chapter have $\varepsilon_r=45$.

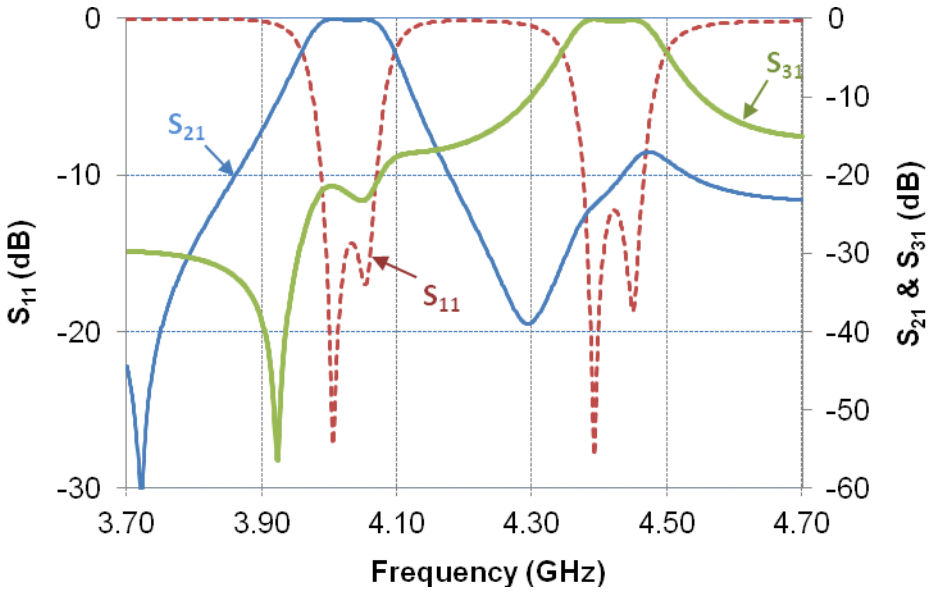

Figure 5-3: Simulated response of the 2x2-pole half-cut multiplexer.

The advantage of such structure is that only one physical line of filter is used, or essentially 2 cavities, compared to the 4 cavities required in the traditional design. This concept can be extended to higher order filters as shown in the filter topology of Figure 5-4. Every box in the figure shows a dual-band cavity, realizing one pole from each filter. The two output ports are denoted by L and L', and the common port is S, which couples directly to the first two resonators. Therefore only N physical resonators are used to realize a two channel multiplexer with N-pole channels, or a 2xN-pole multiplexer.

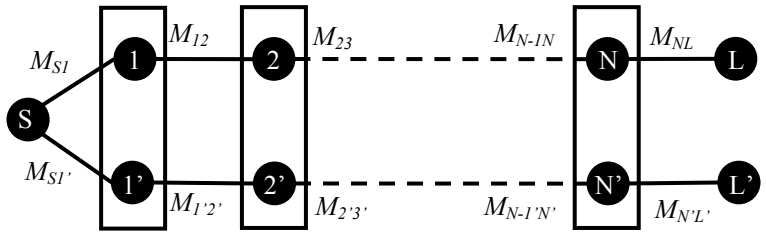

Figure 5-4: Topology of the combined two-channel multiplexer with N-pole channels (2xNpoles).

One major point about the response in Figure 5-3 is the amount of rejection of each filter in the operating frequencies of the other filter. As it can be seen in figure, a worst case rejection of 16 dB is attained. That is for the lower frequency filter, having the transmission S_{21}, its rejection on and around the higher frequency filter is around 16 dB. This is also the case for S_{31} having poor rejection on lower frequencies.

5.4 Rejection Improvement Using Extra Cavities

The out of band rejection issue of Figure 5-3 can be mainly attributed to the existence of the two output probes in the same cavity. Assume the two output probes are placed in the same cavity as shown in Figure 5-1. The output probe for each filter is aligned to only couple to its operating mode. However due to the non-zero thickness of the probes, effects of walls, round corners, etc., there is definitely some coupling of each mode to its non-corresponding output probe. This is one reason that can affect the out of band rejection of the filters.

Another important reason for the rejection degradation however is the direct coupling of the output probes themselves as they exist in the same cavity. That is even if the resonator is removed, there would still be a significant coupling between the ports, as one would create evanescent waveguide propagation within the cavity that would reach the other probe (The cavity is under cut-off at the operation frequencies). Although the two probes are aligned orthogonal to each other and should have minimum coupling, nevertheless existence of this path causes a significant contribution to the rejection of one filter in the other filter's band.

One solution to the above problem is to somehow separate the two output ports, by taking the output of the two filters in different cavities. Doing so promises to avoid some of the issues mentioned in the above problem. With the half-cut structure this can be achieved in several ways.

Consider we have the combined three pole multiplexer structure shown in Figure 5-5 (top). Again, here each resonator is operating in a dual-band fashion, where the lower band is riding on the

½HEE$_{11}$ and the higher frequency band is riding on the ½HEH$_{11}$ mode. The multiplexer can be modified to have the two output ports isolated in separate cavities as shown in Figure 5-5 (bottom).

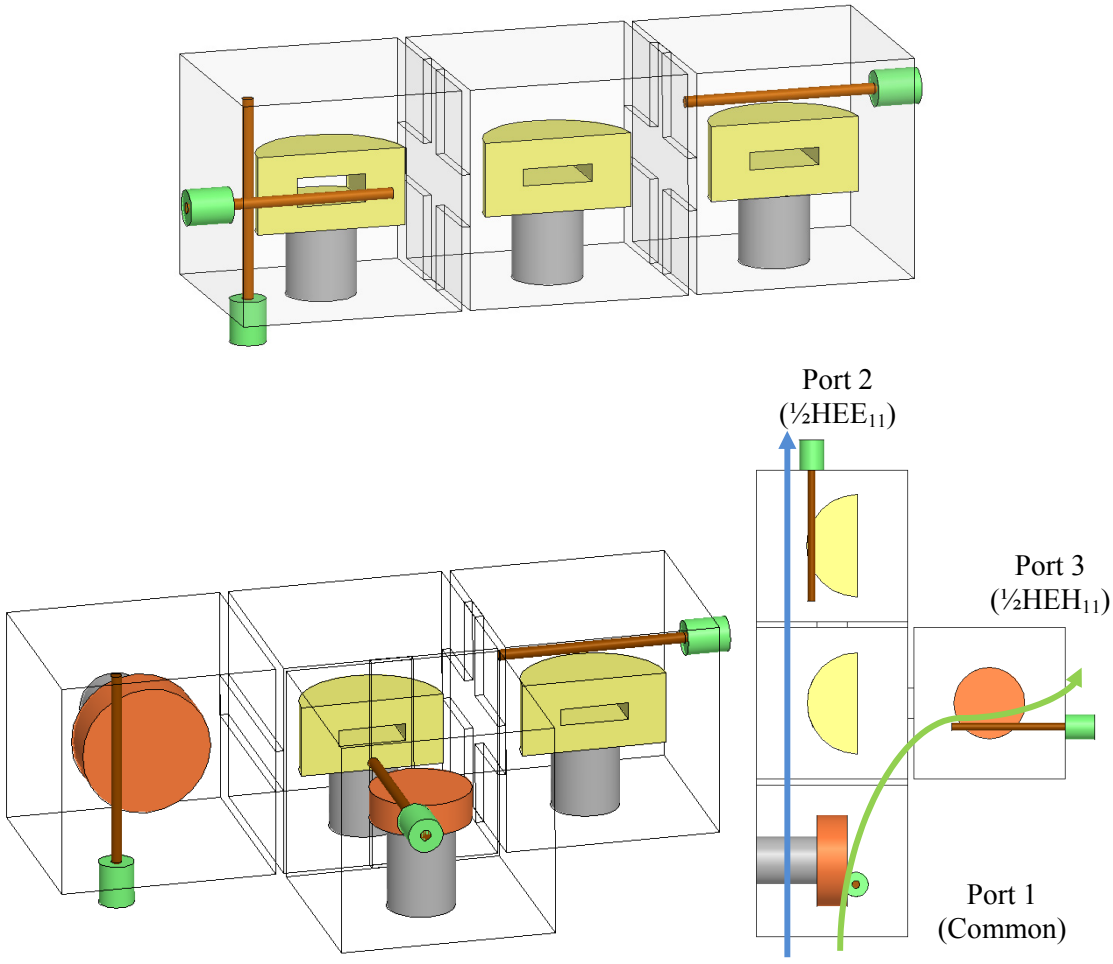

Figure 5-5: (top) 2x3pole multiplexer with single output cavity, and (bottom) modified 2x3 pole multiplexer with separate output cavities.

Here, the middle cavity acts as a junction, allowing to branch off the two filters from each other. The horizontal iris on the front wall is used to couple the ½HEE$_{11}$ mode, while the vertical iris on the side wall is used to couple the ½HEH$_{11}$ mode. The next two cavities on the front and side of the multiplexer can then be dissimilar cavities. The output ports for each filter are then placed in their respective cavities of each filter. In the example in the figure, a single-mode resonance resonator is placed in the two end cavities. They are cylindrical DRs operating in TEH modes. The orientation of the single cavity resonators are chosen so that the polarized modes coupling through the irises would excite the TEH mode. For

example for the extra cavity in the front of the filter, the cylinder is placed vertically. This is because the TEH mode in the cylinder would circulate around the axis of the cylinder, and would not couple through the horizontal iris if the cylinder is placed horizontally.

5.4.1 End-branched combined 2x3-pole MUX

Using this end-branched concept we design a two channel multiplexer having 3-poles each. The device now has two separate filters, each 3-pole. The design center frequencies are 4 GHz and 4.425 GHz, with bandwidths of 1%, and return loss of 13. We design both the fully combined 3-cavity device, and the 4-cavity end-branched device for comparison of performance. The response of the multiplexer with no additional cavities is shown in Figure 5-6. It can be seen that the rejection of the lower band around the frequencies of the higher band is no better than 20 dB. The response in Figure 5-7 is for the end-branched multiplexer with separate output cavities. It can be seen that more than 50 dB rejection for each filter is achieved in the operation frequencies of the other filter. Therefore the above modification to the multiplexer to introduce separate cavities for output, increases out of band rejection for both bands. The spurious performance of the two filters is 1.15 GHz for the lower frequency filter and 615 MHz for the higher frequency filter.

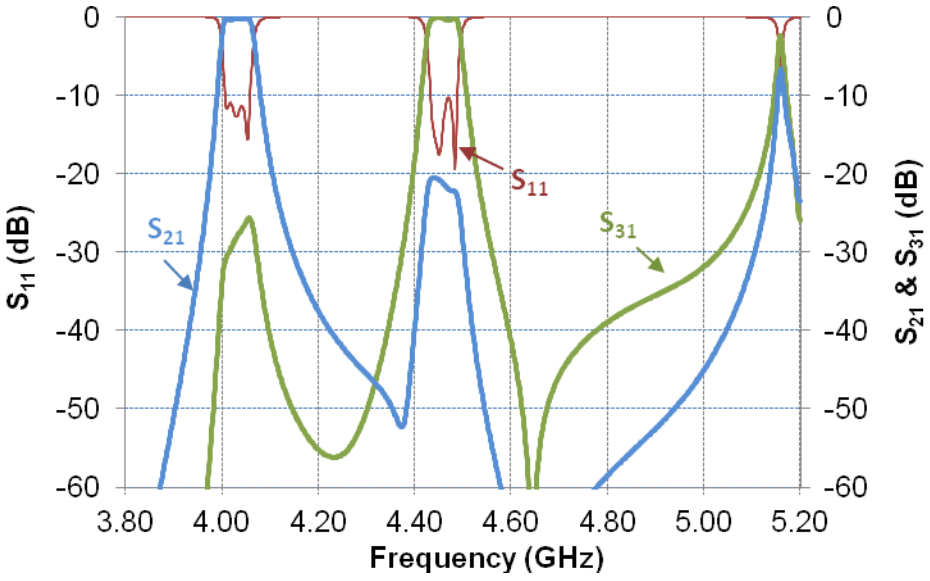

Figure 5-6: Simulated response of the basic 2x3-pole half-cut multiplexer with only 3 cavities.

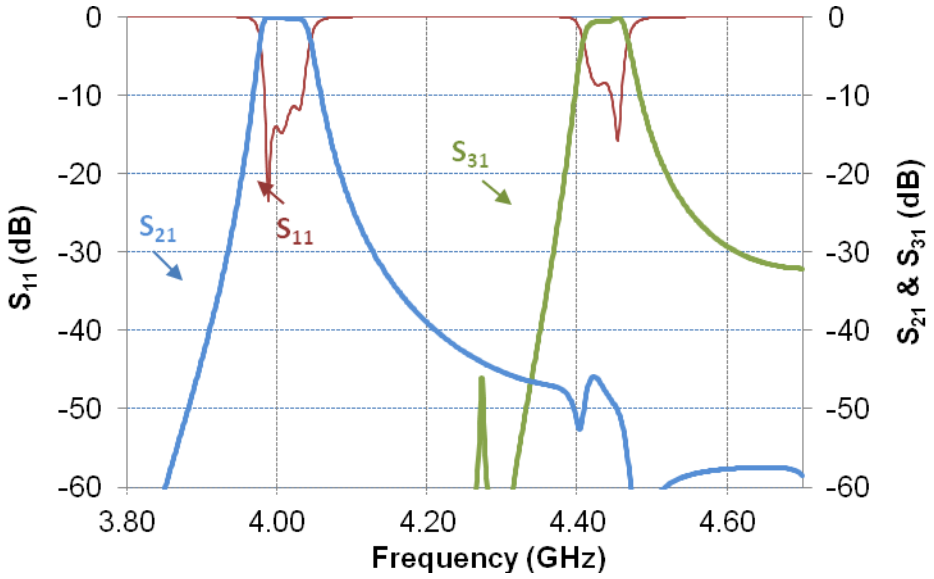

Figure 5-7: Simulated response of the 2x3-pole half-cut multiplexer with separate output cavities.

The fact that we are able to break out the multiplexer in two different paths geometrically, and branch off the two filters in two different orientations is a significant feature of our structure. We saw in Chapter 4 that two bands can coexists in the same cavity owing to the orthogonal modes, and can be coupled simultaneously to adjacent cavities to realize any order filters. However, owing to the unique formation of the two operating modes, and their circulation, we are also given a wide range of flexibility for branching out the two bands at any stage of the filter we so desire. The circulation of the ½HEE_{11} mode allows for a horizontal iris in the front or back walls, as well as irises in the top and bottom walls of the cavity, to couple energy into the next cavity on the other side of the iris, while minimizing the coupling of the ½HEH_{11} mode. On the other hand, a vertical iris placed on any of the side or font walls of the cavity allows for almost exclusive coupling of the ½HEH_{11}, due to its horizontal circulation. This is an important benefit of the half-cut DR when used as a building block for the multiplexer. The orthogonal modes and their coupling do not limit the orientation of the filter to only one direction.

5.4.2 Higher Order End-branched MUX

This idea can be generalized for 2xN-pole multiplexers as shown in the filter topology of Figure 5-8. It can be seen that the first N-1 resonators from each band are placed as a pairs of (1,1') in a dual-band cavity, and the last resonator (N or N'), from each band is placed in a separate cavity.

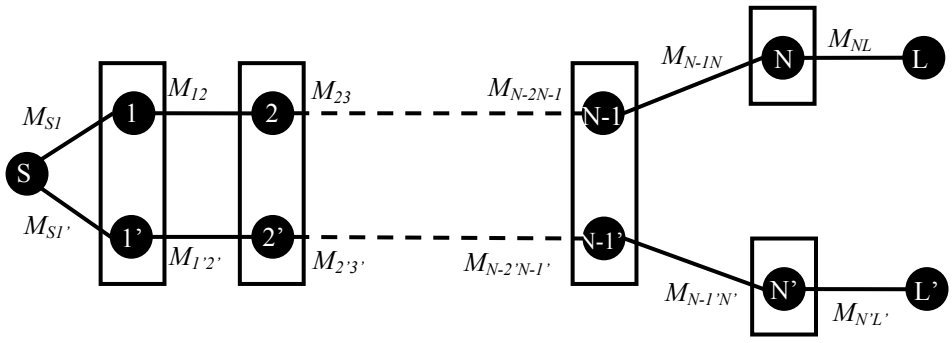

Figure 5-8: Topology of the combined 2xN-pole multiplexer with separate output cavities for rejection improvement.

A higher order multiplexer, 4 poles in each channel was also designed. The structure is shown in Figure 5-9. The first three cavities are shared between the two bands, the third cavity acts as a junction to separate the two filters, and the last two cavities are single TEH mode cavities for separate output ports.

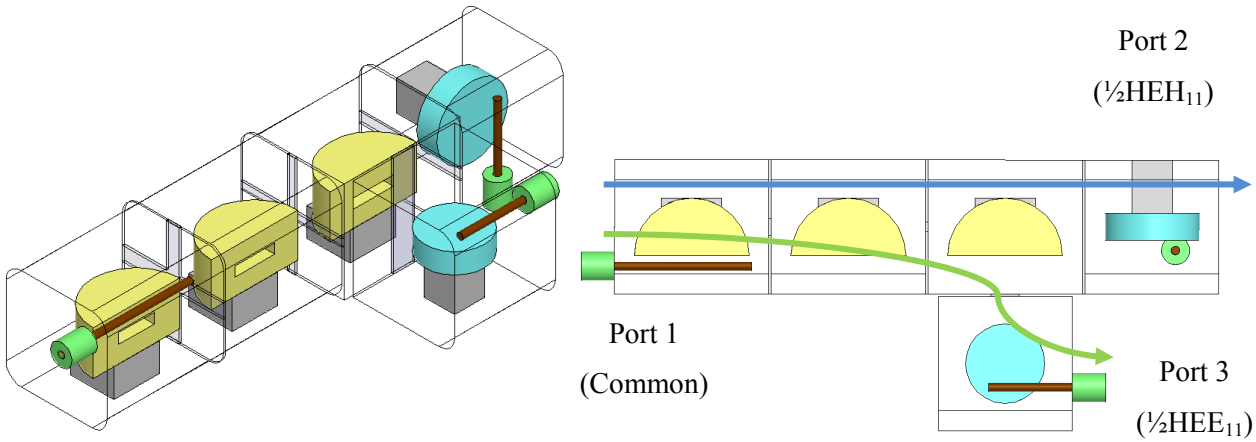

Figure 5-9: Structure of a 2x4-pole half-cut multiplexer with separate output cavities.

The response of the multiplexer is shown in Figure 5-10. The filters were designed for center frequencies of 4.02 GHz, and 4.425 GHz, with return loss of 20 and 25 dB respectively, and 1% bandwidth in each filter. The spurious free window for the lower frequency filter is 1.15 GHz, and for the higher frequency filter is 615 MHz. It can be seen that better than 50 dB out of band rejection is achieved for all frequencies of interest.

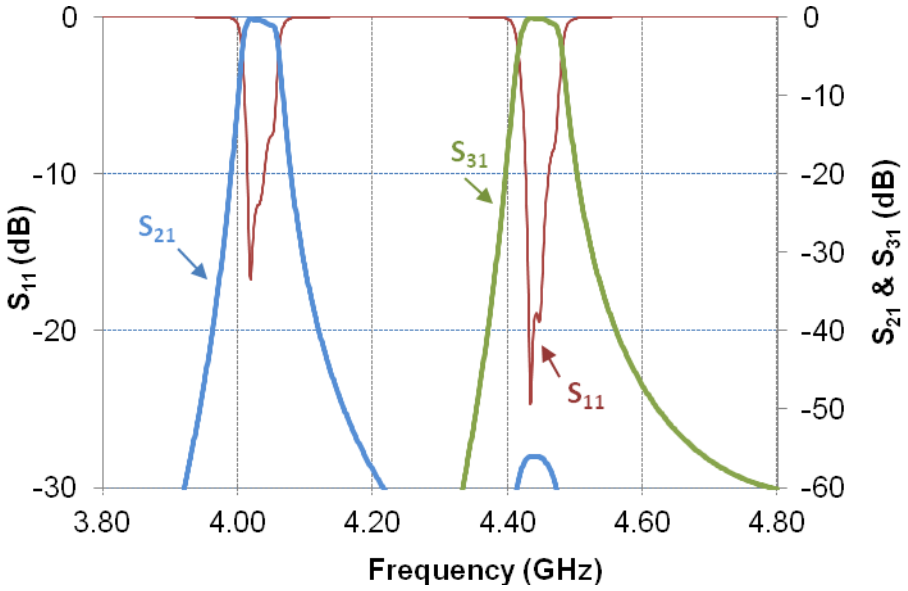

Figure 5-10: Simulated response of the 2x4-pole half-cut multiplexer with separate output cavities.

5.5 Three-port characteristics

The two channel multiplexer is a 3-port device. So far we have only considered the transmission from common port to ports 2 and 3 (S_{21}, S_{31}) and the return loss at port 1 (S_{11}). We must however, among other parameters, also consider S_{23} (S_{32}), which is the transmission between ports 2 and 3, and quantifies the amount of isolation between these two output ports. For the first design presented, the basic 2-pole MUX with no extra cavities (Figure 5-2), the additional 3-port measurements are shown in Figure 5-11. We can see that the transmission between ports 2 and 3 has a maximum of -18 dB, considering all frequencies of interest. In other words, the minimum isolation between the two ports is 18 dB. In this case where no extra cavities are used, the isolation between the two uncommon ports is not high, and this can be mainly attributed to the existence of the two output ports in the same cavity, and the strong coupling path existent between them.

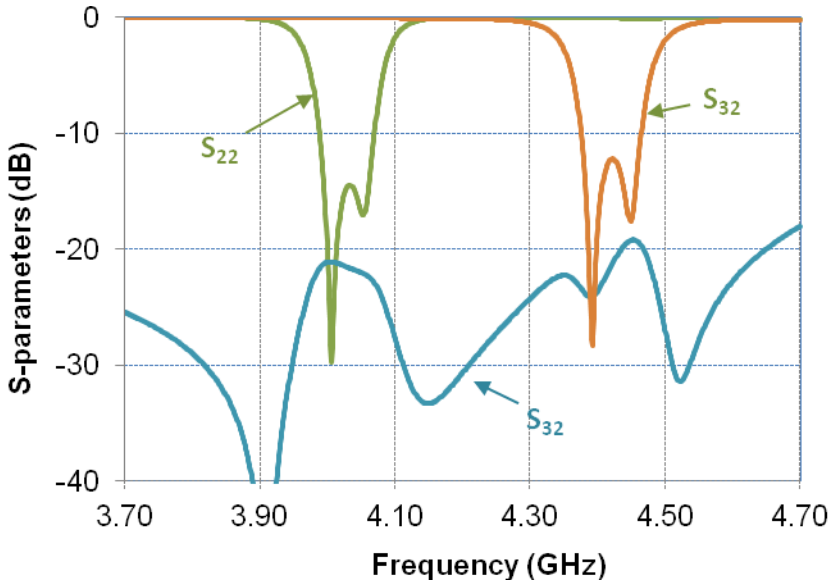

Figure 5-11: Additional simulated 3-port parameters of the 2x2-pole multiplexer of Figure 5-2.

The poor isolation between the two uncommon ports is also apparent in Figure 5-12, the additional 3-port measurements of the 3-cavity combined filter of the structure of Figure 5-5 (top). It can be seen that for the operation frequencies, a worst case isolation of 15 dB is attained between the two uncommon ports.

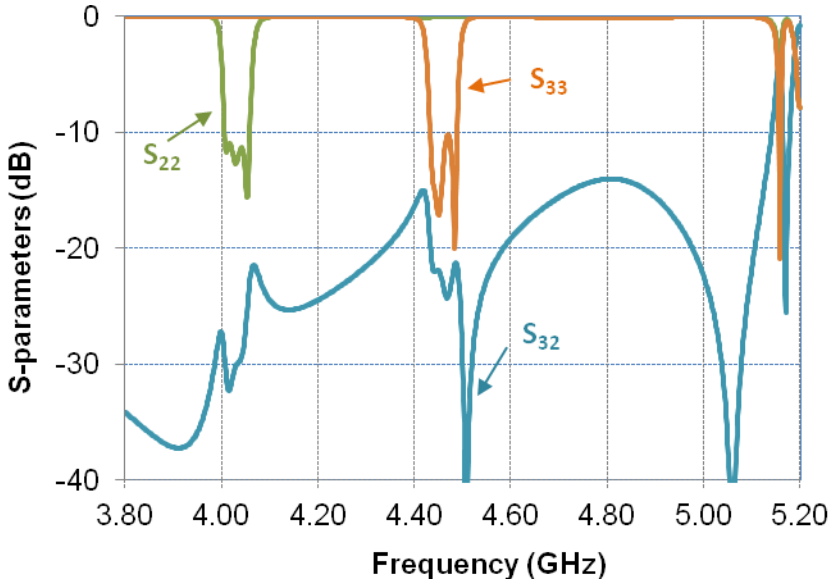

Figure 5-12: Additional simulated 3-port parameters of the 2x3-pole multiplexer of Figure 5-5, having only 3 cavities.

Figure 5-13 shows the additional 3-port S-parameters of the modified end-branched 2x3 pole multiplexer with separate output cavities, and Figure 5-14 shows the additional 3-port S-parameters of the modified 2x4 pole multiplexer with separate output cavities. It can be seen that minimum isolation between ports 2 and 3 is improved to about 43 dB for the 2x3-pole. The isolation between uncommon ports in the 2x4 pole multiplexer is improved to more than 50 dB considering all operation frequencies.

Therefore a major benefit of introducing the extra cavity is isolation improvement between the two uncommon ports, which is an important characteristic for some applications. This improvement is due to the fact that the two ports are now not coupling into the same cavity, and reside in separate enclosures. The amount of transmission still available between ports 2 and 3 is due to the wave that passes through the irises and the middle cavity between the two enclosures of the ports.

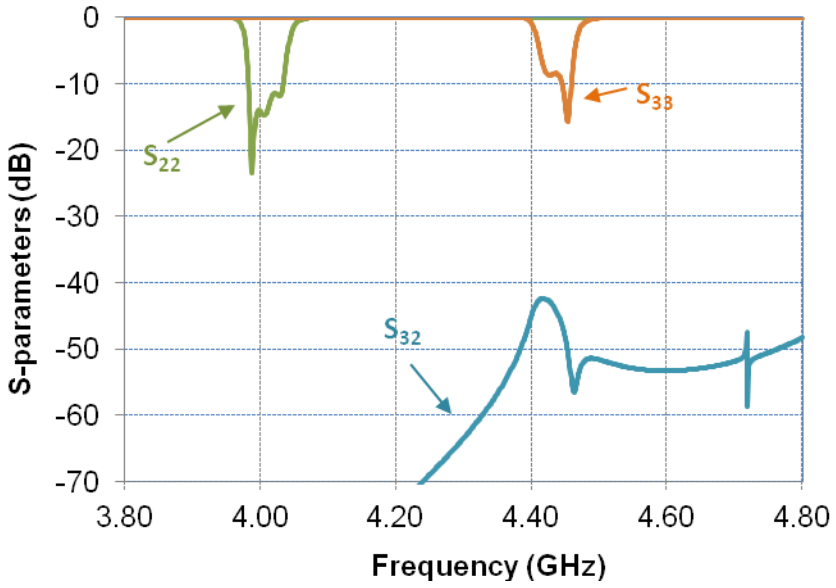

Figure 5-13: Additional simulated 3-port parameters of the 2x3-pole multiplexer of Figure 5-5.

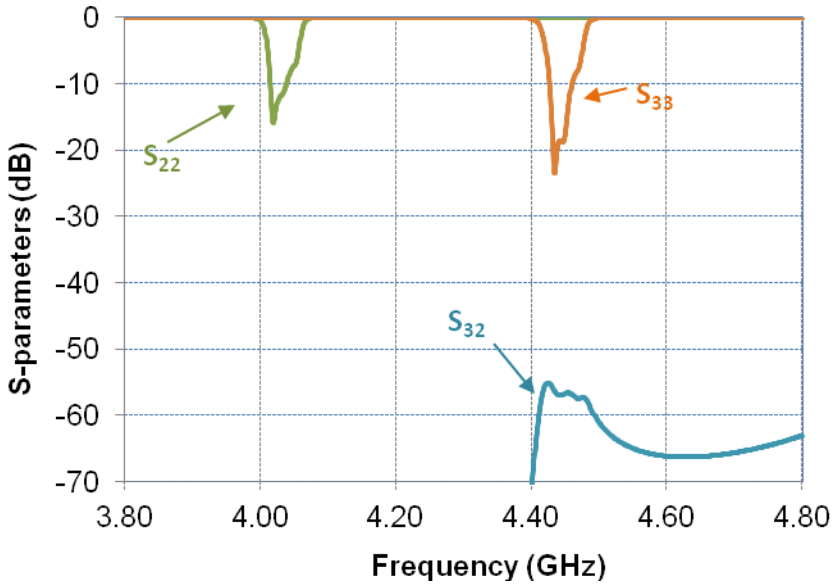

Figure 5-14: Additional simulated 3-port parameters of the 2x4-pole multiplexer of Figure 5-9.

5.6 Multiplexer Size and Mass

As mentioned earlier, the major benefit of the proposed combined two-channel multiplexer is size reduction. In fact the size of the combined MUX with no modifications is almost half of the traditional design, since half as many cavities are used. This is a notable improvement, as half as many metal cavities are required, as well as half as many ceramic resonators, and the overall structure would have approximately half the mass of the traditional design. This level of size and mass reduction is significant for wireless and satellite applications.

To increase out of band rejection of the filters, it was proposed that a separate cavity may be used to isolate the two output ports. This modification however slightly sacrifices the size reduction. For example for a 2x3-pole MUX, a combined design with no separate output cavity requires 3 cavities, end-branched design requires 4 cavities, and the traditional design requires 6 cavities. Therefore the combined design is 50% of the size of traditional MUX, while the end-branched design is 66.67% of the size of the traditional MUX. In others words, in the 2x3-pole MUX, we have increased the size of the combined design by 33% (= [66.67-50]/50) by introducing the extra cavity inhte end-branched method. This size addition however becomes less significant for higher order filters, which are the types of filters that are employed in reality for diplexer and multiplexer systems. In general for a two channel N-pole MUX, the traditional MUX require 2N cavities, whereas the initial combined design requires N cavities, and the end-

branched MUX requires N+1 cavities. As an example, for N=8, a typical order of filter in satellite applications, the size of the combined and the end-branched are respectively 50% and 56.25% of the traditional MUX. Therefore the modified design is only 6.25% larger, but has far better rejection performance.

Addition of a separate cavity for each filter also gives the freedom of placing a dissimilar resonator from the half-cut resonator in the last cavity. This means that we can use a resonator that has a wide spurious free window in the last resonator, and therefore improve the spurious free windows of the two filters. In previous designs we utilized the single mode TEH mode in the last cavities with no particular attention to the spurious performance of the resonator. For example, a modified cylinder with a center hole could have alternatively been used, giving better spurious performance.

Another possible technique is to place dual-mode resonators, e.g. half-cut, in the last dissimilar cavity of the branched design. These two resonances in the last cavity can then be either the last two resonances of the filter, or one resonance plus one extracted pole to improve the rejection of the filter.

The idea of branching is not limited to end-branched method. In the end-branched, one separate output cavity is added for each filter, which increased the out of band rejection of each filter as well as the isolation between the two uncommon ports, while on the other hand increased size. Consider the topology in Figure 5-15. Here, resonator pairs (1,1') up to (m, m') form dual-band cavities. Then the two filters are separated into two branches, one containing resonators m+1 to N of the first filter, and another branch containing resonators m'+1' to N' of the second filter. The branching does not necessarily need to occur at the second last cavity. In the end branched method, we only considered m=N-1, e.g. in the 2x4pole filter example, we had N=4, and m=3, but addition of one separate cavity is not the only option. If less size reduction can be tolerated in a specific application, two or more separate cavities can be used for the last resonators of each branch. In general, the mentioned dual-band resonators can be utilized for any portion of a pair of filters of a multiplexer. The more dual-band resonators are used, the higher the size reduction is achieved. For example in some diplexer applications, high isolation between the two uncommon ports is required. To this end, it would be beneficial to use m=N-2, or in other words branch the filter one resonator sooner, and have two separate cavities for each filter.

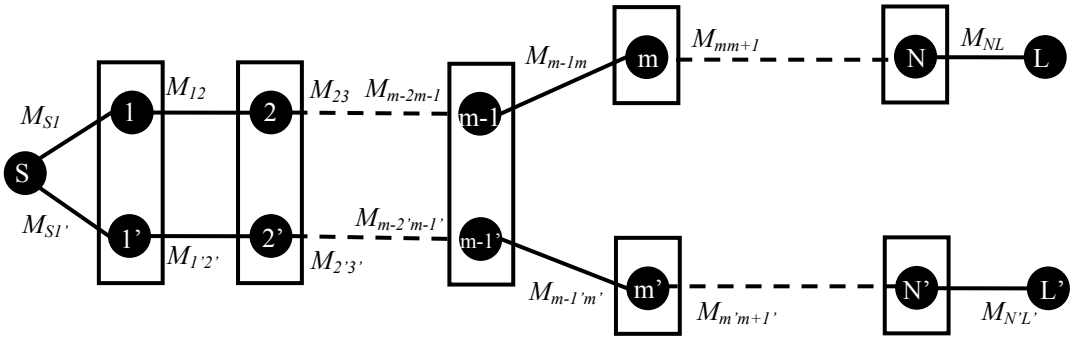

Figure 5-15: Topology of the combined 2xN-pole multiplexer with separate output cavities for rejection improvement.

5.7 Advanced Coupling

By combining the two lines of filter in to one physical line, we have two resonators of different frequency in each cavity. The possible topology of such filter branch was shown in Figure 5-4, Figure 5-8, and Figure 5-15. Another feature of this structure is that we can introduce some inter-band coupling, between the dual-band resonances in all or some cavities, to introduce transmission zeros or improve the out of band rejection of each filter. This is shown in Figure 5-16. In essence, we can use each line of filter, as Non-Resonating Nodes (NRNs) for the other branch of filter. It should be noted that each band still needs to be an operational filter with the same characteristics, therefore certain couplings, e.g. between resonators of the same band, cannot be removed and are still present. The additional proposed couplings are depicted in figure with thick dashed line within each box (cavity).

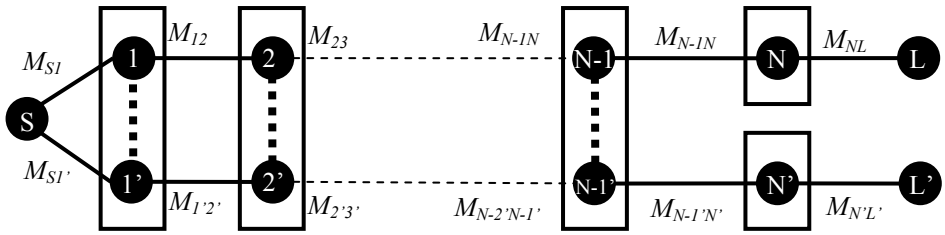

Figure 5-16: Topology of the combined 2xN-pole multiplexer with separate output cavities, with addition of inter-band couplings to increase out of band rejection and utilization of NRNs.

5.8 Applications

The proposed combined MUX and the modified version have several potential applications in microwave systems. Here we briefly indicate some of the major application areas, and the benefits of using the proposed building block in each case. In general, the main advantage is compactness, but as we see, other benefits do arise from these designs.

5.8.1 Manifold-Coupled MUX

A manifold coupled MUX is a MUX in which all channels are present simultaneously, along with a manifold, normally a near lossless transmission line of specific phase length, realized with waveguide or coaxial transmission lines. A typical manifold-couple MUX is shown in Figure 5-17 (top), acting as a channelizer. The same structure can be used as a combiner. In either case, each channel is filtered with a separate physical filter, and the filters are separated by the appropriate phase length in the manifold.

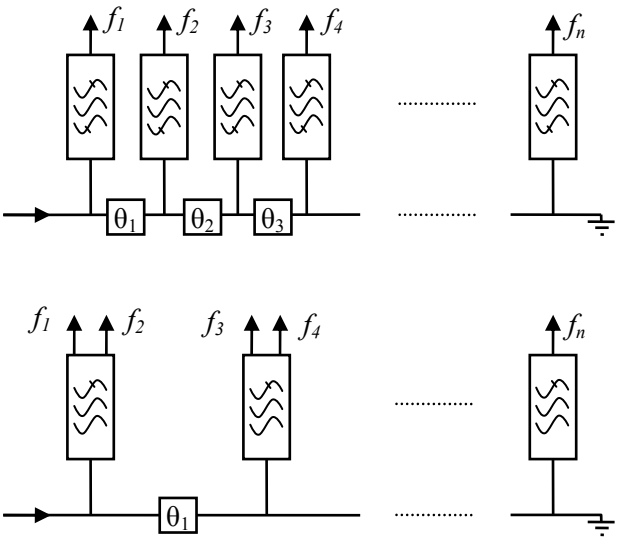

Figure 5-17: (top) traditional manifold coupled MUX [1] and (bottom) proposed manifold coupled MUX scheme using the combined two-channel MUX.

The idea here is to realize every two filters of the manifold-coupled MUX with a single combined MUX proposed in this work, as shown in Figure 5-17 (bottom). This way half as many physical filters allocate space. For example, in a 60 channel system, 30 physical channels are needed, each having

a size equal or slightly higher (if separate cavities are used) compared to the channels of the traditional design. The other benefit is that the manifold would require almost half as many transmission line segments as every two channels are combined.

5.8.2 Tx-Rx Diplexer

The proposed combined two channel MUX can also be used where a transmit-receive diplexer is used. In a typical diplexer, the two filters are designed separately, and then a common junction is designed and optimized to bring together the two paths with proper phase adjustments. For example, a wire T-junction used for coaxial resonator diplexers [1], or a junction at the common port of the diplexer in Figure 5-18 (top). The advantage of our design is in two ways. First of all one physical line of filter is used instead of two filters which makes the size of the overall design considerably smaller as shown in Figure 5-18 (bottom). Secondly, this structure avoids the design of a separate common junction, as the common port (port 1) is designed for both branches of filter simultaneously with right amounts of input coupling for each channel during the filter design stage.

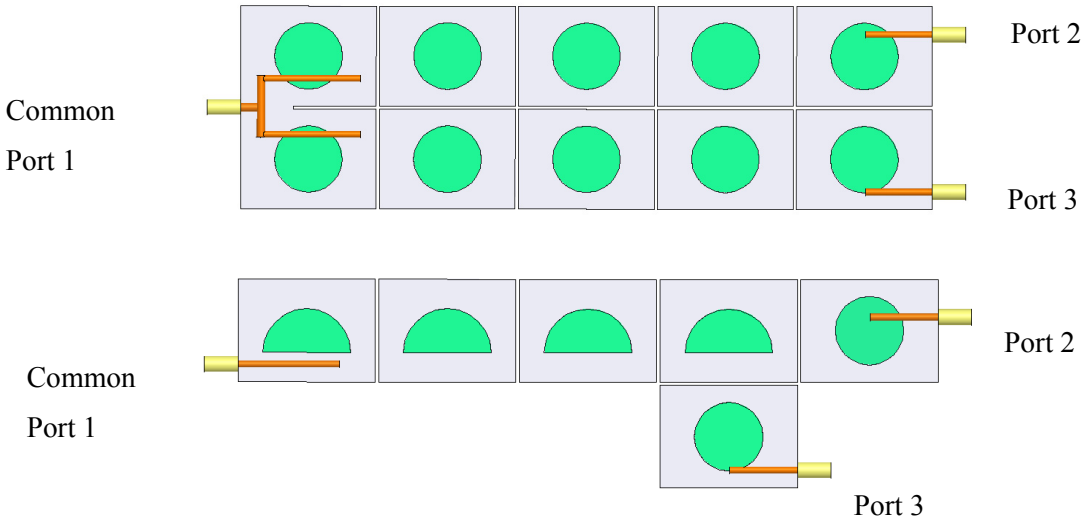

Figure 5-18: (top) 2x5-pole multiplexer with a common junction (bottom) proposed 2x5 pole multiplexer with single probe junction and extra output cavities.

5.8.3 RF Channelizer (IMUX)

A significant application of the proposed design is in the area of RF channelizers, also known as de-multiplexers, or Input multiplexers (IMUX). The functionality here is to split a common frequency

spectrum into a number of RF channels or frequency bands. For example for two types of RF channelizers, Hybrid branching and circulator coupled approach, the proposed design can be used in both as follows.

5.8.3.1 Hybrid Branching MUX

A typical Hybrid branched network for 5-channels is shown in Figure 5-19 (top). Here each 3 dB hybrid splits the signal into two equal paths, until the number of paths equal the number of channels. At the end of each path, channel filters are located. There are some advantages with this approach, mainly simplicity in design. However there is a major drawback which is the high insertion loss exhibited for each path, due to overall number of hybrids. For example, according to [1], the worst case insertion loss for a Ku band IMUX of Figure 5-19 (top) is approximately 12 dB, excluding the filter losses. This methodology can however be modified using the proposed combined multiplexer, as shown in Figure 5-19 (bottom). Here every two channel filters of figure, as well their isolators, and the one hybrid splitting the power between them, is replaced with one combined filter and only one isolator, as shown in Figure 5-19 (bottom). It can be seen from the block diagram that significant size and complexity reduction is introduced, by reducing the number of filters by half, and also using less hybrids and isolators. The added benefit of removing the hybrids is that the insertion loss of channels is significantly improved. In the example of 5-channel MUX, the worst case insertion loss would improve by 3 dB as at least one less hybrid would be used in the longest path.

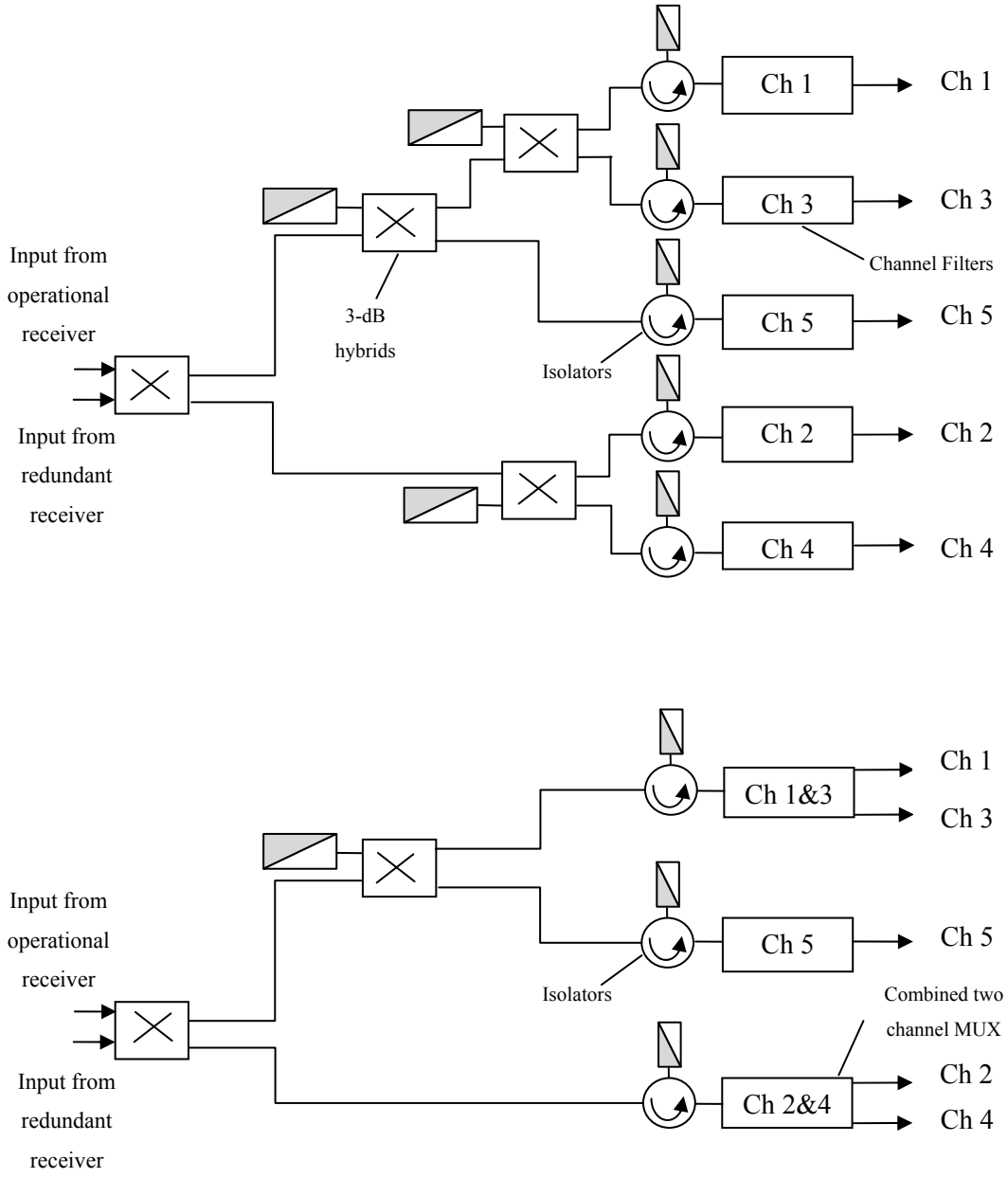

Figure 5-19: (top) traditional hybrid branching IMUX [1] (bottom) proposed hybrid branching IMUX using the novel combined two channel MUX.

5.8.3.2 Circulator-Coupled MUX

The circulator coupled MUX approach which is also referred to as channel dropping MUX, is shown in Figure 5-20 (top), for a 5-channel contiguous channel. The hybrid divides the power in two

paths, and then in each RF path, a channel is branched using a circulator/filter combination. The channel is dropped to the output of the filter, and the rest of the frequencies are forwarded towards the next circulator/filter, where the next channel is dropped. The last stage is a terminating load where all the other channels are absorbed. This approach however can be modified by the combined MUX, and the overall design would simplify to that of Figure 5-20 (bottom). It can be seen that for every two filters we are now using only one circulator, therefore each chain would require half (or half+1 if odd number of channels) as many circulators. We have also reduced the number of physical filters by half, as we have combined every two filters in one physical filter. Therefore significant size and mass reduction, as well as reduction in the overall complexity of the system is achieved.

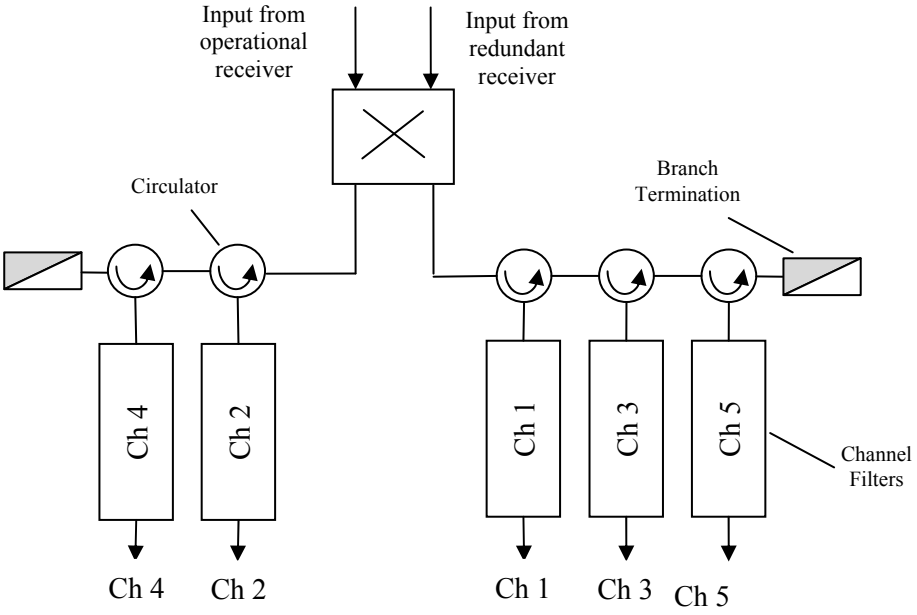

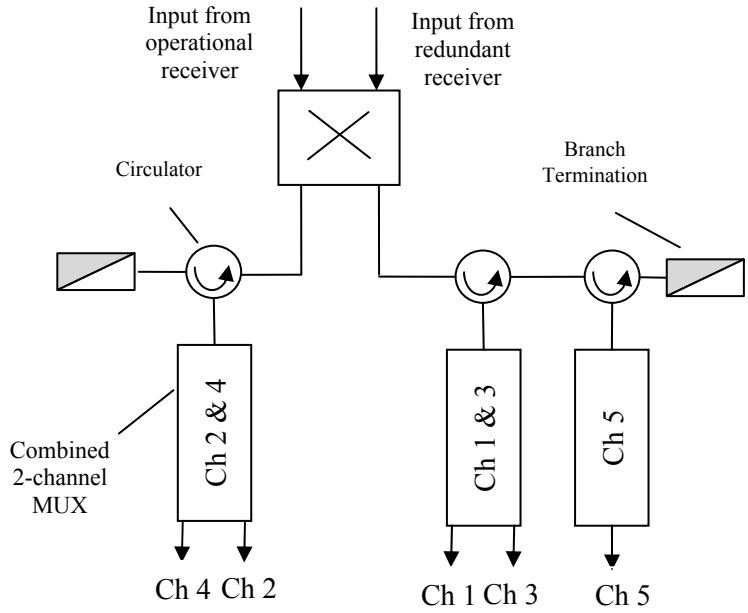

Figure 5-20: (top) traditional circulator coupled or channel dropping deMUX [1] and (bottom) proposed channel dropping scheme using the novel combined MUX.

There is an added benefit of using the new approach. Normally, every circulator in the chain can cause degradation in the response of the next channels in the chain due to its reflections, known and En Passant distortion [1]. Each channel's filter is not affected when put in the chain along with the other channel filters, but the channel's response is affected by the reflections at the input of the non-corresponding filters in the path before reaching the corresponding channel filter. All but the first channel would suffer from such effect. Normally, in order to minimize this issue, non-contiguous channels are used in the consecutive channels of the chain. In the proposed design, less circulators are present. It can be said that the advantage of the proposed design is that at the very least, the first two channels of the chain are unaffected by this distortion, compared to the original design where only the first channel was immune.

5.8.4 RF Combiner (OMUX):

The opposite functionality of the IMUX is the RF combiner or the Output MUX (OMUX), where a number of separate channels are to be combined into one spectrum. This is normally required in a transmit station to be sent to the transmit antenna. There are different methods of OMUX, including the

manifold coupled approach. We saw that by using the proposed design of combined filter in the manifold coupled approach, one can reduce the number of physical branches in a MUX by almost half. This is also the case if the manifold-coupled MUX is used as an OMUX. Therefore in a satellite payload, the size reduction achieved can potentially be both at the channelization and combination of signal, which are the main two bulky parts of the system.

Another output multiplexing method is the Hybrid Coupled Filter Module (HCFM) MUX [1]. Our combined design is also applicable in this case, by combining every two HCFM with different frequencies into the same combined HCFM, and therefore reducing the number of filters by half, as well as halving the total hybrids used.

5.9 Other structures

Other resonators maybe proposed that realize similar dual-band resonator, and therefore may be used in a combined two-channel MUX system. In any case it must be noted that when the branches are combined, it is still necessary that the two bands are not mixed as much as possible, and control over their couplings and frequencies are available.

In general the proposed topologies of Figure 5-4, Figure 5-8, Figure 5-15, and Figure 5-16, maybe used with any physical realization, and offer size and mass reduction compared with their traditional counter parts. For example, the same idea may be applied to other shapes of dielectric resonator, or even other dual-band cavities realized even in other technologies.

5.10 Conclusions

In this chapter we introduced a combined two channel dielectric resonator multiplexer. This novel building block is derived from the dual-band filter, and utilizes orthogonal mode dual-band resonators to combine every two poles from a two channel filters into the same cavity. The design is therefore extremely compact, reducing two physical branches of filter into one, or reducing the size by almost half. Several designs were presented, including the modified MUX with separate output cavities to increase the out of band rejection of the MUX filters, as well as isolation between the uncommon ports. This technique yielded somewhat lesser size reduction, but with better 3-port performance. For example, more than 50dB out of band rejection for channel filters and more than 50 dB isolation between the two uncommon ports was achieved by using only one cavity and no extra coupling scheme. Even higher rejection and isolation levels can be achieved by using two or three dissimilar cavities, which is affordable size addition for high order filter. The proposed design was then investigated for its possible impacts on

various multiplexers and diplexer applications, including the IMUX of satellite payload. It was seen that not only filter size is reduced, but other components such as hybrids and circulators are less used, which yields less system complexity and less insertion loss, in addition to size and mass reduction.

Chapter 6
Conclusions and Future Work

6.1 Contributions of This Work

There are several contributions to the area of microwave filters and systems, resulting from the work done towards this thesis, which can be divided into three major areas.

Firstly, this thesis introduces the first ever quadruple-mode dielectric resonator filter, using a simple cylindrical structure [67]. This filter has significant impact, since despite its compactness, it is a simple structure that is already widely commercially available. Compact 4-n pole filters, as well as mixed mode filters utilizing the quadruple-mode cavity are realizable. Different designs, as well as measurement results are presented for a single cavity 4-pole filter, which validate the concept.

Based on the quadruple-mode operation, a novel dual-mode half-cut dielectric resonator filter is introduced [66] and [67], demonstrating several designs and measurement results backing the proposed concepts. This filter type is demonstrated to be a significant improvement (up to half the size) over existing dual-mode dielectric solutions, and offers significant size and mass reduction with comparable or better performance in other aspects. The work also contains detailed discussions on the different design aspects of the dual-mode half-cut filter, including frequency control, couplings, spurious enhancement, tuning capabilities, and advanced coupling schemes.

The second area of contribution is the novel dual-band dielectric resonator filter, using the half-cut dielectric resonator [68]. This is one of the very few ever reported dielectric resonator based dual-band filters, and to our knowledge, it is the first true single resonator dual-band dielectric resonator filter, which also has fully controllable design parameters for realizing different dual-band filtering functions. Various designs and details of the structure, as well as measurement results are presented that verify the proposed concepts.

The third area of contribution has significant impacts at both device and system level, with the introduction of a novel combined two-channel multiplexer [69], derived from the dual-band dielectric resonator filter. The two channel MUX, combines the two separate physical filter lines into a single physical filter line using the dual-band orthogonal mode resonators. This building block is then demonstrated to have significant impact at the system level for different application areas of multiplexing systems, including various forms of IMUX, OMUX, and Tx-Rx diplexers.

Concepts disclosed in this thesis were filed in [70] and [71], and are under patent pending status.

6.2 Future Work

The dual-mode half-cut dielectric resonator presented in chapter 3 can implement different filtering functions and topologies as mentioned. Therefore various other designs with different filter topologies, e.g. the parallel branch method, in addition to what is presented in this work can be carried out as future work. The half-cut and the quadruple mode dielectric resonator filter can also be extended to designs with higher order filters, e.g. 8-pole or 12-pole designs. The resonators can also be mixed with single mode or other multi-mode resonators to realize mixed mode filters with better spurious performance, especially for the quadruple-mode filter.

The dual-band filters presented in chapter 4 can be extended to include selected additional cavities to the side of the dual-band filter, containing Non-Resonating Nodes, to realize additional transmission zeros and attenuation poles to achieve better out-of band characteristics. More generally, the idea of orthogonal mode dual-band dielectric resonator filter, which is first presented here in this work, can be applied to other dielectric structures, and added benefits may be achieved by using those structures.

The results presented in chapter 5 are in the simulation stage and it is imperative that these designs be fabricated to confirm the proposed concepts. The more advanced coupling schemes briefly discussed in that chapter may also be analyzed for their potentials in providing higher out of band rejection, and possibly higher isolation between uncommon ports. This work is best carried out by devising an analytical approach to find the ideal response based on desired characteristics. Also this method should be applied to the structure in hand, to find the limits of the possible improvements. In addition, other dual-band resonators maybe used with the combined two channel MUX concept, as long as they can provide separate controllable couplings, and branching capabilities.

Bibliography

[1] R. J. Cameron, C. M. Kudsia, and R. R. Mansour, *Microwave Filters for Communication Systems*, New Jersey: J. Wiley & Sons, 2007.

[2] R. J. Cameron, "General Coupling Matrix Synthesis Methods for Chebyshev Filtering Functions," *IEEE Trans. Microw. Theory Tech.*, vol. MTT-47, no.4, pp. 433-442, April 1999.

[3] J. D. Rhodes, *Theory of Electrical Filters*, Wiley, New York, 1976.

[4] A. E. Atia and A.E. Williams, "New Types of Waveguide Bandpass Filters for Satellite Transponders," *Comsat Tech. Review*, vol. 1, No.1, pp. 20-43, Fall 1971.

[5] A. E. Atia and A. E. Williams, "Narrow-Bandpass Waveguide Filters," *IEEE Trans. Microw. Theory Tech.*, vol. MTT-20, No.4, pp. 258-265, April 1972.

[6] A. E. Atia, A. E. Williams, and R. W. Newcomb, "Narrow-band multiple-coupled cavity synthesis", *IEE Trans. Circuit Syst. CAS-21*, pp. 649-655, Sept. 1974.

[7] R. J . Cameron, "Advanced coupling matrix synthesis techniques for microwave filters", *IEEE Trans. Microw. Theory Tech.*, vol. MTT-51, pp. 1-10, Jan. 2003.

[8] R. J. Cameron and R. J. Rhodes, "Asymmetric realizations for dual-mode bandpass filters**,"** *IEEE Trans. Microw. Theory Tech.*, vol. MTT-29, pp. 51-58, Jan. 1981.

[9] S. B. Cohn, "Microwave bandpass filters containing high-Q dielectric resonators," *IEEE Trans. Microwave Theory Tech.*, vol. MTT-16, pp. 218–227, Apr. 1968.

[10] Trans-tech Inc., Ceramics and Advanced Materials, http://www.trans-techinc.com/, 2009.

[11] Y. Kobayashi, N. Fukuoka, and S. Yoshida, "Resonant modes for a shielded-dielectric rod resonator," *Elect. Commun. Japan*, vol. 64-B, 1981-translation, 1983 Scnpta Publishing Co.

[12] D. Kajfez and P. Guillon, *Dielectric Resonators*, 2nd ed., Atlanta: Noble Publishing Corp., 1998

[13] K. A. Zaki and C. Chen, "New results in dielectric-loaded resonators", *IEEE Trans. Microw. Theory Tech*., vol. MTT-34, pp. 815-824, July 1986.

[14] D. L. Rebsch, D. C.Webb, R. A. Moore, and J. D. Cowlishaw, "A mode chart for accurate design of cylindrical dielectric resonators," *IEEE Trans. Microwave Theory Tech.*, vol. MTT-13, pp. 468–469, May 1965.

[15] W. E. Courtney, "Analysis and evaluation of a method of measuring the complex permittivity and permeability of microwave insulators," *IEEE Trans. Microw. Theory Tech.*, vol. MTT-18, pp. 476–485, Aug. 1970.

[16] Y. Kobayashi and S. Tanaka, "Resonant modes of a dielectric rod resonator short-circuited at both ends by parallel conducting plates," *IEEE Trans. Microw. Theory Tech.*, vol. MTT-28, pp. 1077–1085, Oct. 1980.

[17] Y. Kobayashi, N. Fukuoka, and S. Yoshida, "Resonant modes of a shielded dielectric rod resonator," *J. Inst. Electron. Inf. Commun. Eng.*, vol. J64-B, no. 5, pp. 433–440, 1981.

[18] K. A. Zaki and A. E. Atia, "Modes in dielectric-loaded waveguides and resonators," IEEE *Trans. Microw. Theory Tech.*, vol. MTT-31, pp. 1039–1045, Dec. 1983.

[19] S. Amari, and U. Rosenberg, "New in-line dual- and triple-mode cavity filters with non resonating nodes," *IEEE Trans. Microw. Theory Tech.*, vol. MTT-53, pp. 1272–1279, April 2005.

[20] R.R. Bonetti, and A.E. Williams, "Application of Dual TM Modes to Triple- and Quadruple-Mode Filters, *IEEE Trans. Microw. Theory Tech.*, vol. MTT-35, pp. 1143- 1149, Dec 1987.

[21] W. Tang and S.K Chaudhuri, "A True Elliptic-Function Filter Using Triple-Mode Degenerate Cavities," *IEEE Trans. Microw. Theory Tech.*, vol. MTT-32, pp. 1449 – 1454, Nov. 1984.

[22] S. Fok et al., "A Novel Microstrip Square-Loop Dual-Mode Bandpass Filter With Simultaneous Size Reduction and Spurious Response Suppression," *IEEE Trans. Microw. Theory Tech.*, vol. MTT-54, pp. 2033 – 2041, May 2006.

[23] S. J. Fiedziuszko, "Dual-mode dielectric resonator loaded cavity filters," *IEEE Trans. Microwave Theory Tech.*, vol. MTT-30, pp. 1311-1316, Sept. 1982.

[24] I. C. Hunter, J. D. Rhodes, and V. Dassonville, "Triple-mode dielectric resonator hybrid reflection filters," *Proc. Inst. Elect. Eng.*, pt. H, vol. 145, pp. 337–343, Aug. 1998.

[25] V. Walker and I.C. Hunter, "Design of triple mode $TE_{01\delta}$ resonator transmission filters", *IEEE Microwave and Wireless Components Letters*, vol. 12, pp. 215-217, June 2002.

[26] J. Hattori, T. Wada, H. Kubo, and Y. Ishikawa, "2GHz band quadruple mode dielectric resonator filter for cellular base station," in *IEEE MTT-S Intl. Microwave Symp. Dig.*, vol. 2, June 2003, pp. 933-936.

[27] S. J. Fiedziuszko et al., "Dielectric materials, devices, and circuits," *IEEE Trans. on Microwave Theory Tech.*, vol. MTT-50, pp. 706-720, Mar. 2002.

[28] K. Zaki, C. Chen, and A. E. Atia, "Canonical and longitudinal dual-mode dielectric resonator filters," *IEEE Trans. Microwave Theory Tech.*, vol. MTT-35, pp. 1130–1134, Dec. 1987.

[29] Y. Kobayashi and K.Kubo, "Canonical bandpass filters using dual-mode dielectric resonators," in *IEEE MTT-S Int. Microwave Symp. Dig.*, 1987, pp. 137–140.

[30] J. P. Astier and P. Guillon, “Elliptic microwave filter using dual modes of dielectric resonators,” in *European Microwave Conf. Dig.*, Sept. 1985, pp. 335–340.

[31] X.-P. Liang; H.-C. Chang; K.A. Zaki, “Modeling of Cylindrical Dielectric Resonators in Rectangular Waveguides and Cavities,” in *IEEE MTT-S Intl. Microwave Symp. Dig.*, 1993, pp. 597-600.

[32] I. C. Hunter, J. D. Rhodes, and V. Dassonville, “Dual mode filters with conductor loaded dielectric resonators,” *IEEE Trans. Microwave Theory Tech.*, vol. 42, pp. 2304–2311, Dec. 1999.

[33] C. Wang, K. A. Zaki, A. E. Atia, and T. G. Dolan, “Dielectric combline resonators and filters,” *IEEE Trans. Microwave Theory Tech.*, vol. 46, pp. 2501–2506, Dec. 1998.

[34] Y. Kobayashi and M. Minegishi, “A bandpass filter using electrically coupled TM dielectric rod resonators,” in *IEEE MTT-S Int. Microwave Symp. Dig.*, 1988, pp. 507–510.

[35] S. Yamashita and M. Makimoto, “Miniaturized coaxial resonator partially loaded with high-dielectric constant microwave ceramics,” *IEEE Trans. Microwave Theory Tech.*, vol. MTT-31, pp. 697–703, Sept. 1983.

[36] S. Kobayashi and K. Saito, “A miniaturized ceramic bandpass filter for cordless phone systems,” in *IEEE Int. Microwave Symp. Dig.*, vol. 2, 1995, pp. 391–394.

[37] R. Zhang, and R. R. Mansour, “Low-Cost Dielectric-Resonator Filters With Improved Spurious Performance”, *IEEE Trans. Microwave Theory Tech.*, vol. MTT-55, pp. 2168-2175, Oct. 2007.

[38] T. Nishikawa, K. Wakino, K. Tsunoda, Y. Ishikawa, “Dielectric high-power bandpass filter using quarter-cut $TE_{01\delta}$ image resonator for cellular base stations,” *IEEE Trans. Microwave Theory Tech.*, vol. MTT-35, pp. 1150-1155, Dec. 1987.

[39] R. R. Mansour, S. Ye, S. F. Peik, V. Dokas, B. Flitzpatrick , “Quasi-dual-mode resonators**,”** *IEEE Trans. Microwave Theory Tech.*, vol. MTT-48, pp. 2576-2481, Dec. 2000.

[40] Mixed Modes Cylindrical Planar Dielectric Resonator Filters with Rectangular Enclosure

[41] K. Watkino et al. “Dielectric resonator and microwave using the same,” US patent 4,028,652 June 1977.

[42] R. D. Fuller et al. “Ring shaped dielectric resonator with adjustable tuning screw extending upwardly into ring opening,” US patent 4,630,012 Dec. 1986.

[43] J. Hattori et al. “Dielectric resonator,” US patent 4,706,052, Nov. 1987.

[44] Y. Kobayashi and M. Miura, “Optimum design for shielded dielectric rod and ring resonators for obtaining best mode separation,” *IEEE MU-S Symp. Dig.*, pp. 184-186, 1984.

[45] T. Itoh and R.S. Rudokas, "New method for computing the resonant frequencies of dielectric resonators," *IEEE Trans. Microw. Theorv Tech*., vol. MTT-25, pp. 52-54, Jan. 1977.

[46] Ansoft Corporation, Ansoft HFSS, http://www.ansoft.com/products/hf/hfss/, 2009.

[47] CST, CST Microwave Studio, http://www.cst.com/, 2009.

[48] P. Vincent, "Computation of the resonant frequency of a dielectric resonator by a differential method," *Applied Physics*, vol. A-31, pp.51-54, 1983.

[49] M. Jaworski and M.W. Pospieszalski, "An accurate solution of the cylindrical dielectric resonator problem," *IEEE Trans. Microwave Theory Tech*, vol. MTT-27, pp. 639-643, July 1979.

[50] Yu. G. Kapustin, "Design of circular waveguide resonator with dielectric disk," *Izvestiva Vuzov. Radiofizika*, vol. 25, pp. 1337-1344, Nov. 1982.

[51] Y. Zhang, K. A. Zaki, J. A. Ruiz-Cruz, and A. E. Atia, "Analytical synthesis of generalized multi-band microwave filters," *IEEE MTT-S Int. Microw. Symp. Dig.*, Jun. 2007, pp. 1273–1276.

[52] M. Mokhtaari, J. Bornemann, K. Rambabu, and S. Amari, "Coupling matrix design of dual and triple passband filters," *IEEE Trans. Microw. Theory Tech.*, vol. 55, no. 11, pp. 3940–3946, Nov. 2006.

[53] G. Macchiarella and S. Tamiazzo, "Design techniques for dual passband filters," *IEEE Trans. Microwave Theory Tech.*, vol. 53, no. 11, pp. 3265-327 1, Nov.2005.

[54] S. Amari and M. Bekheit "A new class of dual-Mode dual-Band waveguide filters" *IEEE Trans. Microwave Theory Tech.*, Vol. 56, no. 8, pp.1938-1944, Aug. 2008.

[55] G. Macchiarella and S. Tamiazzo, "Dual-band filters for base station multi-band combiners," in *IEEE MTT-S Int. Microw. Symp. Dig.*, Jun. 2007, pp. 1289–1292.

[56] V. Lunot, F. Seyfert, S. Bila, and A. Nasser, "Certified computation of optimal multiband filtering functions," *IEEE Trans. Microw. TheoryTech.*, vol. MTT-56, no. 1, pp. 105–112, Jan. 2008.

[57] P. Lenoir et al., "Synthesis and design of asymmetrical dual-band bandpass filters based on equivalent network simplification," *IEEE Trans. Microw. Theory Tech.*, vol. MTT-54, pp. 3090-3097, Jul. 2006.

[58] S. W. Chen, K. A. Zaki, and R. G. West, "Tunable, temperature-compensated dielectric resonators and filters," *IEEE Trans. Microw. Theor. Tech.*, vol. MTT-38, pp. 1046–1052, Aug. 1990.

[59] R. Zhang, R. R. Mansour, "Dual-band dielectric-resonator filters", *IEEE Trans. Microw. Theory Tech.*, vol. MTT-57, pp. 1760-1766, July 2009.

[60] E. G. Cristal and G. L. Matthaei, "A technique for the design of multiplexers having contiguous channels," *IEEE Trans. Microw. Theory Tech.*, vol. MTT-12, pp. 88-93, Jan. 1964.

[61] A. E. Atia, "Computer aided design of waveguide multiplexers," *IEEE Trans. Microw. Theory Tech.*, vol. MTT-22, pp. 322-336, March 1974.

[62] J. D. Rhodes and R. Levy, "Design of general manifold multiplexers," *IEEE Trans. Microw. Theory Tech.*, vol. MTT-27, pp. 11-123, 1979.

[63] D. Doust et al., "Satellite multiplexing using dielectric resonator filters," *Microw. J.,* vol. 32, pp. 93-166, Dec. 1989.

[64] C. Kudsia, R. Cameron, and W. C. Tang, "Innovation in microwave filters and multiplexing networks for communication satellite systems," *IEEE Trans. Microw. Theory Tech.*, vol. MTT-40, pp. 1133-1149, June 1992.

[65] W. C. Tang et al., "Dielectric resonator output multiplexer for C-band satellite applications" in *IEEE Int. Microwave Symp. Dig.*, vol. 85, Jun. 1985, pp. 343-345.

[66] M. Memarian and R. R. Mansour, "Dual-mode half-cut dielectric resonator filter," in *IEEE Int. Microwave Symp. Dig,* vol., Jun 2009, pp. 1465-1468.

[67] M. Memarian and R. R. Mansour, "Quad-mode and dual-mode dielectric resonator filters", submitted to *IEEE Trans. Microw. Theory Tech.*, 2009.

[68] M. Memarian and R. R. Mansour, "Dual-band half-cut dielectric resonator filters", in *European Microw Conf.*, vol. ?, Oct. 2009, pp. ?.

[69] M. Memarian and R. R. Mansour, "Compact dual-band filters and multiplexers in dielectric resonator technology", in preparation for *IEEE Trans. Microw. Theory Tech.,* 2009.

[70] M. Memarian and R. R. Mansour, "Method of operation and construction of dual-mode filters, quad-mode filters, dual-band filters, and diplexer/multiplexer devices using full or half-cut dielectric resonators," US Patent 12/479,263, filed June 2009.

[71] M. Memarian and R. R. Mansour, "Method of operation and construction of dual-mode filters, quad-mode filters, dual-band filters, and diplexer/multiplexer devices using full or half-cut dielectric resonators," EU Patent, filed July 2009.